

Electronic Supplementary Information

Electronic, steric and catalytic properties of N-heterocyclic carbene rhodium(I) complexes linked to (metallo)porphyrins

Ludivine Poyac,^a Stefano Scoditti,^b Xavier Dumail,^a Michel Granier,^a Sébastien Clément,^a Rafael Gramage-Doria,^c Charles H. Devillers^d and Sébastien Richeter,^{*a}

sebastien.richeter@umontpellier.fr

- ^a ICGM, Univ Montpellier, CNRS, ENSCM, Montpellier 34293, France.
^b Department of Chemistry and Chemical Technologies, Univ of Calabria, Via P. Bucci, Rende 87036, Italy.
^c ISCR, Univ Rennes, CNRS, UMR 6226, Rennes 35000, France
^d ICMUB UMR 6302, CNRS, Univ Bourgogne Franche-Comté, 9 avenue Alain Savary, Dijon 21078, France.

Table of contents

Experimental section	4
Synthesis and characterization of new compounds	5
Spectra of new compounds	10
Catalytic studies	41
General procedure for catalytic studies	41
Monitoring of the reactions by gas chromatography (GC)	41
Time profile of the reactions.....	42
Monitoring of the reactions by ¹ H NMR spectroscopy	43
Monitoring of the catalysis reactions by UV-visible absorption spectroscopy	44
Stability of 2H-C-Rh(cod)Cl and Ni-C-Rh(cod)Cl	45
Monitoring of the stability of complexes 2H-C-Rh(cod)Cl and Ni-C-Rh(cod)Cl by ¹³ C{ ¹ H} NMR spectroscopy	45
Monitoring of the stability of Ni-C-Rh(cod)Cl by UV-visible absorption spectroscopy	46
Monitoring of the stability of complexe Ni-C-Rh(cod)Cl by Electrospray Ionization Time-of-Flight mass spectrometry.	47

Table of Figures

Figure S1. Full range (top) and partial (bottom) ^1H NMR spectrum (500 MHz, CD_2Cl_2) of 2H-A-Cl	10
Figure S2. Full range (top) and partial (bottom) $^{13}\text{C}\{^1\text{H}\}$ NMR spectrum (125.7 MHz, CD_2Cl_2) of 2H-A-Cl	10
Figure S3. ESI-TOF (positive mode) mass spectrum of 2H-A-Cl	11
Figure S4. Full range (top) and partial (bottom) ^1H NMR spectrum (400 MHz, CD_2Cl_2) of Zn-A-Cl	11
Figure S5. Full range (top) and partial (bottom) $^{13}\text{C}\{^1\text{H}\}$ NMR spectrum (125.7 MHz, CD_2Cl_2) of Zn-A-Cl	12
Figure S6. ESI-TOF (positive mode) mass spectrum of Zn-A-Cl	12
Figure S7. ^1H NMR spectrum (400 MHz, CD_2Cl_2) of Ni-A-Cl	13
Figure S8. Full range (top) and partial (bottom) $^{13}\text{C}\{^1\text{H}\}$ NMR spectrum (125.7 MHz, CD_2Cl_2) of Ni-A-Cl	13
Figure S9. ESI-TOF (positive mode) mass spectrum of Ni-A-Cl	14
Figure S10. Full range (top) and partial (bottom) ^1H NMR spectrum (400 MHz, CD_2Cl_2) of 2H-A-Rh(cod)Cl	14
Figure S11. Full range (top) and partial (bottom) $^{13}\text{C}\{^1\text{H}\}$ NMR spectrum (150.9 MHz, CD_2Cl_2) of 2H-A-Rh(cod)Cl	15
Figure S12. ^1H - ^1H COSY NMR spectrum (600 MHz, CD_2Cl_2) of 2H-A-Rh(cod)Cl	16
Figure S13. ^1H - $^{13}\text{C}\{^1\text{H}\}$ HSQC NMR spectrum (600 MHz, CD_2Cl_2) of 2H-A-Rh(cod)Cl	16
Figure S14. Full range (top), partial (bottom) ^1H - $^{13}\text{C}\{^1\text{H}\}$ HMBC NMR spectra (600 MHz, CD_2Cl_2) of 2H-A-Rh(cod)Cl	17
Figure S15. ^1H - ^1H ROESY NMR spectra (600 MHz, CD_2Cl_2) of 2H-A-Rh(cod)Cl	18
Figure S16. ESI-TOF (positive mode) mass spectrum of 2H-A-Rh(cod)Cl	18
Figure S17. Full range (top) and partial (bottom) ^1H NMR spectrum (600 MHz, CD_2Cl_2) of Zn-A-Rh(cod)Cl	19
Figure S18. Full range (top) and partial (bottom) $^{13}\text{C}\{^1\text{H}\}$ NMR spectrum (150.9 MHz, CD_2Cl_2) of Zn-A-Rh(cod)Cl	20
Figure S19. ESI-TOF (positive mode) mass spectrum (left) of Zn-A-Rh(cod)Cl . Experimental (a) and calculated (b) isotopic patterns (right)	20
Figure S20. Full range (top) and partial (bottom) ^1H NMR spectrum (400 MHz, CD_2Cl_2) of Ni-A-Rh(cod)Cl	21
Figure S21. $^{13}\text{C}\{^1\text{H}\}$ NMR spectrum (150.9 MHz, CD_2Cl_2) of Ni-A-Rh(cod)Cl	22
Figure S22. ESI-TOF positive mode mass spectrum (left) of Ni-A-Rh(cod)Cl . Experimental (a) and calculated (b) isotopic patterns.....	22
Figure S23. Full range (top) and partial (bottom) ^1H NMR spectrum (400 MHz, CD_2Cl_2) of 2H-C-PF₆ ..	23
Figure S24. $^{19}\text{F}\{^1\text{H}\}$ spectrum (376.5 MHz, CD_2Cl_2) of 2H-C-PF₆	23
Figure S25. $^{13}\text{C}\{^1\text{H}\}$ NMR spectrum (150.9 MHz, $\text{DMSO}-d_6$) of 2H-C-PF₆	24
Figure S26. ESI-TOF positive mode mass spectrum of porphyrin 2H-C-PF₆	24
Figure S27. Full range (top) and partial (bottom) ^1H NMR spectrum (400 MHz, CD_2Cl_2) of Zn-C-PF₆	25
Figure S28. $^{13}\text{C}\{^1\text{H}\}$ NMR spectrum (125.7 MHz, CD_2Cl_2) of Zn-C-PF₆	25
Figure S29. $^{19}\text{F}\{^1\text{H}\}$ NMR spectrum (376.5 MHz, CD_2Cl_2) of Zn-C-PF₆	26
Figure S30. ESI-TOF (positive mode) mass spectrum of Zn-C-PF₆	26
Figure S31. ^1H NMR spectrum (400 MHz, CD_2Cl_2) of Ni-C-PF₆	27
Figure S32. A) Full range B) Partial $^{13}\text{C}\{^1\text{H}\}$ NMR spectrum (125.7 MHz, CD_2Cl_2) of Ni-C-PF₆ . C) $^{19}\text{F}\{^1\text{H}\}$ (376.5 MHz, CD_2Cl_2) of Ni-C-PF₆	27
Figure S33. ESI-TOF (positive mode) mass spectra of Ni-C-PF₆	28
Figure S34: Full range (top) and partial (bottom) ^1H NMR spectrum (600 MHz, CD_2Cl_2) of 2H-C-Rh(cod)Cl	29
Figure S35. Full range (top) and partial (bottom) $^{13}\text{C}\{^1\text{H}\}$ NMR spectrum (150.9 MHz, CD_2Cl_2) of 2H-C-Rh(cod)Cl	29
Figure S36. Full range (top) and partial (bottom) ^1H - ^1H COSY NMR spectrum (600 MHz, CD_2Cl_2) of 2H-C-Rh(cod)Cl	30

Figure S37. ^1H - $^{13}\text{C}\{^1\text{H}\}$ HSQC NMR spectrum (600 MHz, CD_2Cl_2) of 2H-C-Rh(cod)Cl	30
Figure S38. Full range (top) and partial (bottom) ^1H - $^{13}\text{C}\{^1\text{H}\}$ HMBC NMR spectrum (600 MHz, CD_2Cl_2) of 2H-C-Rh(cod)Cl	31
Figure S39. ^1H - ^1H ROESY NMR spectra (600 MHz, CD_2Cl_2)	31
Figure S40. ESI-TOF (positive mode) mass spectrum of 2H-C-Rh(cod)Cl (left). Experimental (a) and theoretical (b) isotopic patterns (right).....	32
Figure S41. Full range (top) and partial (bottom) ^1H NMR spectrum (600 MHz, CD_2Cl_2) of Zn-C-Rh(cod)Cl	33
Figure S42. Full range (top) and partial $^{13}\text{C}\{^1\text{H}\}$ NMR spectrum (150.9 MHz, CD_2Cl_2) of Zn-C-Rh(cod)Cl	33
Figure S43. ESI-TOF (positive mode) mass spectrum of porphyrin Zn-C-Rh(cod)Cl (right). Experimental (a) and theoretical (b) isotopic patterns (left).....	34
Figure S44. Full range (top) and partial (bottom) ^1H NMR spectrum (600 MHz, CD_2Cl_2) of Ni-C-Rh(cod)Cl	35
Figure S45. Full range (top) and partial (bottom) $^{13}\text{C}\{^1\text{H}\}$ NMR spectrum (150.9 MHz, CD_2Cl_2) of Ni-C-Rh(cod)Cl	35
Figure S46. Full range ^1H - ^1H COSY NMR spectra (600 MHz, CD_2Cl_2) of porphyrin Ni-C-Rh(cod)Cl	36
Figure S47. Full range (top) and partial (bottom) ^1H - $^{13}\text{C}\{^1\text{H}\}$ HSQC NMR spectrum (600 MHz, CD_2Cl_2) of Ni-C-Rh(cod)Cl	36
Figure S48. Full range (top) and partial (bottom) ^1H - $^{13}\text{C}\{^1\text{H}\}$ HMBC NMR spectrum (600 MHz, CD_2Cl_2) of Ni-C-Rh(cod)Cl	37
Figure S49. Full range ^1H - ^1H ROESY NMR spectrum (600 MHz, CD_2Cl_2) of Ni-C-Rh(cod)Cl	37
Figure S50. ESI-TOF (positive mode) mass spectrum of Ni-C-Rh(cod)Cl (left). Experimental (a) and calculated (b) isotopic patterns (right)	38
Figure S51. DFT optimized structures of complexes M¹-A-Rh(cod)Cl , M¹-B-Rh(cod)Cl and M¹-C-Rh(cod)Cl with $\text{M}^1 = 2\text{H}$, Zn and Ni (meso <i>p</i> -tolyl groups and H omitted for clarity).....	39
Figure S52. Steric maps of the complexes M¹-A-Rh(cod)Cl , M¹-B-Rh(cod)Cl and M¹-C-Rh(cod)Cl with $\text{M}^1 = 2\text{H}$, Zn and Ni in optimized geometries of the corresponding complexes calculated with the SambVca 2.1 tool with the following standard inputs: Bondi radii 1.17 Å, $\text{Rh}-\text{C}_{\text{NHC}}$ 2.00 Å, $r_{\text{sphere}} = 3.50$ Å, mesh spacing 0.10 Å, H atoms excluded. ¹⁵	40
Figure S53. GC chromatograms obtained from reaction mixtures with Ni-A-Rh(cod)Cl (top) and Ni-C-Rh(cod)Cl (bottom) at 100°C with $t=0$ (left) and $t=3\text{h}$ (right).	41
Figure S54: Time profiles of the conjugated addition of phenylboronic acid to cyclohexen-2-one catalysed by IMe-Rh(cod)Cl (black), IMe-Rh(cod)Cl + NiP (orange) at 60°C and 100°C (top); Time profiles of the same reaction catalysed by M¹-A-Rh(cod)Cl , M¹-B-Rh(cod)Cl and M¹-C-Rh(cod)Cl ($\text{M}^1 = 2\text{H}$ in blue, Zn in green and Ni in red) at 60°C and 100°C.....	42
Figure S55. ^1H NMR spectra of the reaction mixtures with Ni-A-Rh(cod)Cl (top) and Ni-C-Rh(cod)Cl (bottom) complexes at $t = 0$ (up) and $t = 3$ hours (down). A drop of the reaction mixtures was taken at $t = 0$ and $t = 3\text{h}$ and diluted with CD_2Cl_2 for ^1H NMR spectroscopy analysis.	43
Figure S56. UV-visible absorption spectra in CH_2Cl_2 of the reaction mixtures of the conjugated addition of phenylboronic acid to cyclohexen-2-one at 100°C catalysed by M¹-A-Rh(cod)Cl , M¹-B-Rh(cod)Cl and M¹-C-Rh(cod)Cl ($\text{M}^1 = \text{Ni}$, Zn , 2H) at $t = 0$, blue and $t = 3\text{h}$, green.	44
Figure S57. Monitoring of the stability of complexes 2H-C-Rh(cod)Cl (top) and Ni-C-Rh(cod)Cl (bottom) in the presence of KOH (100 eq) in toluene at 100 °C ($t = 0$, black; $t = 0.5$ h, blue; $t = 3$ h, orange) by $^{13}\text{C}\{^1\text{H}\}$ NMR spectroscopy (500 MHz, CD_2Cl_2).	45
Figure S58: Monitoring of the stability of complex Ni-C-Rh(cod)Cl in the presence of KOH (100 eq) in toluene at 100 °C ($t = 0$, black; $t = 0.5$ h, blue; $t = 1\text{h}$, green, $t = 2\text{h}$, purple, $t = 3\text{h}$, orange) by UV-visible absorption spectroscopy in CH_2Cl_2	46
Figure S59: Monitoring of the stability of complex Ni-C-Rh(cod)Cl (m/z calc for $\text{C}_{52}\text{H}_{44}\text{N}_6\text{NiRh} [\text{M}-\text{Cl}]^+$: 913.2030) in the presence of KOH (100 eq) in toluene at 100 °C ($t = 0.5\text{h}$ (top) and $t = 3\text{h}$ (bottom), by ESI-TOF mass spectrometry.	47

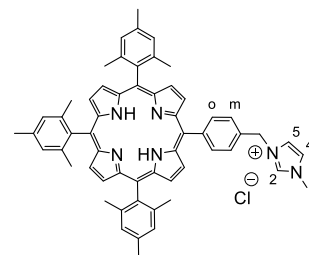
Experimental section

Materials. Reactions that needed inert atmosphere were performed under argon using Schlenk techniques and oven-dried glassware. All solvents were obtained from commercial suppliers and used as received. Dry THF was obtained by a PureSolve MD5 solvent purification system from Innovative Technology. Trifluoroacetic acid and pyrrole distilled under reduced pressure before use were purchased from Fluorochem. Boron trifluoride diethyl etherate (46%), paraformaldehyde (95%), phenyllithium 1.9 M in dibutyl ether, 2,3-dichloro-5,6-dicyano-1,4-benzoquinone (98%), sodium nitrite (99.9%), sodium hydride (99%) and 1-methylimidazole were purchased from Sigma Aldrich. Zinc acetate dihydrate (97%), 2,4,6-trimethylbenzaldehyde (98%), nickel(II) bis(acetylacetonate) (95%), *p*-tolualdehyde (98%), dimethyl carbonate (99%), imidazole (99%), iodomethane (99%), potassium hexafluorophosphate (95%) were purchased from Alfa Aesar. Potassium *tert*-butoxide (97%) was purchased from TCI and 2,3,5,6-tetrachloro-1,4-benzoquinone from Fluka (97%). Chloro(1,5-cyclooctadiene)rhodium(I) dimer was purchased from Alfa Aesar. TLC were carried out on Merck DC Kieselgel 60 F-254 aluminium sheets and spots were visualized with UV-lamp ($\lambda = 254/365$ nm) if necessary. Purifications were performed by silica gel Geduran® Si 60 for column chromatography (Merck 40–63 μ m). Compound **IME** was synthesized following the procedure described in the literature.¹ Porphyrin **2H-1** was synthesized following Lindsey's procedure.² Porphyrins **Ni-2**, **2H-2** and **Zn-2** were synthesized following our previously reported procedures.³ Porphyrins **Ni-B-BF₄**, **2H-B-BF₄** and **Zn-B-BF₄** were synthesized following our previously reported procedures.⁴ Rhodium(I) complexes **Ni-B-Rh(cod)Cl**, **2H-B-Rh(cod)Cl** and **Zn-B-Rh(cod)Cl** were synthesised following our previously reported procedures.^{4,5} Porphyrin **Ni-3** was synthesized following our previously reported procedure.⁶ Porphyrin **2H-3** and **Zn-3** were synthesized following our previous reported procedure.⁷

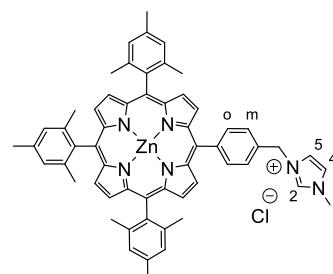
Instrument and methods. NMR spectroscopy and mass spectrometry were performed at the Laboratoire de Mesures Physiques of the University of Montpellier. ¹H, COSY, ROESY, HSQC, HMBC, ROESY ¹³C{¹H}, ¹⁹F spectra were recorded on Bruker 400 MHz Avance III HD, 500 MHz Avance III or 600 MHz Avance III spectrometers at 298 K. CD₂Cl₂, CDCl₃, and DMSO-*d*₆ solvents were purchased from Eurisotop, France and used as received. ¹H and ¹³C{¹H} NMR spectra were calibrated to TMS on the basis of the relative chemical shift of the residual non-deuterated solvent as an internal standard. Chemical shifts (δ) are expressed in ppm from the residual non-deuterated solvent signal and coupling constants values (J) are expressed in Hz. Abbreviations used for ¹H NMR spectra are as follows: s, singlet; d, doublet; t, triplet; m, multiplet, br, broad. High resolution mass spectra analysis (HRMS) were recorded on a ESI Bruker MicroToF QII instrument in positive/negative modes or ESI-TOF Q instruments in positive/negative modes. UV-visible absorption spectra were recorded with a JASCO V-750 UV-visible spectrophotometer in 10 mm quartz cells (Hellma); λ_{max} is expressed in nm and molar extinction coefficients ϵ (L.mol⁻¹.cm⁻¹) are expressed as log ϵ . GC measurements were performed using Agilent 8860 GC with a FID detector and a column HP-5 (0.320 mm x 30 m x 0.25 μ m).

Synthesis and characterization of new compounds

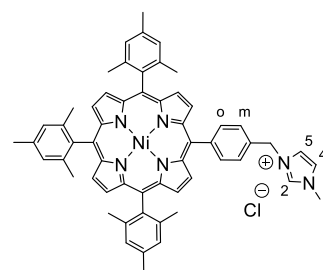
Synthesis of 2H-A-Cl. In a 250 mL two neck round bottom flask, **2H-1** (820 mg, 1.038 mmol, 1 eq) was added and degassed with argon. The solid was dissolved in CH₃CN (70 mL) and stirred. Then, 1-methylimidazole (8.52 g, 101.33 mmol, 100 eq) was added and the mixture was heated at reflux for 24 hours. The progress of the reaction was monitored by TLC analysis. Once finished, the solvent was evaporated and the excess of 1-methylimidazole was removed by distillation. Recrystallization from CH₂Cl₂/Et₂O afforded porphyrin **2H-A-Cl** as a purple solid in 91% yield (822 mg, 0.943 mmol). **¹H NMR** (400 MHz, CD₂Cl₂): δ 11.40 (s, 1H, H₂), 8.76 (d, ³J_{H,H} = 4.7 Hz, 2H, H_{β-pyr}), 8.67 (d, ³J_{H,H} = 4.8 Hz, 2H, H_{β-pyr}), 8.63 (br s, 4H, H_{β-pyr}), 8.27 (d, ³J_{H,H} = 7.6 Hz, 2H, H_o), 7.86 (d, ³J_{H,H} = 7.6 Hz, 2H, H_m), 7.45 (s, 1H, H₅), 7.30 (s, 1H, H₄), 7.29 (s, 6H, H_{mes meta}), 5.95 (s, 2H, CH₂), 4.15 (s, 3H, N-CH₃), 2.61 (s, 9H, H_{methyl para}), 1.86 (s, 6H, H_{methyl ortho}), 1.83 (s, 12H, H_{methyl ortho}), -2.62 (s, 2H, NH) ppm. **¹³C{¹H} NMR** (100.1 MHz, CH₂Cl₂): δ 144.0, 140.1, 140.0, 139.9, 139.8, 138.8, 138.6, 138.5, 135.9, 133.5, 131.0, 128.3, 127.8, 123.8, 122.3, 118.7, 118.6, 118.5, 37.3, 22.0, 21.9, 21.7 ppm. **UV-Vis** (DMSO): λ_{max} (log ε) = 419 (3.82), 514 (2.70), 548 (2.24), 590 (2.14), 646 (2.01) nm. **HRMS** (ESI⁺): *m/z* calc for C₅₈H₅₅N₆⁺ [M-Cl]⁺: 835.4483, found: 835.4488



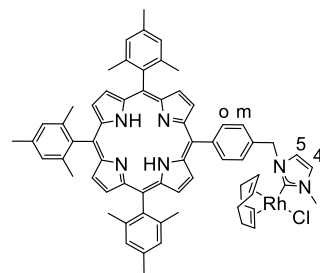
Synthesis of Zn-A-Cl. In a Schlenk tube, porphyrin **2H-A-Cl** (101 mg, 0.116 mmol, 1 eq) was added and degassed with argon/vacuum cycles. Chloroform was added (20 mL) and the obtained solution was stirred under argon. Then, a solution of Zn(OAc)₂·2H₂O (28.0 mg, 0.127 mmol, 1.1 eq) in methanol (5 mL) was prepared and added under argon. The obtained mixture was stirred overnight for 16 hours. Metalation reaction was monitored by UV-visible absorption spectroscopy. Once finished, the solvent was evaporated and the solid residue was recrystallized from CH₂Cl₂/*n*-hexane giving porphyrin **Zn-A-Cl** as a purple solid in 96% yield (104 mg, 0.111 mmol). **¹H NMR** (400 MHz, DMSO-*d*₆): δ 9.47 (s, 1H, H₂), 8.64 (d, ³J_{H,H} = 4.6 Hz, 2H, H_{β-pyr}), 8.56 (d, ³J_{H,H} = 4.6 Hz, 2H, H_{β-pyr}), 8.52 (m, 4H, H_{β-pyr}), 8.22 (d, ³J_{H,H} = 7.8 Hz, 2H, H_o), 8.09 (d, ³J_{H,H} = 1.7 Hz, 1H, H₅), 7.88 (d, ³J_{H,H} = 1.7 Hz, 1H, H₄), 7.77 (d, ³J_{H,H} = 7.8 Hz, 2H, H_m), 7.30 (d, ³J_{H,H} = 3.2 Hz, 6H, H_{mes meta}), 5.79 (s, 2H, CH₂), 3.98 (s, 3H, N-CH₃), 2.57 (d, ³J_{H,H} = 2.8 Hz, 9H, H_{methyl para}), 1.78 (s, 18H, H_{methyl ortho}) ppm. **¹³C{¹H} NMR** (125.7 MHz, CD₂Cl₂): δ 150.3, 150.3, 149.9, 149.7, 144.8, 139.7, 139.7, 139.6, 139.6, 137.9, 137.8, 135.7, 132.4, 131.9, 131.4, 131.4, 130.8, 128.0, 128.0, 127.4, 123.8, 122.1, 119.1, 119.0, 118.7, 22.1, 21.8, 21.7, 21.6 ppm. **UV-Vis** (DMSO): λ_{max} (log ε) = 429 (5.23), 562 (3.69), 601 (3.28) nm. **HRMS** (ESI⁺): *m/z* calc for C₅₈H₅₃N₆Zn⁺ [M-Cl]⁺: 897.3618, found: 897.3623



Synthesis of Ni-A-Cl. In a Schlenk tube, porphyrin **2H-A-Cl** (122 mg, 0.140 mmol, 1eq) was introduced and degassed with argon/vacuum cycles. Anhydrous toluene was added (20 mL) and the obtained solution was stirred under argon. Then, Ni(acac)₂ (71.9 mg, 0.280 mmol, 2 eq) was added and the mixture was heated at 40°C for 16 hours. Metalation reaction was monitored by UV-visible absorption spectroscopy. Once finished, the solvent was evaporated and the solid residue was recrystallized from CH₂Cl₂/*n*-hexane giving porphyrin **Ni-A-Cl** as a purple solid in 95% yield (123 mg, 0.132 mmol). **¹H NMR** (400 MHz, CD₂Cl₂): δ 11.45 (s, 1H, H₂), 8.71 (d, ³J_{H,H} = 4.5 Hz, 2H, H_{β-pyr}), 8.62 (d, ³J_{H,H} = 4.6 Hz, 2H, H_{β-pyr}), 8.56 (br s, 4H, H_{β-pyr}), 8.27 (d, ³J_{H,H} = 7.7 Hz, 2H, H_o), 7.80 (d, ³J_{H,H} = 7.7 Hz, 2H, H_m), 7.44 (s, 1H, H₅), 7.29 (s, 1H, H₄), 7.29–7.23 (m, 6H, H_{mes meta}), 5.92 (s, 2H, CH₂), 4.15 (s, 3H, N-CH₃), 2.65 – 2.55 (m, 9H, H_{methyl para}), 1.87–1.76 (m, 18H, H_{methyl ortho}) ppm. **¹³C{¹H} NMR** (125.7 MHz, CD₂Cl₂): δ 143.0, 142.9, 142.8, 139.4, 138.4, 137.5, 137.5, 135.0, 133.5, 132.5, 132.1, 132.0, 131.6, 128.2, 124.0, 122.4, 117.7, 117.7, 117.6, 21.6, 21.6 ppm. **UV-Vis** (DMSO): λ_{max} (log ε) = 429 (4.76), 527 (3.61), 555 (2.95) nm. **HRMS** (ESI⁺): *m/z* calc for C₅₈H₅₃N₆Ni⁺ [M-Cl]⁺: 891.3680, found: 891.3685.

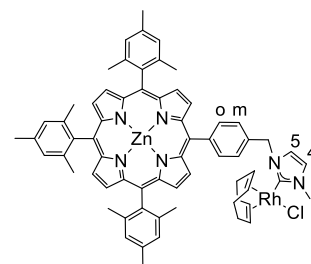


Synthesis of 2H-A-Rh(cod)Cl. Porphyrin **2H-A-Cl** (400 mg, 0.459 mmol, 1 eq), [Rh(cod)Cl]₂ (159 mg, 0.322 mmol, 0.7 eq), and *t*-BuOK (72 mg, 0.643 mmol, 1.4 eq) were degassed under argon for 10 minutes. Then, anhydrous THF (150 mL) was added and the reaction mixture was stirred at room temperature under argon atmosphere for 16 hours. Once finished according to TLC analysis, the solvent was evaporated and the residue was purified by silica gel column chromatography (eluent: CH₂Cl₂ to CH₂Cl₂/MeOH 97:3 (v:v)). Recrystallization from CH₂Cl₂/*n*-pentane afforded the porphyrin **2H-A-Rh(cod)Cl** as a purple solid in 45% yield (226 mg, 0.209 mmol).



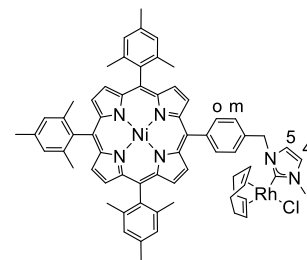
¹H NMR (600 MHz, CD₂Cl₂): δ 8.80 (d, ³J_{H,H} = 4.8 Hz, 2H, H_{β-pyr}), 8.67 (d, ³J_{H,H} = 4.6 Hz, 2H, H_{β-pyr}), 8.63 (s, 4H, H_{β-pyr}), 8.22 (d, ³J_{H,H} = 7.7 Hz, 2H, H_o), 7.79 (d, ³J_{H,H} = 7.7 Hz, 2H, H_m), 7.30 (s, 6H, H_{mes meta}), 7.09 (d, ³J_{H,H} = 1.9 Hz, 1H, H₅), 7.02 (d, ³J_{H,H} = 1.9 Hz, 1H, H₄), 6.26 (d, ³J_{H,H} = 14.8 Hz, 1H, CH₂), 5.99 (d, ³J_{H,H} = 14.8 Hz, 1H, CH₂), 5.12–5.00 (m, 2H, CH-cod), 4.19 (s, 3H, N-CH₃), 3.54–3.43 (m, 2H, CH-cod), 2.62 (2s, 9H, H_{methyl para}), 2.59–2.39 (m, 4H, CH₂-cod), 2.08–1.96 (m, 4H, CH₂-cod), 1.87–1.85 (2s, 18H, H_{methyl ortho}), –2.59 (s, 2H, NH) ppm. **¹³C{¹H} NMR** (150.9 MHz, CD₂Cl₂): δ 184.2 (d, ¹J_{Rh,C} = 51.5 Hz, C-Rh), 142.4, 140.0, 138.2, 138.6, 138.4, 137.2, 135.4, 128.3, 127.0, 123.3, 121.4, 119.2, 118.5, 118.4, 99.0 (br d, ¹J_{CH(cod)-Rh} = 8.1 Hz), 68.8 (br dd, ¹J_{CH(cod)-Rh} = 14.7 Hz), 38.3, 33.7, 33.4, 29.7, 29.3, 22.0, 21.9, 21.7 ppm. **UV-Vis** (DMSO): λ_{max} (log ε) = 419 (5.56), 515 (4.41), 548 (3.93), 591 (3.88), 646 (3.66) nm. **HRMS** (ESI⁺): *m/z* calc for C₆₆H₆₇ClN₆Rh⁺ [M+H]⁺: 1081.4165, found: 1081.4171.

Synthesis of Zn-A-Rh(cod)Cl. Porphyrin **Zn-A-Cl** (80.0 mg, 0.0856 mmol, 1 eq), [Rh(cod)Cl]₂ (29.6 mg, 0.060 mmol, 0.7eq), and *t*-BuOK (14.4 mg, 0.128 mmol, 1.5 eq) were degassed under argon for 10 min. Then, anhydrous THF (30 mL) was added and the reaction mixture was stirred at room temperature under argon atmosphere for 16 hours. Once finished according to TLC analysis, the solvent was evaporated and the residue was purified by silica gel column chromatography (eluent: CH₂Cl₂ to CH₂Cl₂/MeOH 95:5 (v:v)). Recrystallization from CH₂Cl₂/*n*-pentane afforded the porphyrin **Zn-A-Rh(cod)Cl** as a purple solid in 35% yield (34 mg, 0.0297 mmol).



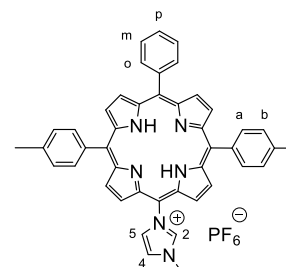
¹H NMR (600 MHz, CD₂Cl₂): δ 8.85 (d, ³J_{H,H} = 4.6 Hz, 2H, H_{β-pyr}), 8.72 (d, ³J_{H,H} = 4.6 Hz, 2H, H_{β-pyr}), 8.68 (s br, 4H, H_{β-pyr}), 8.22 (d, ³J_{H,H} = 7.9 Hz, 2H, H_o), 7.76 (d, ³J_{H,H} = 7.9 Hz, 2H, H_m), 7.29 (s, 6H, H_{mes meta}), 7.10 (d, ³J_{H,H} = 1.9 Hz, 1H, H₅), 7.03 (d, ³J_{H,H} = 1.9 Hz, 1H, H₄), 6.25 (d, ³J_{H,H} = 14.8 Hz, 1H, CH₂), 5.98 (d, ³J_{H,H} = 14.8 Hz, 1H, CH₂), 5.06–4.97 (m, 2H, CH_{cod}), 4.18 (s, 3H, N-CH₃), 3.51–3.44 (m, 2H, CH_{cod}), 2.61 (s, 9H, H_{methyl para}), 2.36–2.32 (m, 4H, CH₂ cod), 2.12–2.06 (m, 4H, CH₂ cod), 1.83 (2s, 18H, H_{methyl ortho}) ppm. **¹³C{¹H} NMR** (150.9 MHz, CD₂Cl₂) δ 183.5, (d, ¹J_{Rh,C} = 51.0 Hz) 143.0, 143.0, 142.93, 142.8, 141.3, 139.4, 138.3, 137.6, 137.5, 137.1, 134.5, 132.6, 132.0, 132.0, 131.9, 131.5, 128.2, 127.1, 123.2, 121.3, 118.4, 117.6, 117.4, 98.9 (br dd, ¹J_{CH(cod)-Rh} = 3.5 and 7.1 Hz), 68.8 (br dd, ¹J_{CH(cod)-Rh} = 7.4 and 17.8 Hz), 38.2, 33.7, 33.3, 30.2, 29.6, 29.3, 28.5, 21.6, 21.6 ppm. **UV-Vis** (DMSO): λ_{max} (log ε) = 420 (5.66), 549 (4.23), 576 (3.38) nm. **HRMS** (ESI⁺): *m/z* calc for C₆₆H₆₄N₆RhZn⁺ [M-Cl]⁺: 1107.3533, found: 1107.3541.

Synthesis of Ni-A-Rh(cod)Cl. Porphyrin **Ni-A-Cl** (80.0 mg, 0.0862 mmol, 1 eq), [Rh(cod)Cl]₂ (29.8 mg, 0.060 mmol, 0.7 eq), and *t*-BuOK (14.5 mg, 0.129 mmol, 1.5 eq) were degassed under argon for 10 min. Then, anhydrous THF (30 mL) was added and the reaction mixture was stirred at room temperature under argon atmosphere for 16 hours. Once finished according to TLC analysis, solvent was evaporated and the residue was purified by silica gel column chromatography (eluent: CH₂Cl₂ to CH₂Cl₂/MeOH 95:5 (v:v)). Recrystallization from CH₂Cl₂/*n*- afforded the porphyrin **Ni-A-Rh(cod)Cl** as a purple solid in 38% yield (37 mg, 0.0325 mmol).



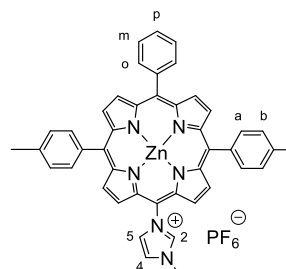
¹H NMR (600 MHz, CD₂Cl₂): δ 8.70 (d, ³J_{H,H} = 4.8 Hz, 2H, H_{β-pyr}), 8.56 (d, ³J_{H,H} = 4.8 Hz, 2H, H_{β-pyr}), 8.54 (s, 4H, H_{β-pyr}), 8.02 (d, ³J_{H,H} = 8.0 Hz, 2H, H_o), 7.71 (d, ³J_{H,H} = 8.0 Hz, 2H, H_m), 7.22 (s, 6H, H_{mes meta}), 7.03 (d, ³J_{H,H} = 1.8 Hz, 1H, H₅), 7.00 (d, ³J_{H,H} = 1.8 Hz, 1H, H₄), 6.24 (d, ³J_{H,H} = 14.8 Hz, 1H, CH₂), 5.90 (d, ³J_{H,H} = 14.8 Hz, 1H, CH₂), 5.06–4.98 (m, 2H, CH_{cod}), 4.16 (s, 3H, N-CH₃), 3.49–3.40 (m, 2H, CH_{cod}), 2.55 (2s, 9H, H_{methyl para}), 2.47–2.40 (m, 4H, CH_{2 cod}), 2.07–1.94 (m, 4H, CH_{2 cod}), 1.80 (s, 18H, H_{methyl ortho}) ppm. ¹³C{¹H} NMR (150.9 MHz, CD₂Cl₂): δ 183.6, (d, ¹J_{Rh,C} = 51.2 Hz) 150.3, 150.3, 143.2, 139.7, 139.7, 138.0, 136.8, 135.2, 132.5, 131.51, 131.4, 130.9, 129.1, 128.1, 126.7, 123.2, 121.4, 120.0, 119.2, 119.1, 98.9 (br dd, ¹J_{CH(cod)-Rh} = 6.8 Hz), 68.8 (br dd, ¹J_{CH(cod)-Rh} = 13.1 and 17.5 Hz), 38.2, 33.7, 33.4, 29.6, 29.3, 28.5, 25.1, 22.0, 21.9, 21.7 ppm. **UV-Vis** (DMSO): λ_{max} (log ε) = 420 (5.68), 527(4.13), 555 (3.46) nm. **HRMS** (ESI⁺): *m/z* calc for C₆₆H₆₄N₆NiRh⁺ [M-Cl]⁺: 1101.3595, found: 1101.3571.

Synthesis of porphyrin 2H-C-PF₆. Porphyrin **2H-3** (152 mg, 0.240 mmol, 1 eq) was dissolved in dry THF (40 mL) under argon atmosphere. Then, iodomethane (1.50 mL, 24.02 mmol, 100 eq) was added and the reaction mixture was stirred at 40°C for 16 hours under argon atmosphere. Once finished according to TLC analysis, a solution of KPF₆ (221 mg, 1.20 mmol, 5 eq) in water (10 mL) was added dropwise and the reaction was stirred at room temperature for 2 hours. Then, the mixture was concentrated and the resulting solid was filtered off and washed with *n*-pentane to give porphyrin **2H-C-PF₆** as a purple solid in 96% yield (182 mg, 0.229 mmol).



¹H NMR (400 MHz, CD₂Cl₂): δ 9.37 (s br, 1H, H₂), 9.07 (d, ³J_{H,H} = 4.7 Hz, 2H, H_{β-pyr}), 8.92 (d, ³J_{H,H} = 4.7 Hz, 2H, H_{β-pyr}), 8.89 (d, ³J_{H,H} = 4.7 Hz, 2H, H_{β-pyr}), 8.72 (d, ³J_{H,H} = 4.8 Hz, 2H, H_{β-pyr}), 8.42 (s br, 1H, H₅), 8.20 (d, ³J_{H,H} = 7.1 Hz, 2H, H_o), 8.14-8.05 (m, 4H, H_a), 7.93 (s br, 1H, H₄), 7.87-7.76 (m, 3H, H_m and H_p), 7.65-7.60 (m, 4H, H_b), 4.47 (s, 3H, N-CH₃), 2.71 (s, 6H, CH_{3 tolyl}), -2.85 (s, 2H, NH) ppm. ¹³C{¹H} NMR (150.9 MHz, DMSO-*d*₆): δ 142.5, 140.9, 137.8, 137.5, 134.4, 134.3, 130.2, 128.5, 127.9, 127.1, 123.3, 123.0, 121.8, 108.7, 36.8, 21.1 ppm. ¹⁹F NMR (376.5 MHz, CD₂Cl₂): δ -73.8 ppm (d, ¹J_{F,P} = 711.2 Hz). ppm. **UV-Vis** (DMSO): λ_{max} (log ε) = 418 (5.64), 514 (4.26), 549 (3.79), 586 (3.77), 641 (3.47) nm. **MS** (ESI⁺): *m/z* calc for C₄₄H₃₅N₆⁺ [M-PF₆]⁺: 647.29, found 647.29. **MS** (ESI⁻): *m/z* calc for PF₆⁻: 144.96, found 144.97.

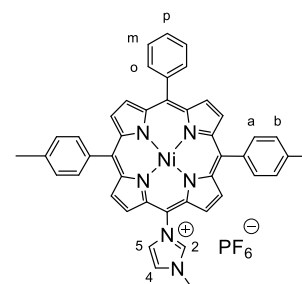
Synthesis of porphyrin Zn-C-PF₆. Porphyrin **Zn-3** (142 mg, 0.204 mmol, 1 eq) was dissolved in dry THF (40 mL) under argon atmosphere. Then, iodomethane (1.30 mL, 20.40 mmol, 100 eq) was added and the reaction mixture was stirred at 40°C for 16 hours under argon atmosphere. Once finished according to TLC analysis, a solution of KPF₆ (188 mg, 1.02 mmol, 5 eq) in water (10 mL) was added dropwise and the reaction was stirred at room temperature for 2 hours. Then, the mixture was concentrated and the resulting solid was filtered off and washed with *n*-pentane to give porphyrin **Zn-C-PF₆** as a purple solid in 90% yield (158 mg, 0.184 mmol).



¹H NMR (400 MHz, CD₂Cl₂): δ 9.41 (s br, 1H, H₂), 9.13 (d, ³J_{H,H} = 4.7 Hz, 2H, H_{β-pyr}), 8.99 (d, ³J_{H,H} = 4.7 Hz, 2H, H_{β-pyr}), 8.97 (d, ³J_{H,H} = 4.7 Hz, 2H, H_{β-pyr}), 8.77 (d, ³J_{H,H} = 4.7 Hz, 2H, H_{β-pyr}), 8.44 (s br, 1H, H₅), 8.21–8.17 (m, 2H, H_o), 8.13-8.00 (m, 4H, H_a), 7.91 (s br, 1H, H₄), 7.86–7.74 (m, 3H, H_m and H_p), 7.64–7.55 (m, 4H, H_b), 4.47 (s, 3H, N-CH₃), 2.72 (s, 6H, CH_{3 tolyl}) ppm. ¹³C{¹H} NMR (125.7 MHz, CD₂Cl₂): δ 165.8, 152.2, 151.4, 151.1, 147.1, 142.7, 141.0, 139.4, 138.3, 135.3, 135.1, 135.0, 134.9, 133.6, 133.2, 131.0, 130.1, 128.4, 128.0, 127.2, 126.6, 123.9, 123.2, 108.0, 63.5, 38.0, 30.2, 21.8 ppm.

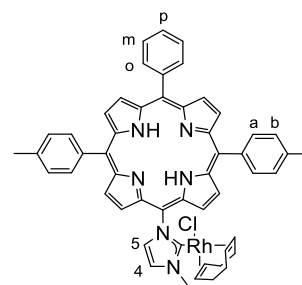
¹⁹F NMR (376.5 MHz, CD₂Cl₂): δ -72.8 ppm (d, ¹J_{F,P} = 707.8 Hz) ppm. **UV-Vis** (DMSO): λ_{max} (log ε) = 427 (5.66), 557(4.25), 600 (3.77) nm. **MS** (ESI+): *m/z* calc for C₄₄H₃₃N₆Zn⁺ [M-PF₆]⁺: 709.21, found: 709.16. **MS** (ESI-): *m/z* calc for PF₆⁻: 144.96, found 144.97.

Synthesis of porphyrin Ni-C-PF₆. Porphyrin Ni-3 (154 mg, 0.223 mmol, 1 eq) was dissolved in dry THF (40 mL) under argon atmosphere. Then, iodomethane (1.39 mL, 22.34 mmol, 100 eq) was added and the reaction mixture was stirred at 40°C for 16 hours under argon atmosphere. Once finished according to TLC analysis, a solution of KPF₆ (205.6 mg, 1.12 mmol, 5 eq) in water (10 mL) was added dropwise and the reaction mixture was stirred at room temperature for 2 hours. Then, the mixture was concentrated and the resulting solid was filtered off and washed with *n*-pentane to give porphyrin Ni-C-PF₆ as a purple solid in 92% yield (174 mg, 0.205 mmol). **¹H**

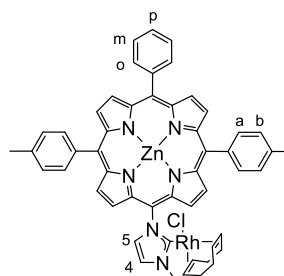


NMR (500 MHz, CD₂Cl₂): δ 9.78 (s br, 1H, H₂), 8.94 (d, ³J_{H,H} = 5.0 Hz, 2H, H_{β-pyr}), 8.81 (d, ³J_{H,H} = 5.0 Hz, 2H, H_{β-pyr}), 8.79 (d, ³J_{H,H} = 5.0 Hz, 2H, H_{β-pyr}), 8.67 (d, ³J_{H,H} = 5.0 Hz, 2H, H_{β-pyr}), 8.20 (t, ³J_{H,H} = 1.8 Hz, ⁴J_{H,H} = 1.8 Hz, 1H, H_δ), 8.01 (d, ³J_{H,H} = 6.6 Hz, 2H, H_o), 7.91 (t, ³J_{H,H} = 1.8 Hz, ⁴J_{H,H} = 1.8 Hz, 1H, H₄), 7.88 (d, ³J_{H,H} = 7.3 Hz, 4H, H_a), 7.79–7.68 (m, 3H, H_m and H_p), 7.53 (d, ³J_{H,H} = 7.3 Hz, 4H, H_b), 4.50 (s, 3H, N-CH₃), 2.65 (s, 6H, CH₃ tolyl) ppm. **¹³C{¹H} NMR** (125.7 MHz, CD₂Cl₂): δ 145.1, 144.5, 144.2, 141.03, 140.8, 140.5, 138.9, 137.6, 135.5, 134.3, 133.9, 133.6, 130.0, 128.8, 128.4, 127.6, 127.3, 123.9, 122.1, 38.70, 27.5, 21.8 ppm. **¹⁹F NMR** (376.5 MHz, CD₂Cl₂): δ -72.8 ppm (d, ¹J_{F,P} = 711.2 Hz). **UV-Vis** (DMSO): λ_{max} (log ε) = 413 (4.91), 526 (3.74), 555 (3.34) nm. **MS** (ESI+): *m/z* calc for C₄₄H₃₃N₆Ni [M-PF₆]⁺: 703.21, found 703.21. **MS** (ESI-): *m/z* calc for PF₆⁻: 144.96, found 144.97.

Synthesis of porphyrin H2-C-Rh(cod)Cl. Porphyrin 2H-C-PF₆ (103 mg, 0.1299 mmol, 1 eq), [Rh(cod)Cl]₂ (52.8 mg, 0.1071 mmol, 0.8 eq) and *t*-BuOK (17.5 mg, 0.1559 mmol, 1.2 eq) were degassed under argon for 10 min. Then, anhydrous THF (45 mL) was added and the reaction mixture was stirred at room temperature under argon atmosphere for 16 hours. Once finished according to TLC analysis, the solvent was evaporated and the residue was purified by silica gel column chromatography (eluent: CH₂Cl₂ to CH₂Cl₂/MeOH 98:2 (v:v)). The first red fraction was collected and concentrated to give porphyrin Ni-C-Rh(cod)Cl a purple solid in 61% yield (71 mg, 0.0795 mmol). **¹H NMR** (600 MHz, CD₂Cl₂): δ 9.72 (d, ³J_{H,H} = 4.9 Hz, 1H, H_{β-pyr}), 8.99 (d, ³J_{H,H} = 4.9 Hz, 1H, H_{β-pyr}), 8.91 (d, ³J_{H,H} = 4.7 Hz, 1H, H_{β-pyr}), 8.89 (d, ³J_{H,H} = 4.7 Hz, 1H, H_{β-pyr}), 8.86 (d, ³J_{H,H} = 4.8 Hz, 1H, H_{β-pyr}), 8.82 (d, ³J_{H,H} = 4.7 Hz, 1H, H_{β-pyr}), 8.81 (d, ³J_{H,H} = 4.7 Hz, 1H, H_{β-pyr}), 8.48 (d, ³J_{H,H} = 4.8 Hz, 1H, H_{β-pyr}), 8.24–8.18 (m br, 3H, 2H_o+1H_a), 8.11–8.05 (m br, 3H, H_a), 8.00 (d, ³J_{H,H} = 1.8 Hz, 1H, H_δ), 7.84–7.74 (m, 3H, 2H_m+1H_p), 7.63 (d br, ³J_{H,H} = 8.2 Hz, 1H, H_b), 7.58 (d, ³J_{H,H} = 8.2 Hz, 3H, H_b), 7.42 (d, ³J_{H,H} = 1.8 Hz, H₄), 4.62 (m, 1H, H_{cod}), 4.57 (s, 3H, N-CH₃), 4.32 (m, 1H, H_{cod}), 3.63 (m, 1H, H_{cod}), 2.71 (2s, 6H, CH₃ tolyl), 2.37 (m, 1H, H_{cod}), 1.94 (m, 1H, H_{cod}), 1.72 (m, 1H, H_{cod}), 1.62 (m, 1H, H_{cod}), 1.20 (m, 1H, H_{cod}), 0.82–0.75 (m, 1H, H_{cod}), 0.20 (m, 1H, H_{cod}), 0.00 (m, 1H, H_{cod}), -1.04 (m, 1H, H_{cod}), -2.67 (s, 2H, NH) ppm. **¹³C{¹H} NMR** (150.9 MHz, CD₂Cl₂): δ 189.4 (d, ¹J_{Rh,C} = 51.2 Hz), 142.5, 139.2, 138.4, 135.2, 135.1, 135.0, 130.9, 128.5, 128.3, 128.1, 127.3, 122.4, 121.9, 121.8, 121.5, 115.4, 97.5 (d, ¹J_{CH(cod)-Rh} = 6.6 Hz), 97.2 (d, ¹J_{CH(cod)-Rh} = 7.0 Hz), 68.5 (d, ¹J_{CH(cod)-Rh} = 14.4 Hz), 66.8 (d, ¹J_{CH(cod)-Rh} = 13.8 Hz), 39.7, 35.2, 29.9, 29.0, 27.6, 21.8 ppm. **UV-Vis** (DMSO): λ_{max} (log ε) = 418 (5.14), 520 (4.26), 593 (3.83), 649 (3.49) nm. **HRMS** (ESI+): *m/z* calc for C₅₂H₄₆N₆Rh [M-Cl]⁺: 857.2833, found 857.2849.

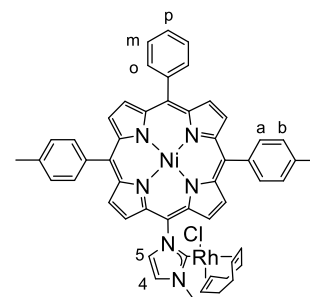


Synthesis of porphyrin Zn-C-Rh(cod)Cl. Porphyrin Zn-C-PF₆ (101 mg, 0.1180 mmol, 1 eq), [Rh(cod)Cl]₂ (48.0 mg, 0.0973 mmol, 0.8 eq) and *t*-BuOK (15.9 mg, 0.1417 mmol, 1.2 eq) were degassed under argon for 10 min. Then, anhydrous THF (45 mL) was added and the reaction mixture was stirred at room temperature under argon atmosphere for 16 hours. Once finished according to TLC analysis, the solvent was evaporated and the residue was purified by silica gel column chromatography (eluent: CH₂Cl₂ to CH₂Cl₂/MeOH 98:2 (v:v)). The first red fraction was collected and



concentrated to give a purple solid in 66% yield (75 mg, 0.0784 mmol). **¹H NMR** (600 MHz, CD₂Cl₂): δ 9.63 (d br, ³J_{H,H} = 4.7 Hz, 1H, H_{β-pyrr}), 9.00 (d, ³J_{H,H} = 4.7 Hz, 1H, H_{β-pyrr}), 8.99 (d, ³J_{H,H} = 4.7 Hz, 1H, H_{β-pyrr}), 8.96-8.93 (m, 4H, H_{β-pyrr}), 8.62 (d, ³J_{H,H} = 4.7 Hz, 1H, H_{β-pyrr}), 8.24-8.19 (m br, 3H, H_o+H_a), 8.13-8.03 (2m br, 3H, H_a), 7.99 (s, ³J_{H,H} = 1.9 Hz, 1H, H₅), 7.81-7.77 (m, 3H, H_m+H_p), 7.63-7.57 (m br, 4H, H_b), 7.43 (d, ³J_{H,H} = 1.9 Hz, 1H, H₄), 4.61 (m, 1H, H_{cod}), 4.58 (s, 3H, N-CH₃), 4.21 (m, 1H, H_{cod}), 3.64 (m, 1H, H_{cod}), 2.70 (s, 6H, CH_{3 tolyl}), 2.37 (m, 1H, H_{cod}), 2.00–1.86 (m, 2H, 2H_{cod}), 1.67–1.56 (m, 1H, H_{cod}), 1.14-1.09 (m, 1H, H_{cod}), 0.51 (m, 1H, H_{cod}), 0.28 (m, 1H, H_{cod}), 0.09 (m, 1H, H_{cod}), -0.89 (m, 1H, H_{cod}) ppm. **¹³C{¹H} NMR** (125.7 MHz, CD₂Cl₂): δ 188.6 (br d, ¹J_{Rh,C} = 63.4 Hz), 152.4, 151.8, 151.1, 150.7, 150.5, 150.3, 143.1, 140.0, 138.0, 135.0, 134.9, 133.5, 133.4, 132.9, 132.7, 132.6, 132.5, 130.9, 128.1, 128.0, 127.8, 127.1, 121.1, 97.1 (br d, ¹J_{CH(cod)-Rh} = 29.8 Hz, 2 CH(cod)), 68.4 (d, ¹J_{CH(cod)-Rh} = 17.1 Hz), 66.9 (d, ¹J_{CH(cod)-Rh} = 12.7 Hz), 39.5, 35.0, 31.4, 28.8, 27.7, 21.7 ppm. **UV-Vis** (DMSO): λ_{max} (log ε) = 413 (5.14), 532 (4.20), 560 (3.82) nm. **HRMS** (ESI+): *m/z* calc for C₅₂H₄₆N₆Rh [M-Cl]⁺: 919.1962, found 919.1968.

Synthesis of porphyrin Ni-C-Rh(cod)Cl. Porphyrin Ni-C-PF₆ (122 mg, 0.1436 mmol, 1 eq), [Rh(cod)Cl]₂ (53.1 mg, 0.1077 mmol, 0.75 eq) and *t*BuOK (20.7 mg, 0.1844 mmol, 1.3 eq) were degassed under argon for 10 min. Then, anhydrous THF (45 mL) was added and the reaction mixture was stirred at room temperature under argon atmosphere for 16 hours. Once finished according to TLC analysis, the solvent was evaporated and the residue was purified by silica gel column chromatography (eluent: CH₂Cl₂ to CH₂Cl₂/MeOH 98:2 (v:v)). The first red fraction was collected and concentrated to give porphyrin Ni-C-Rh(cod)Cl a purple solid in 72% yield



(99 mg, 0.1042 mmol). **¹H NMR** (600 MHz, CD₂Cl₂): δ 9.49 (d, ³J_{H,H} = 5.0 Hz, 1H, H_{β-pyrr}), 8.84 (d, ³J_{H,H} = 5.0 Hz, 1H, H_{β-pyrr}), 8.81 (d, ³J_{H,H} = 4.9 Hz, 1H, H_{β-pyrr}), 8.78 (d, ³J_{H,H} = 4.9 Hz, 1H, H_{β-pyrr}), 8.76 (d, ³J_{H,H} = 4.9 Hz, 1H, H_{β-pyrr}), 8.76 (s, 2 H_{β-pyrr}), 8.44 (d, ³J_{H,H} = 4.9 Hz, 1H, H_{β-pyrr}), 8.04 (d br, ³J_{H,H} = 7.1 Hz, 2H, H_o), 7.92 (d, ³J_{H,H} = 1.9 Hz, 1H, H₅) 7.95–7.85 (m, 4H, H_a), 7.76–7.68 (m, 3H, 2H_m and 1H_p), 7.55–7.50 (m, 4H, H_b), 7.37 (d, ³J_{H,H} = 1.8 Hz, 1H, H₄), 4.56 (m, 1H, H_{cod}), 4.48 (s, 3H, N-CH₃), 4.26 (m, 1H, H_{cod}), 3.53 (m, 1H, H_{cod}), 2.65 (2s, 3+3H, CH_{3 tolyl}), 2.33 (m, 1H, H_{cod}), 1.95 (m, 1H, H_{cod}), 1.63 (m, 2H, 2H_{cod}), 1.26 (m, 1H, H_{cod}), 0.85 (m, 1H, H_{cod}), 0.37 (m, 1H, H_{cod}), 0.20 (m, 1H, H_{cod}), -0.62 (m, 1H, H_{cod}) ppm. **¹³C{¹H} NMR** (150.9 MHz, CD₂Cl₂): δ 189.3 (d, ¹J_{Rh,C} = 51.3 Hz), 145.2, 144.7, 144.1, 143.5, 143.6, 143.6, 143.5, 142.6, 141.3, 138.4, 138.2, 134.2, 134.2, 133.9, 133.7, 133.1, 132.9, 132.8, 132.7, 130.0, 128.5, 128.3, 128.2, 128.1, 127.5, 121.7, 121.1, 120.9, 120.6, 115.8, 97.6 (d, ¹J_{CH(cod)-Rh} = 8.0 Hz), 97.3 (d, ¹J_{CH(cod)-Rh} = 8.0 Hz), 68.3 (d, ¹J_{CH(cod)-Rh} = 16.0 Hz), 66.8 (d, ¹J_{CH(cod)-Rh} = 15.1 Hz), 39.5, 35.0, 30.3, 29.0, 27.8, 21.8 ppm. **UV-Vis** (DMSO): λ_{max} (log ε) = 413 (5.17), 532 (4.20), 560 (3.82) nm. **HRMS** (ESI+): *m/z* calc for C₅₂H₄₄N₆NiRh [M-Cl]⁺: 913.2030 found 913.2034.

Synthesis of complexes M¹-Rh-(CO)₂Cl. Rhodium(I) complexes M¹-A-Rh(cod)Cl, M¹-B-Rh(cod)Cl and M¹-C-Rh(cod)Cl were dissolved and stirred in CH₂Cl₂ (10⁻³ M in 5 mL). Then, carbon monoxide was bubbled through the solutions for 15 minutes and the corresponding rhodium(I) complexes M¹-A-Rh(CO)₂Cl, M¹-B-Rh(CO)₂Cl and M¹-C-Rh(CO)₂Cl were obtained. These complexes were not isolated and aliquots of the reaction mixtures were sampled for IR spectroscopy analyses. Carbonyl stretching frequencies were found to be in the range 2080-2082 and 2000-2002 cm⁻¹. These data are in agreement with those reported in the literature for known complexes of the type *cis*-[(NHC)RhCl(CO)₂].⁸

Spectra of new compounds

Porphyrin 2H-A-Cl

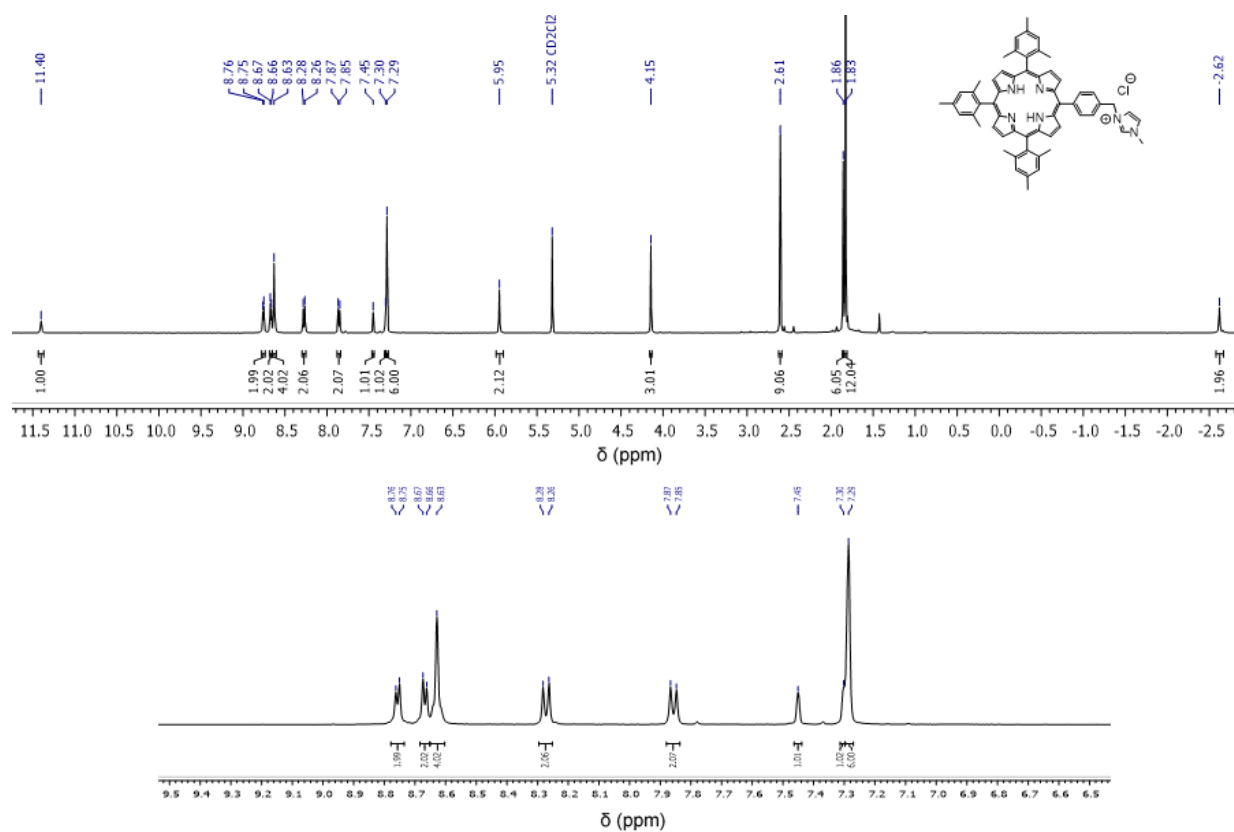


Figure S1. Full range (top) and partial (bottom) ^1H NMR spectrum (500 MHz, CD_2Cl_2) of 2H-A-Cl

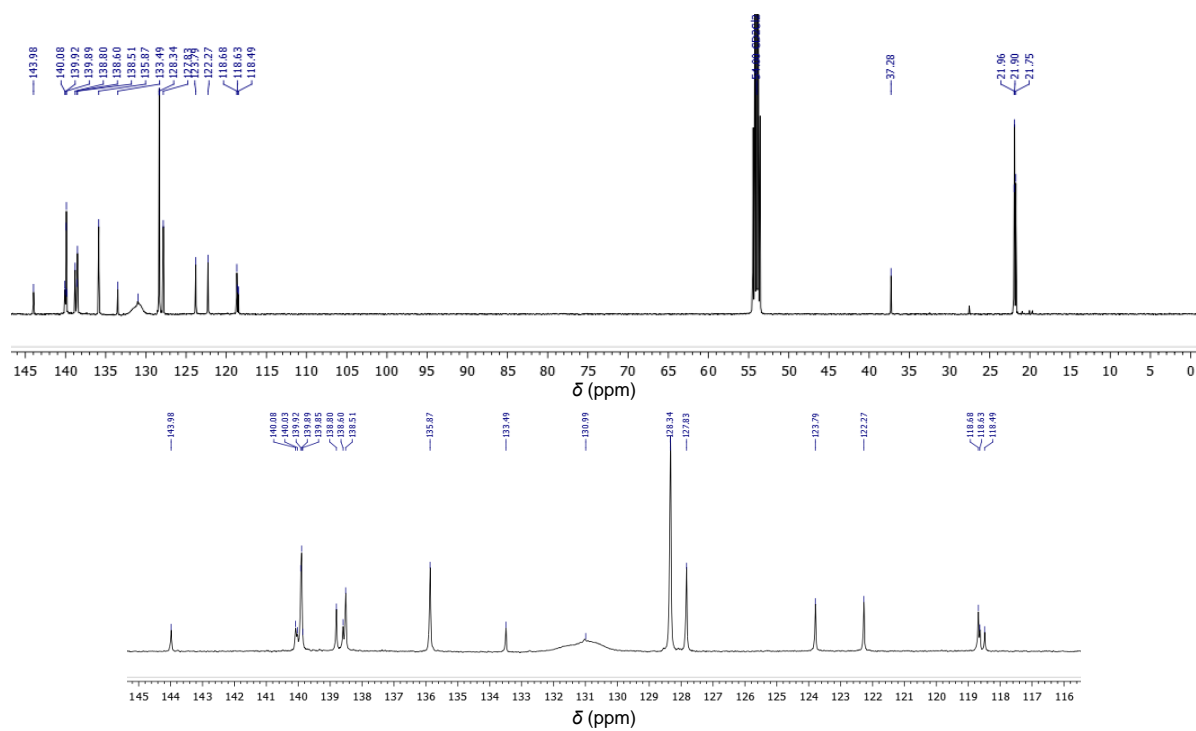


Figure S2. Full range (top) and partial (bottom) $^{13}\text{C}\{^1\text{H}\}$ NMR spectrum (125.7 MHz, CD_2Cl_2) of 2H-A-Cl

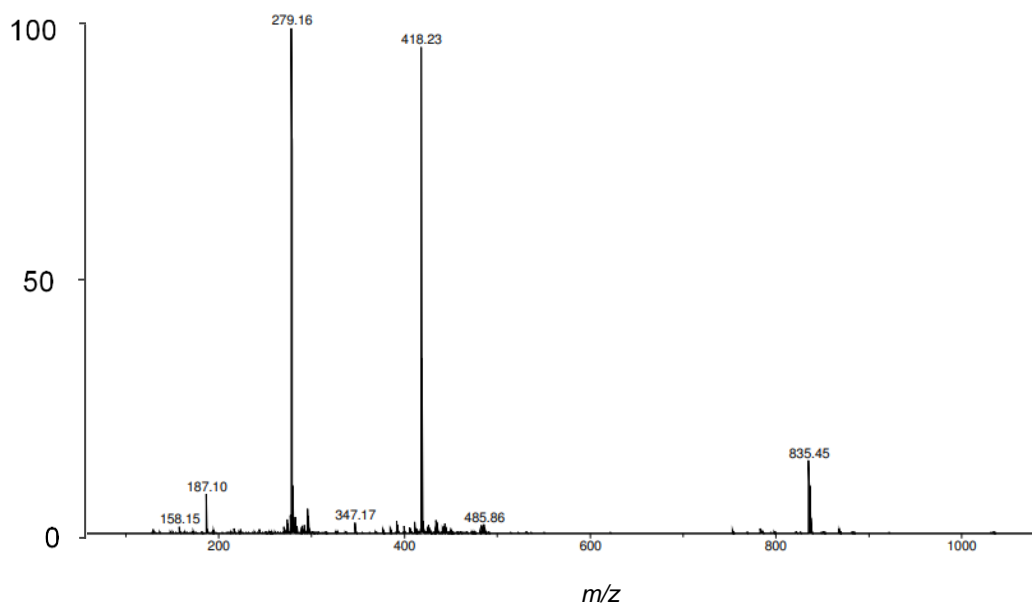


Figure S3. ESI-TOF (positive mode) mass spectrum of **2H-A-Cl**

Porphyrin Zn-A-Cl

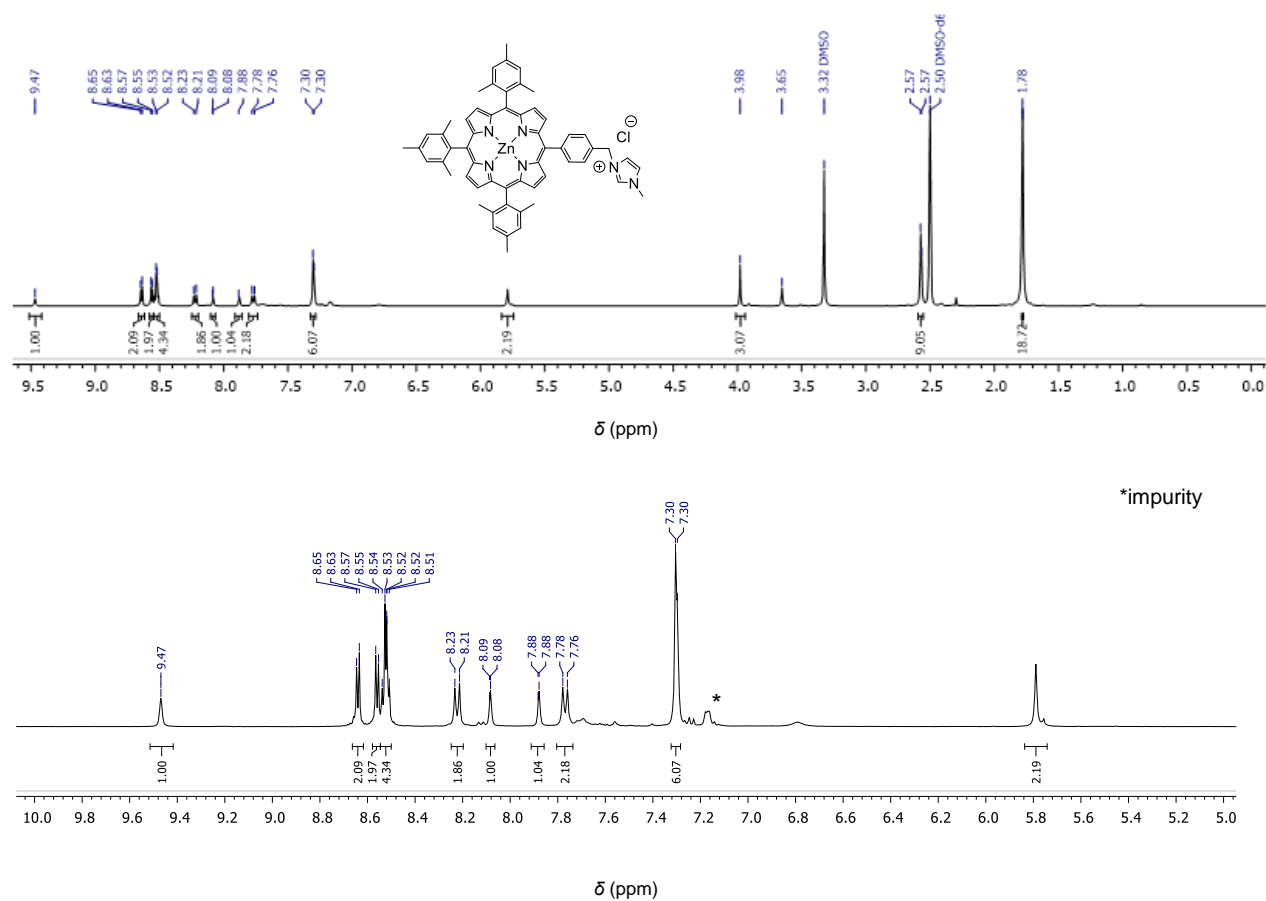


Figure S4. Full range (top) and partial (bottom) ^1H NMR spectrum (400 MHz, CD_2Cl_2) of **Zn-A-Cl**

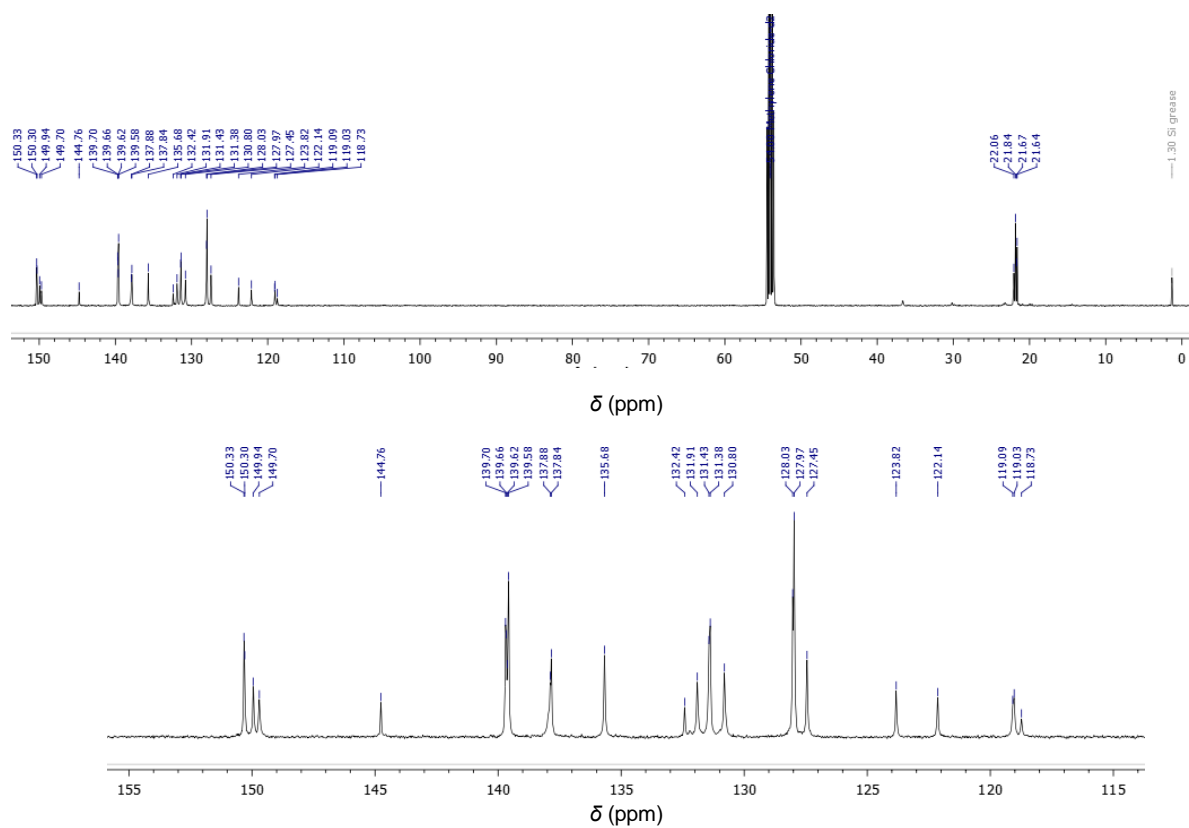


Figure S5. Full range (top) and partial (bottom) $^{13}\text{C}\{^1\text{H}\}$ NMR spectrum (125.7 MHz, CD_2Cl_2) of Zn-A-Cl

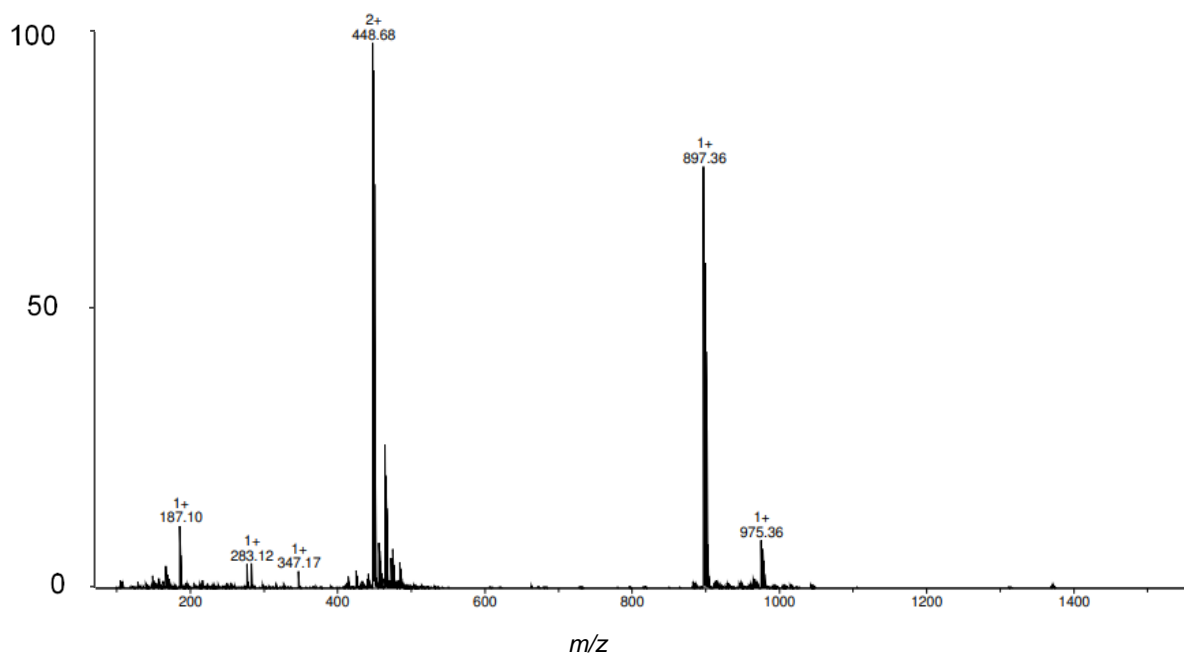
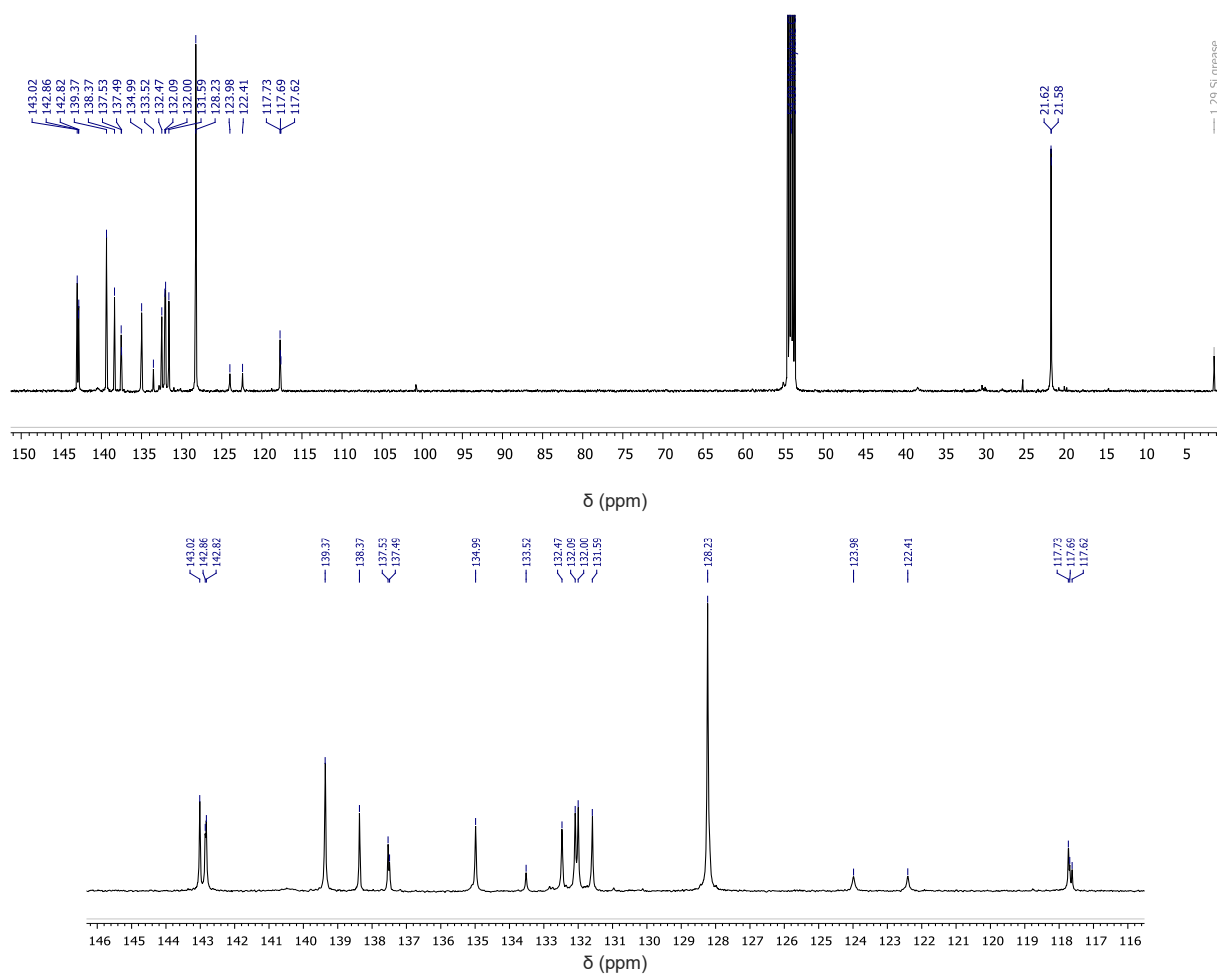
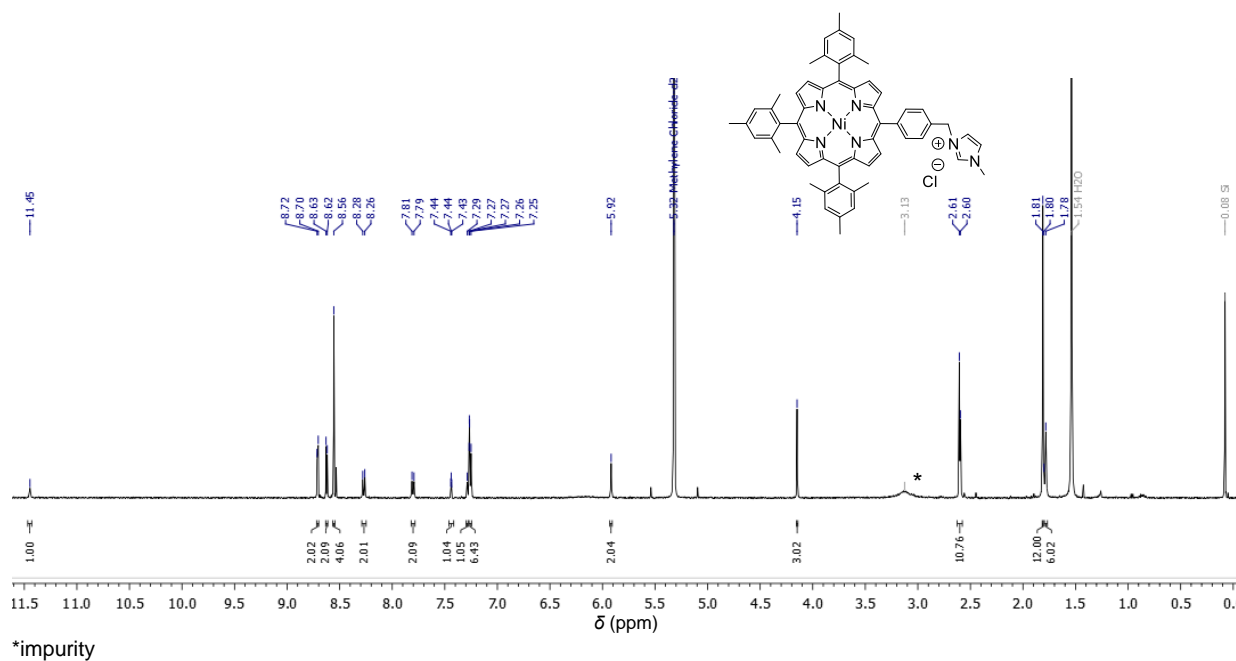


Figure S6. ESI-TOF (positive mode) mass spectrum of Zn-A-Cl

Porphyrin Ni-A-Cl



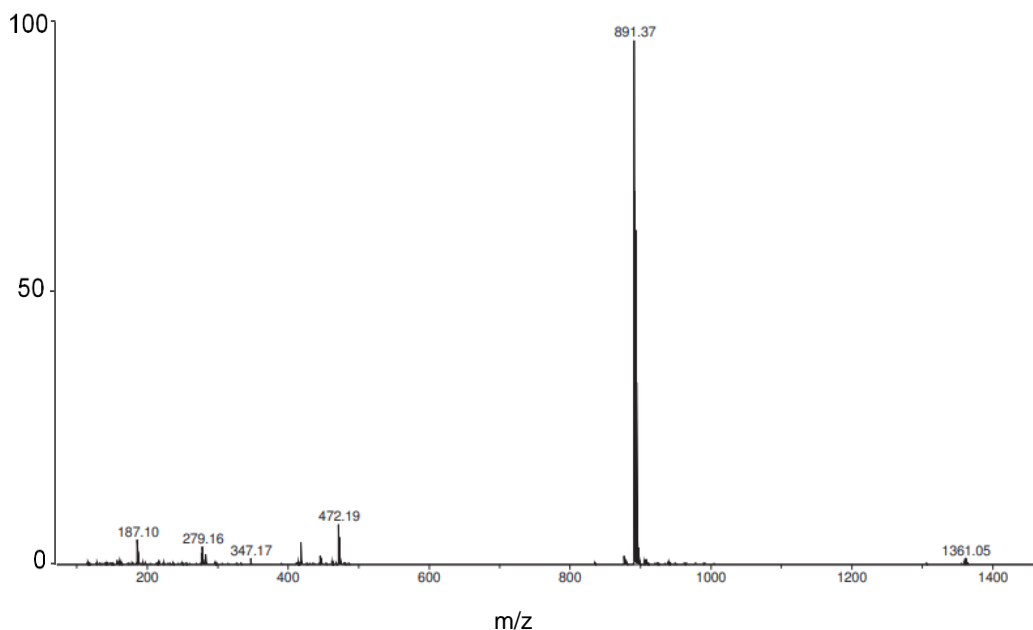


Figure S9. ESI-TOF (positive mode) mass spectrum of Ni-A-Cl

Porphyrin 2H-A-Rh(cod)Cl

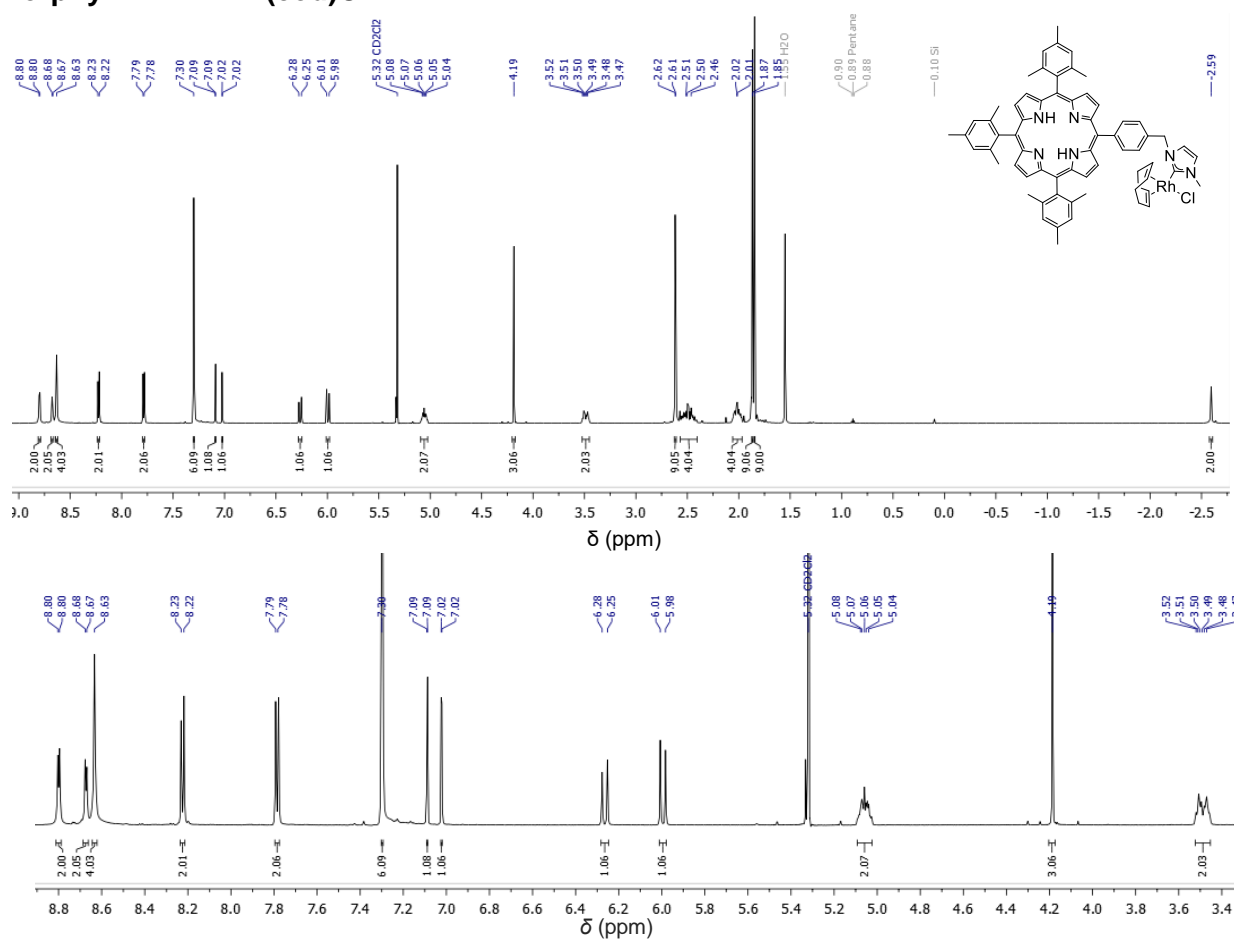


Figure S10. Full range (top) and partial (bottom) ^1H NMR spectrum (400 MHz, CD_2Cl_2) of 2H-A-Rh(cod)Cl

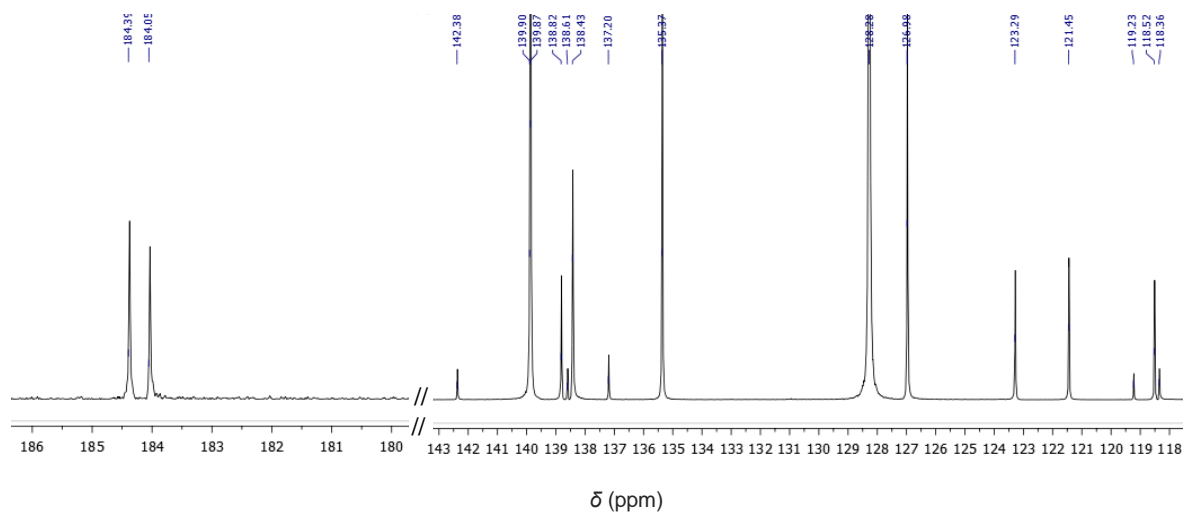
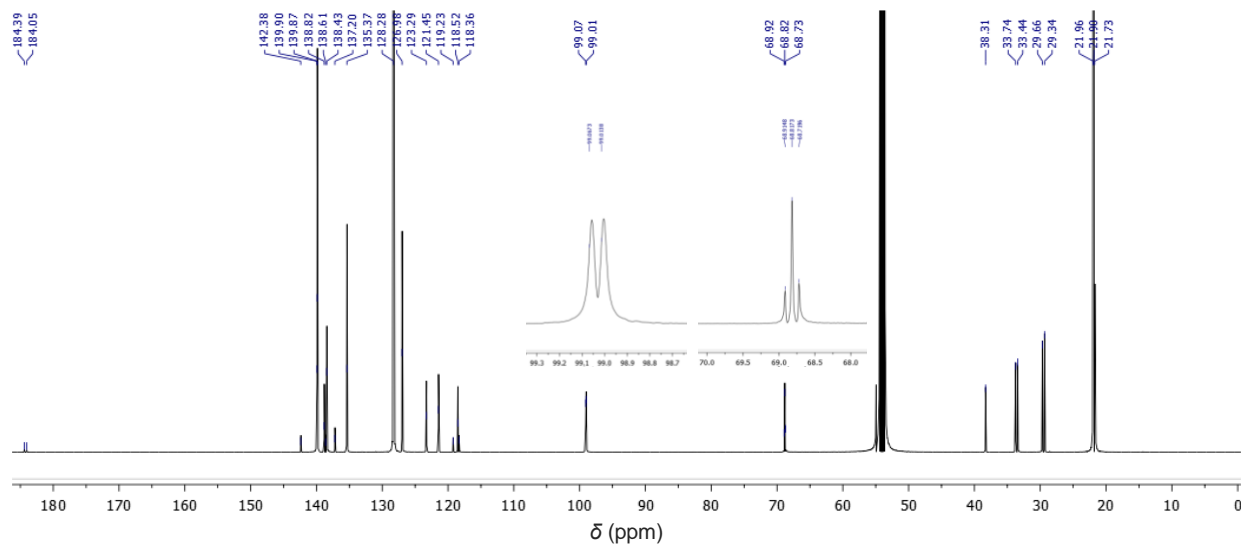


Figure S11. Full range (top) and partial (bottom) $^{13}\text{C}\{^1\text{H}\}$ NMR spectrum (150.9 MHz, CD_2Cl_2) of **2H-A-Rh(cod)Cl**

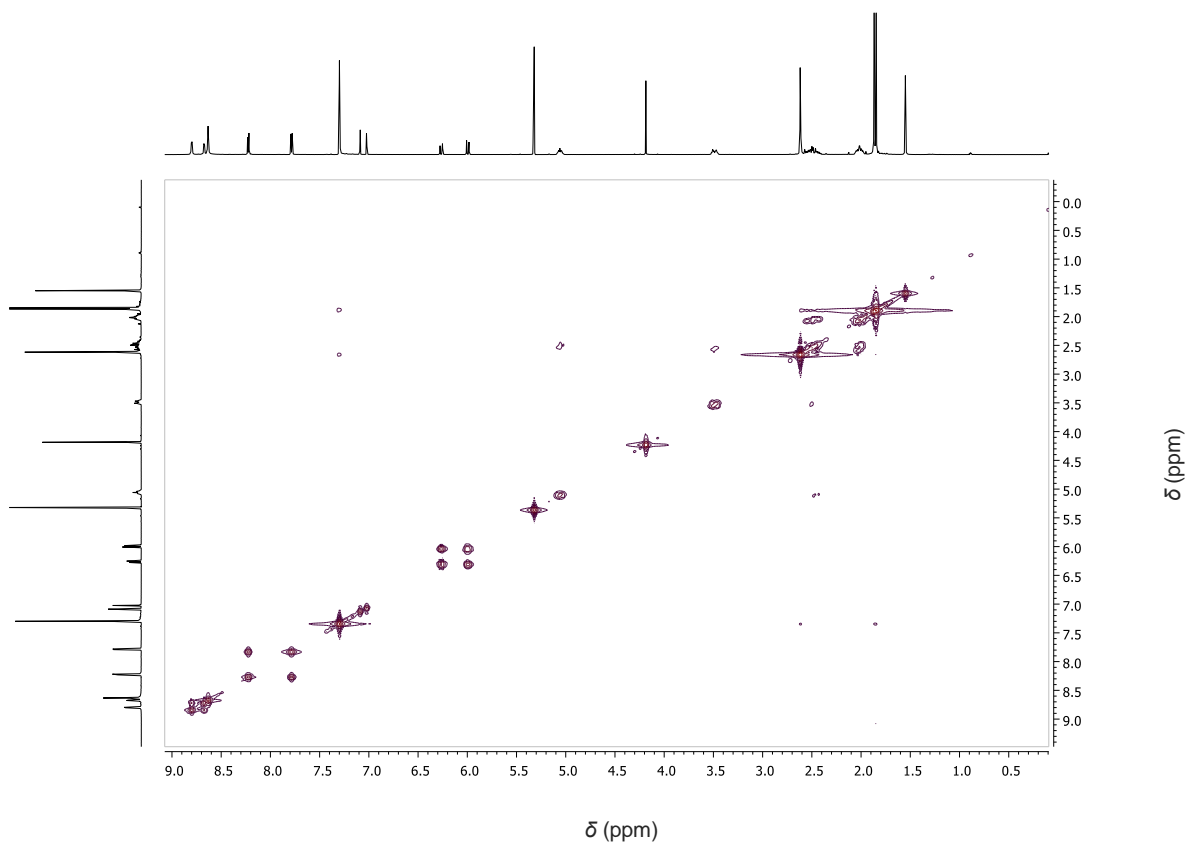


Figure S12. ^1H - ^1H COSY NMR spectrum (600 MHz, CD_2Cl_2) of **2H-A-Rh(cod)Cl**

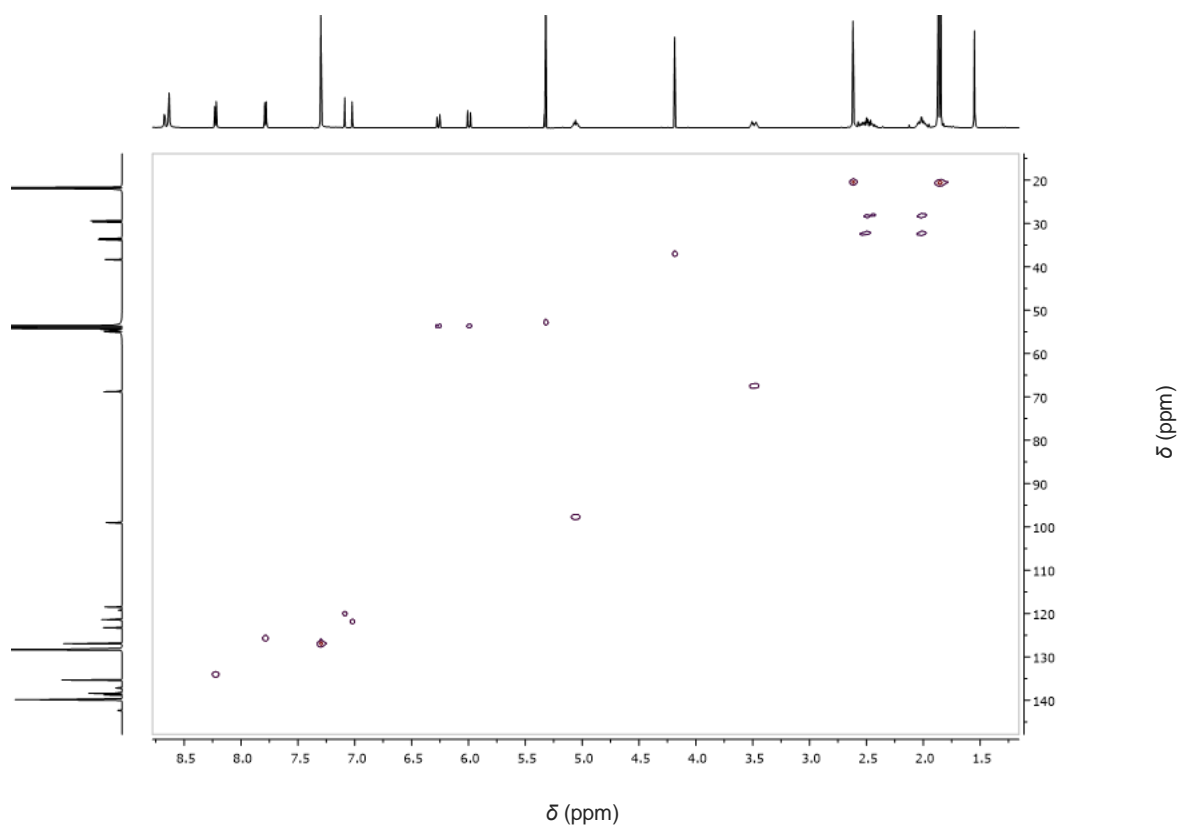


Figure S13. ^1H - $^{13}\text{C}\{^1\text{H}\}$ HSQC NMR spectrum (600 MHz, CD_2Cl_2) of **2H-A-Rh(cod)Cl**

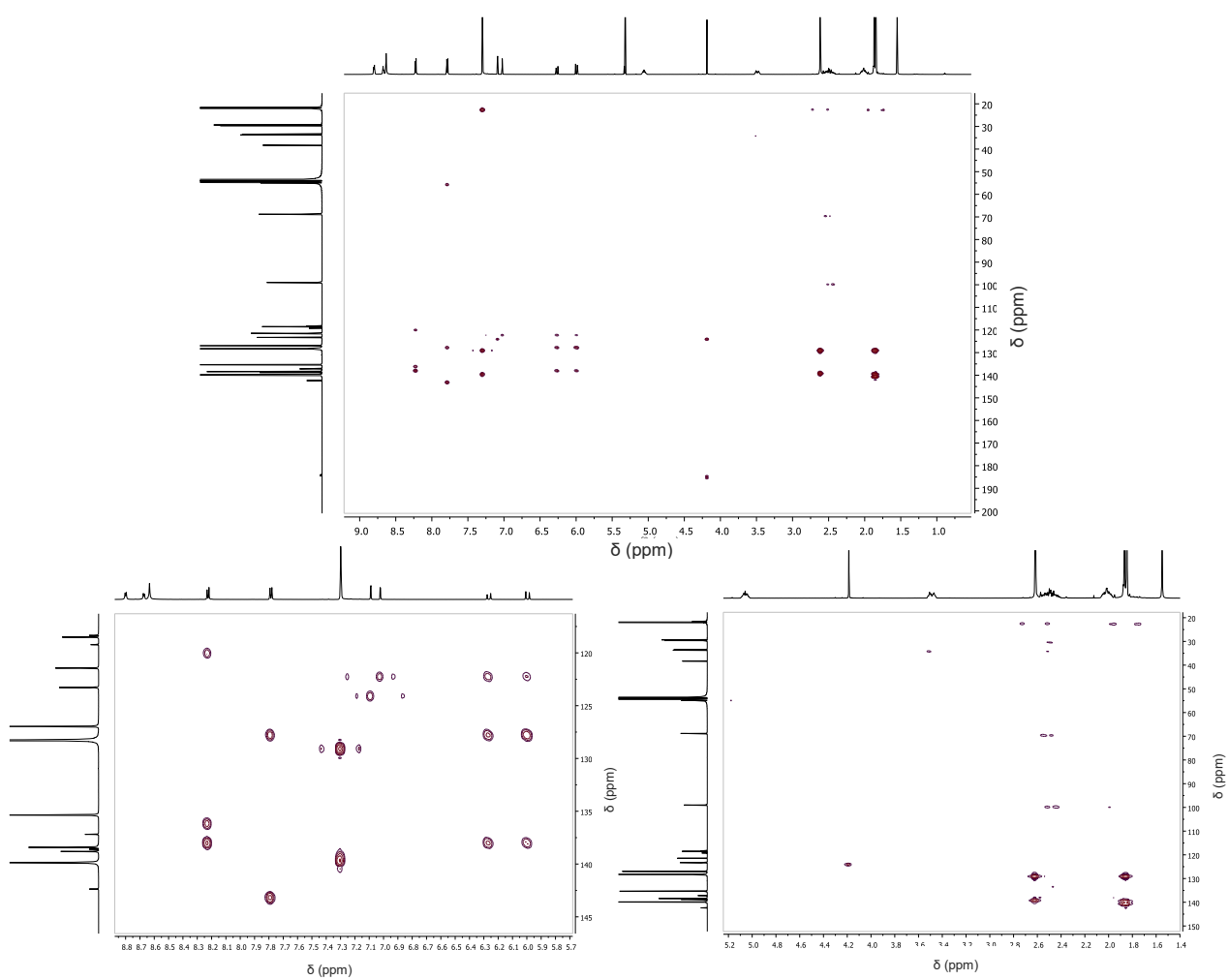


Figure S14. Full range (top), partial (bottom) ^1H - $^{13}\text{C}\{^1\text{H}\}$ HMBC NMR spectra (600 MHz, CD_2Cl_2) of **2H-A-Rh(cod)Cl**

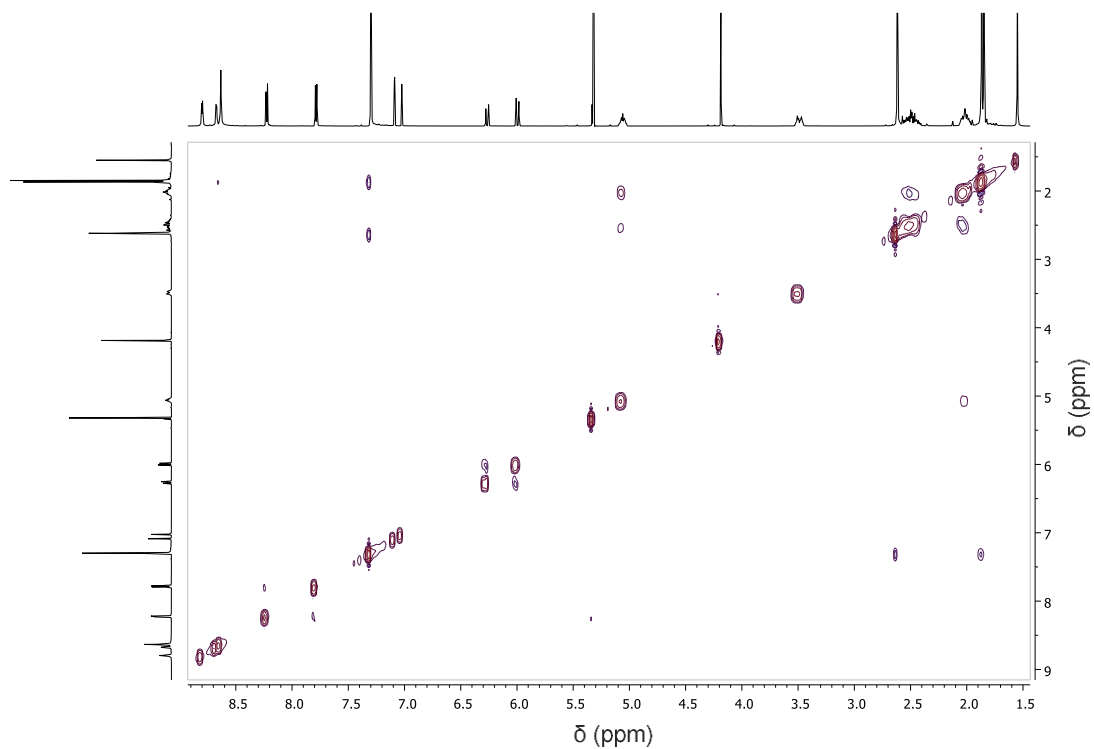


Figure S15. ^1H - ^1H ROESY NMR spectra (600 MHz, CD_2Cl_2) of **2H-A-Rh(cod)Cl**

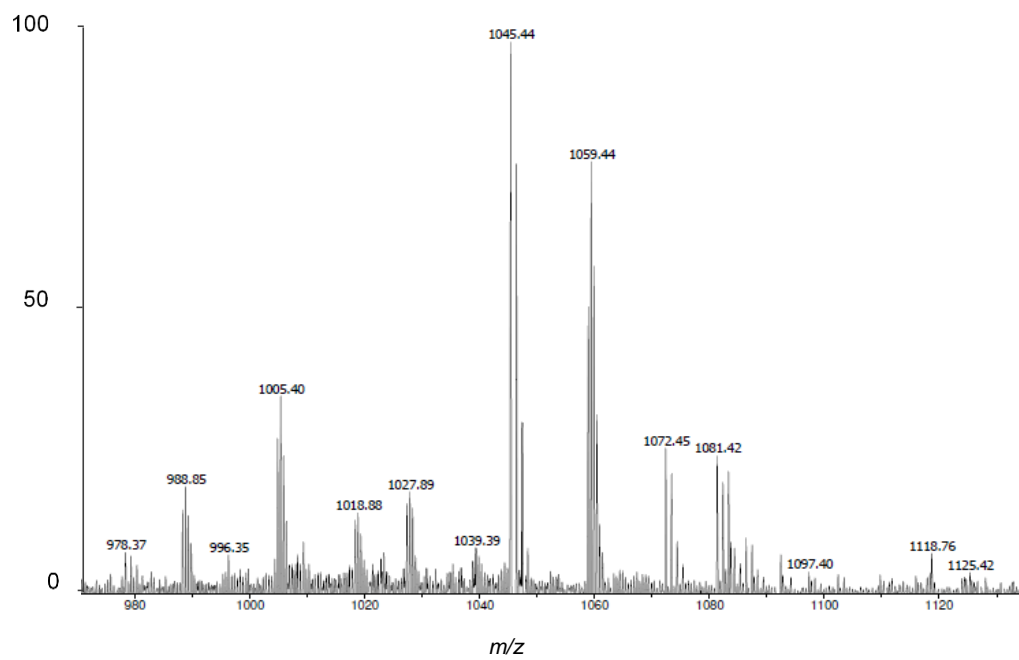


Figure S16. ESI-TOF (positive mode) mass spectrum of **2H-A-Rh(cod)Cl**

Porphyrin Zn-A-Rh(cod)Cl

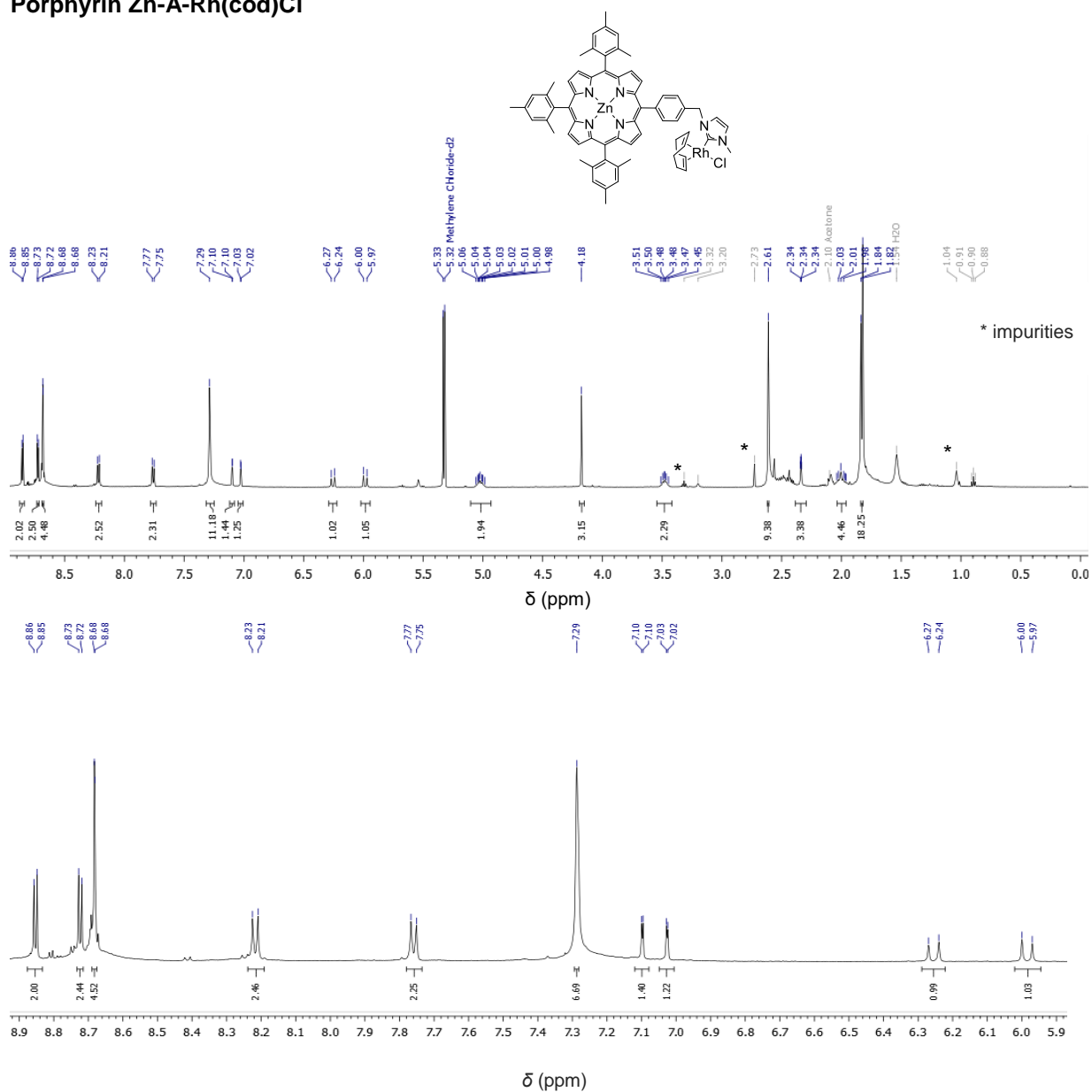


Figure S17. Full range (top) and partial (bottom) ^1H NMR spectrum (600 MHz, CD_2Cl_2) of **Zn-A-Rh(cod)Cl**

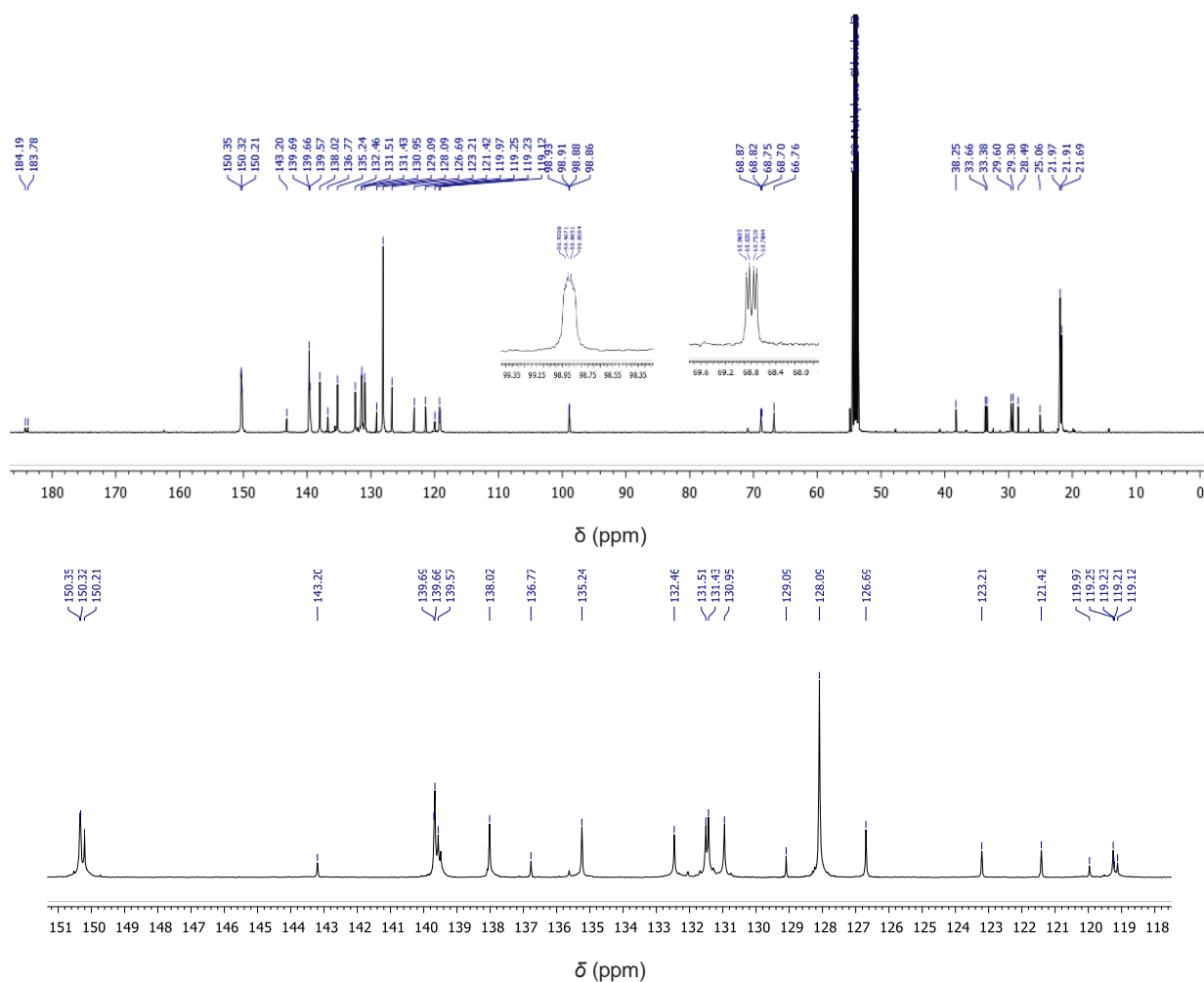


Figure S18. Full range (top) and partial (bottom) $^{13}\text{C}\{^1\text{H}\}$ NMR spectrum (150.9 MHz, CD_2Cl_2) of Zn-A-Rh(cod)Cl

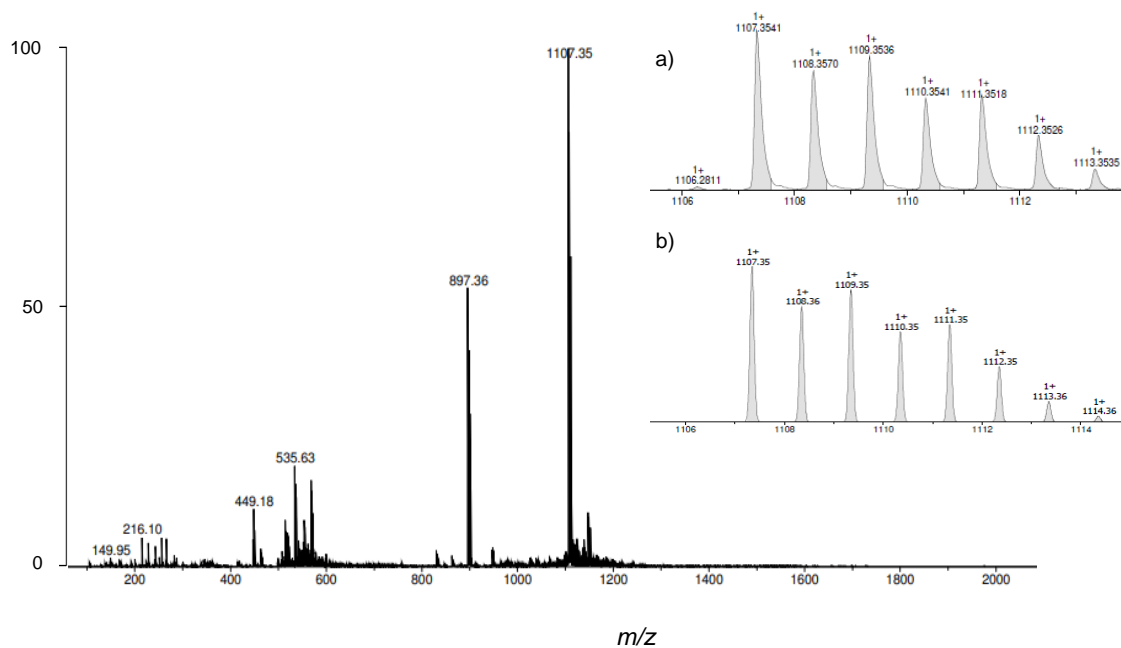
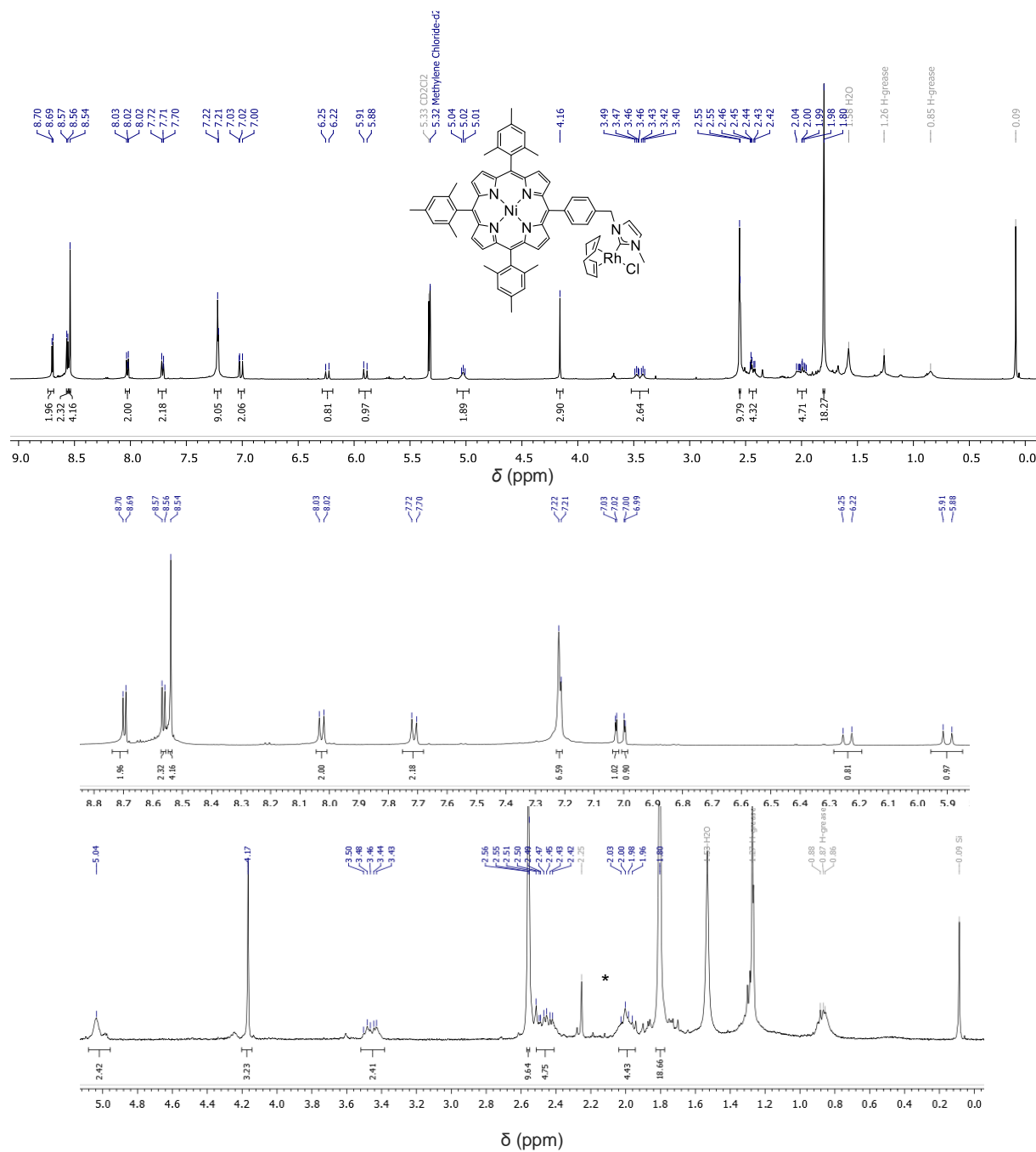


Figure S19. ESI-TOF (positive mode) mass spectrum (left) of Zn-A-Rh(cod)Cl . Experimental (a) and calculated (b) isotopic patterns (right)

Porphyrin Ni-A-Rh(cod)Cl



*Impurity

Figure S20. Full range (top) and partial (bottom) ^1H NMR spectrum (400 MHz, CD_2Cl_2) of **Ni-A-Rh(cod)Cl**

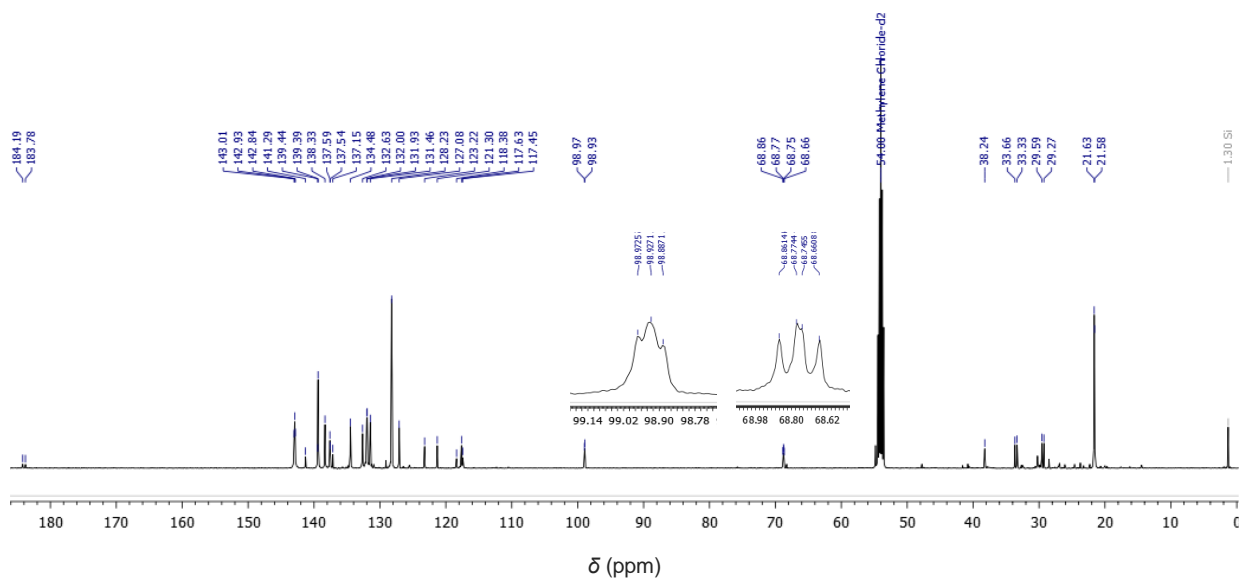


Figure S21. $^{13}\text{C}\{^1\text{H}\}$ NMR spectrum (150.9 MHz, CD_2Cl_2) of **Ni-A-Rh(cod)Cl**

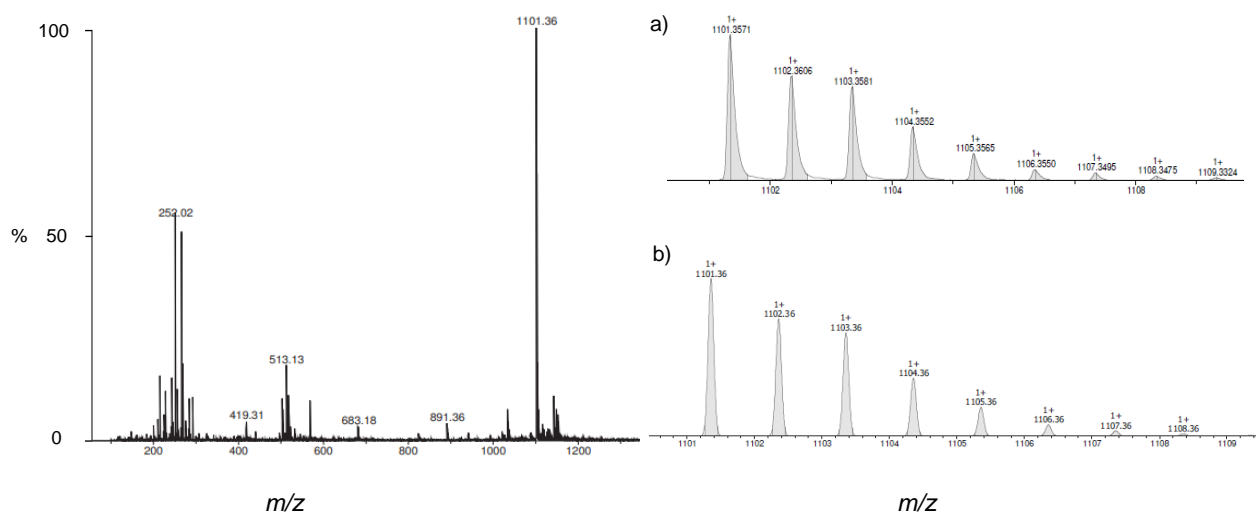


Figure S22. ESI-TOF positive mode mass spectrum (left) of **Ni-A-Rh(cod)Cl**. Experimental (a) and calculated (b) isotopic patterns

Porphyrin 2H-C-PF₆

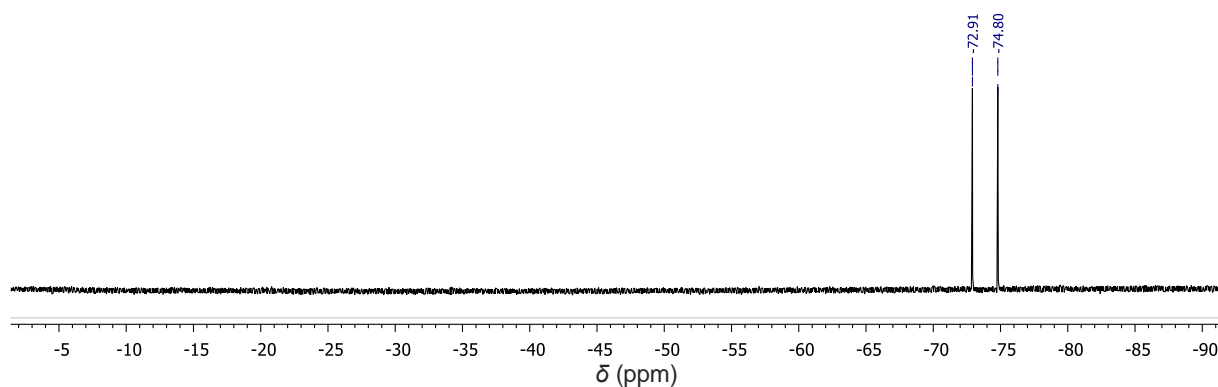
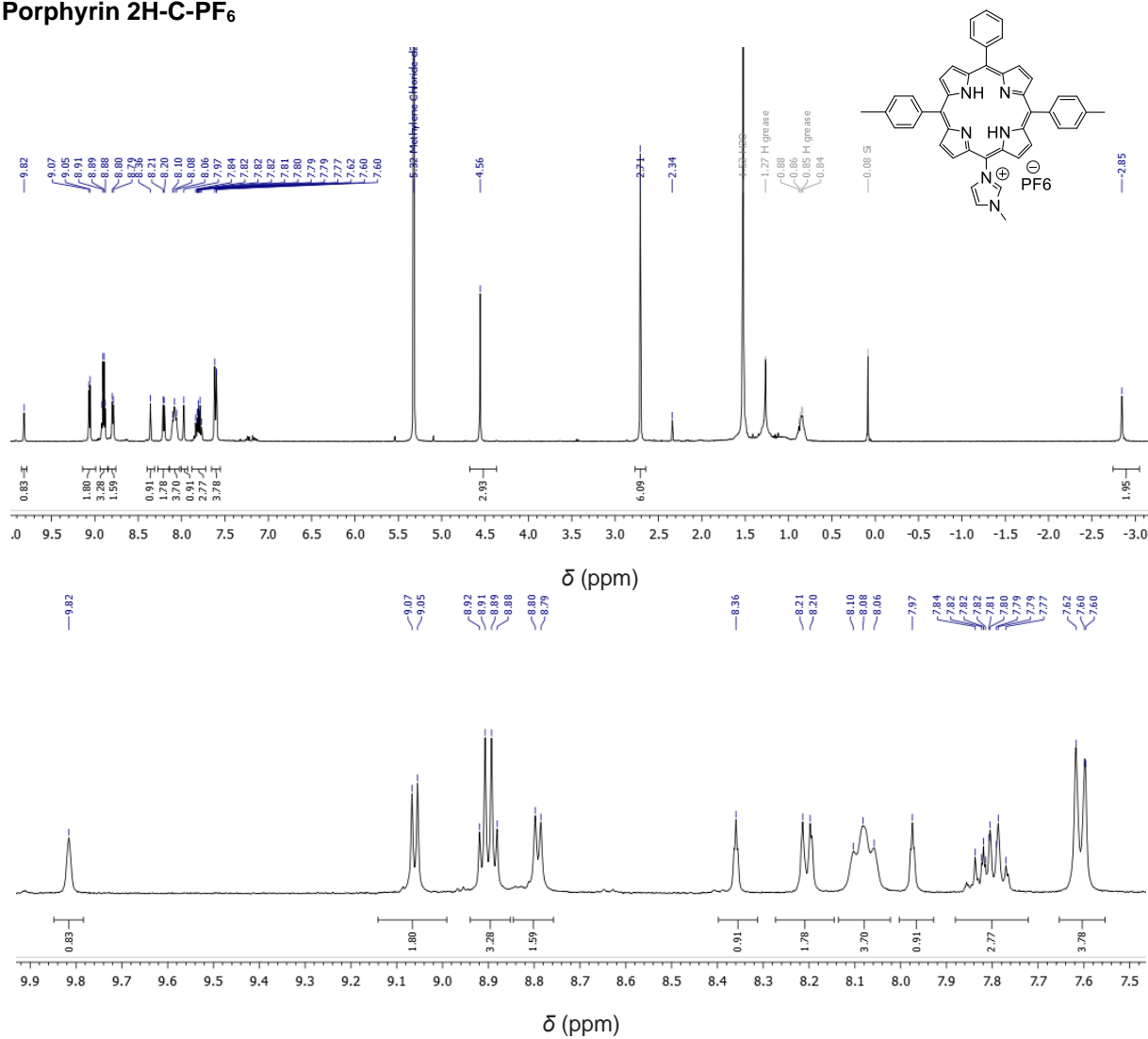


Figure S24. ¹⁹F {¹H} spectrum (376.5 MHz, CD₂Cl₂) of 2H-C-PF₆

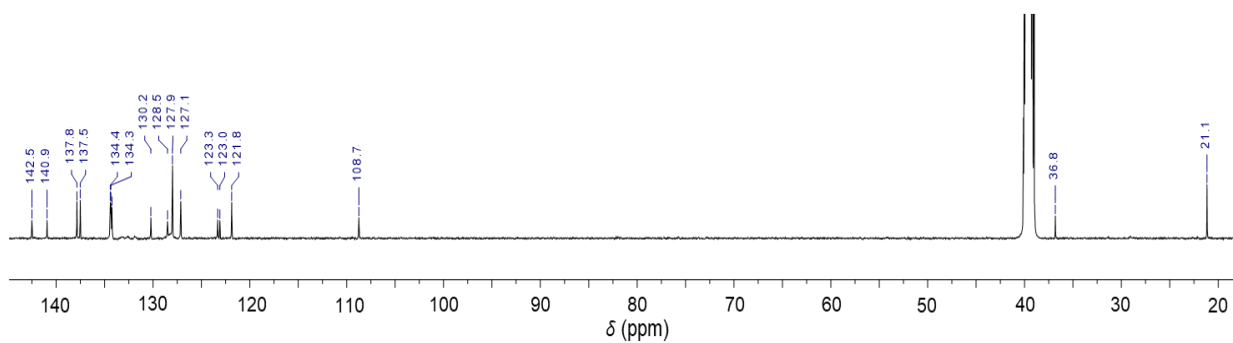


Figure S25. $^{13}\text{C}\{^1\text{H}\}$ NMR spectrum (150.9 MHz, DMSO-*d*₆) of 2H-C-PF₆

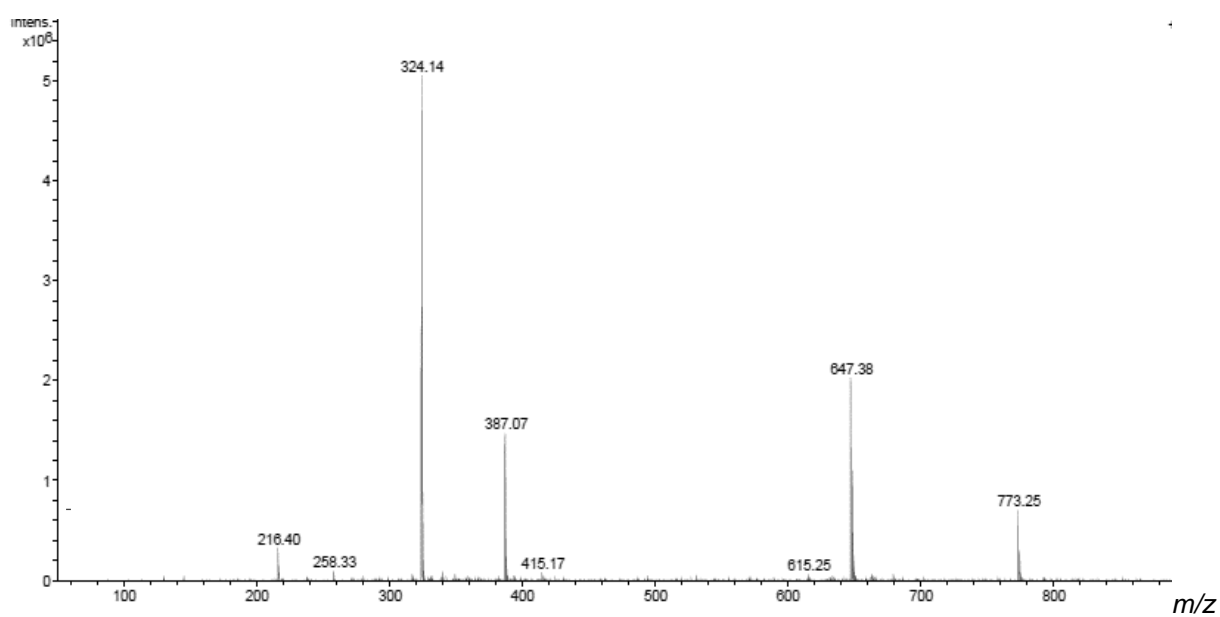


Figure S26. ESI-TOF positive mode mass spectrum of porphyrin 2H-C-PF₆

Porphyrin Zn-C-PF₆

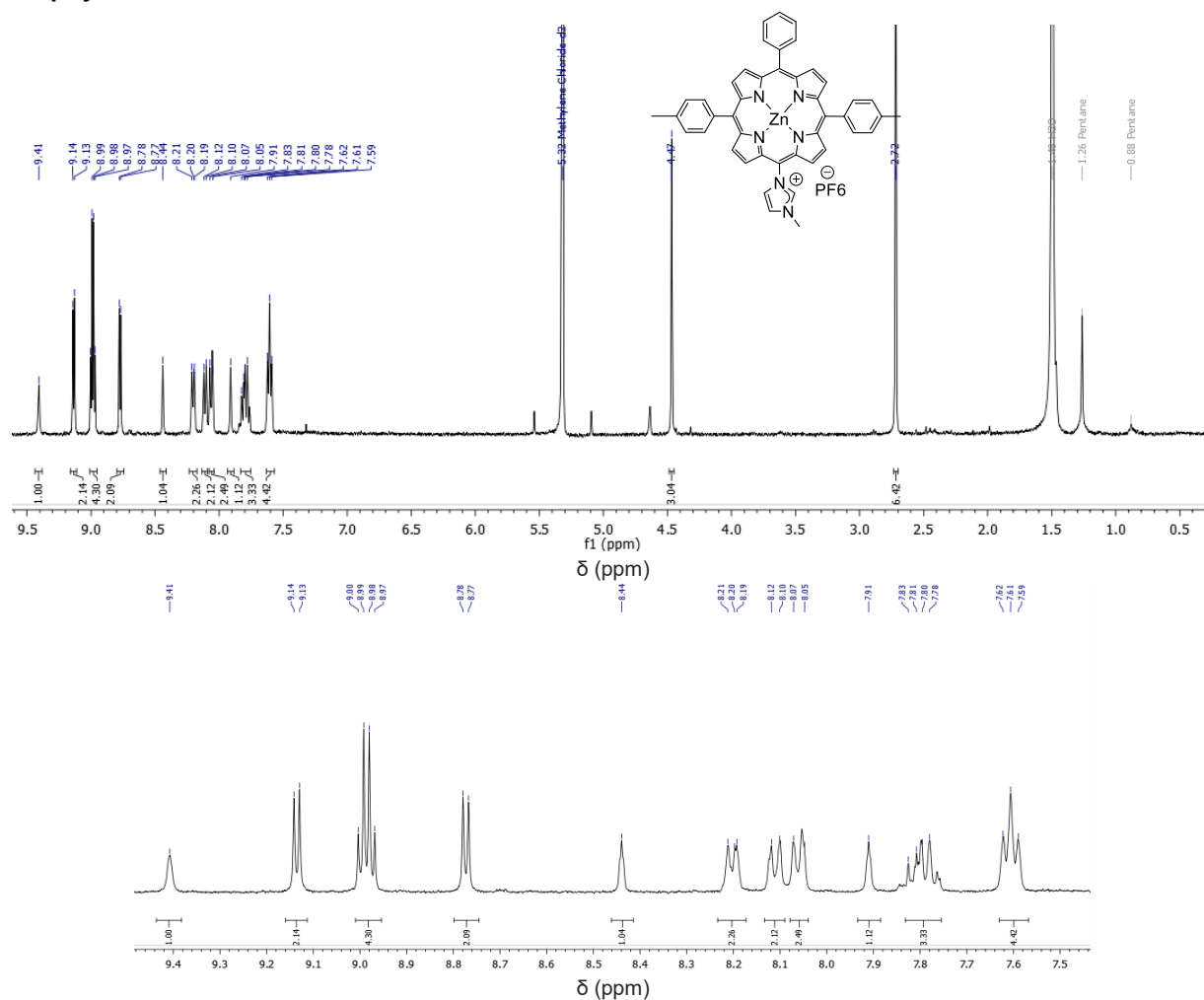


Figure S27. Full range (top) and partial (bottom) ¹H NMR spectrum (400 MHz, CD₂Cl₂) of Zn-C-PF₆

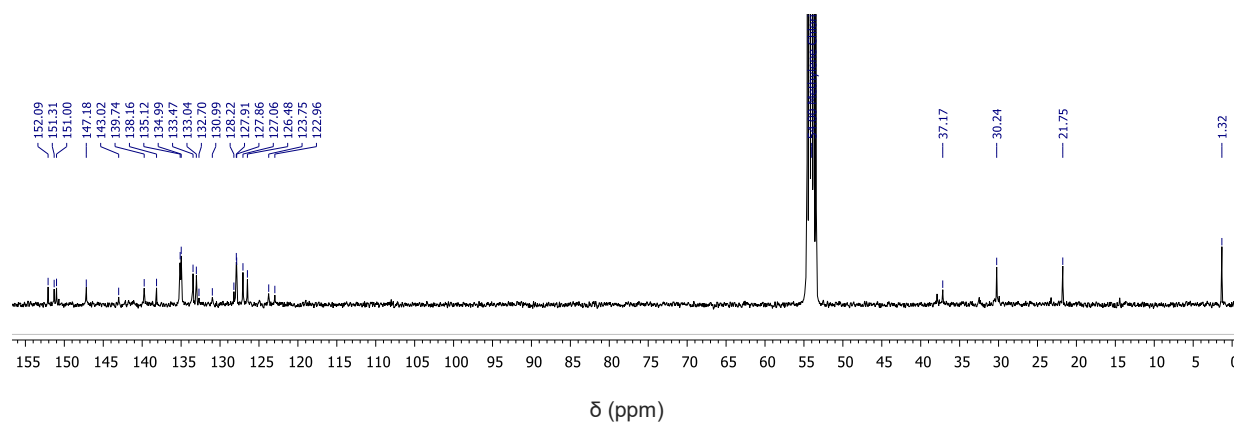


Figure S28. ¹³C{¹H} NMR spectrum (125.7 MHz, CD₂Cl₂) of Zn-C-PF₆

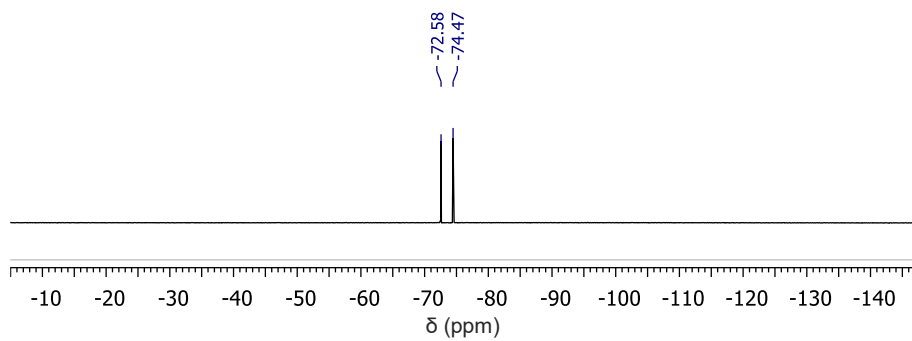


Figure S29. $^{19}\text{F}\{^1\text{H}\}$ NMR spectrum (376.5 MHz, CD_2Cl_2) of **Zn-C-PF₆**

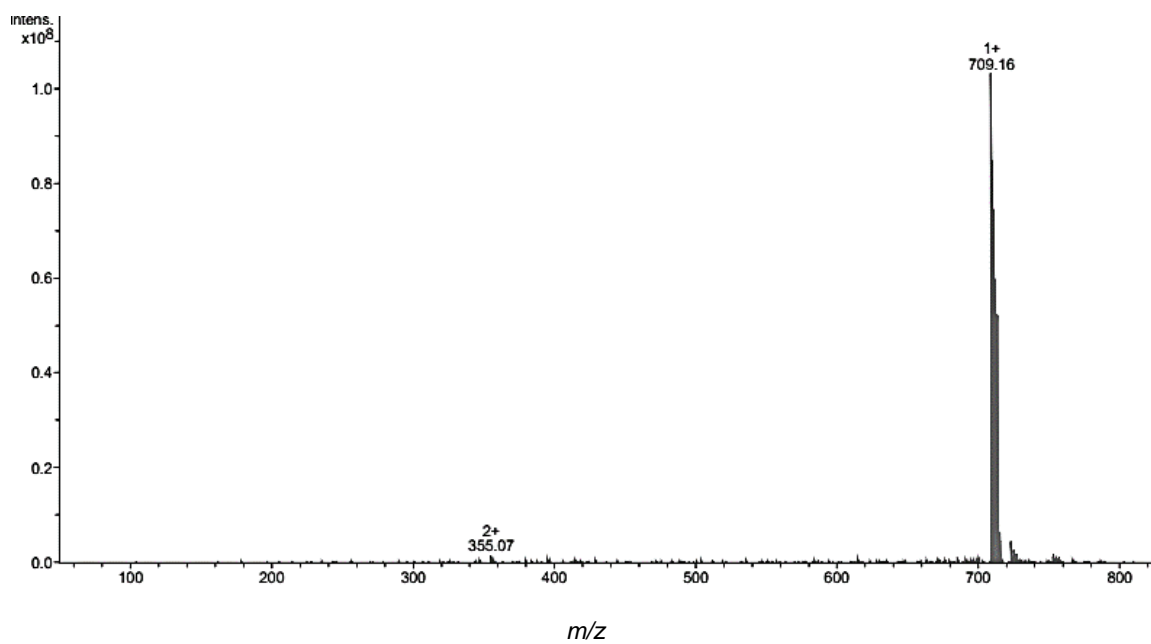


Figure S30. ESI-TOF (positive mode) mass spectrum of **Zn-C-PF₆**

Porphyrin Ni-C-PF₆

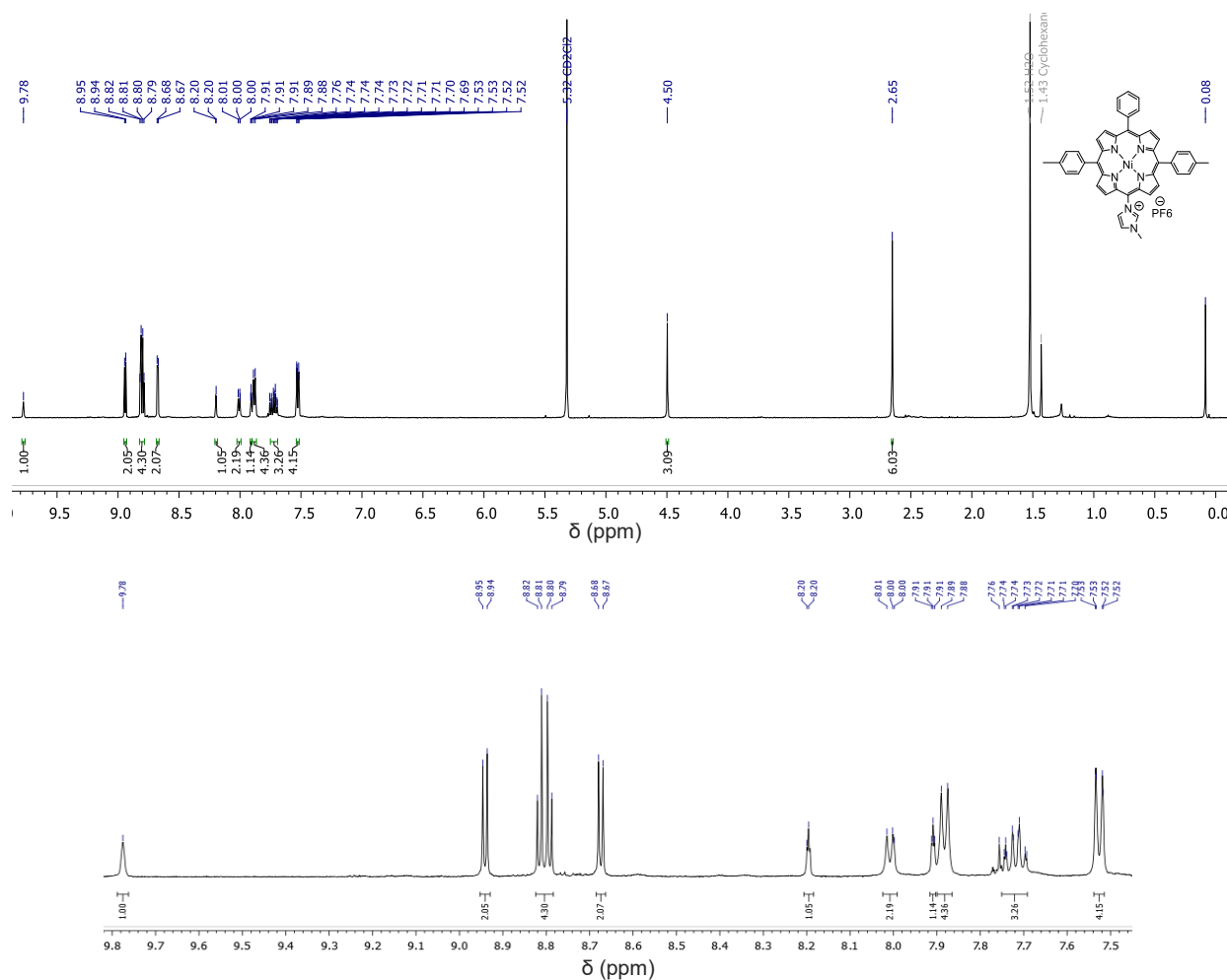


Figure S31. ¹H NMR spectrum (400 MHz, CD₂Cl₂) of Ni-C-PF₆

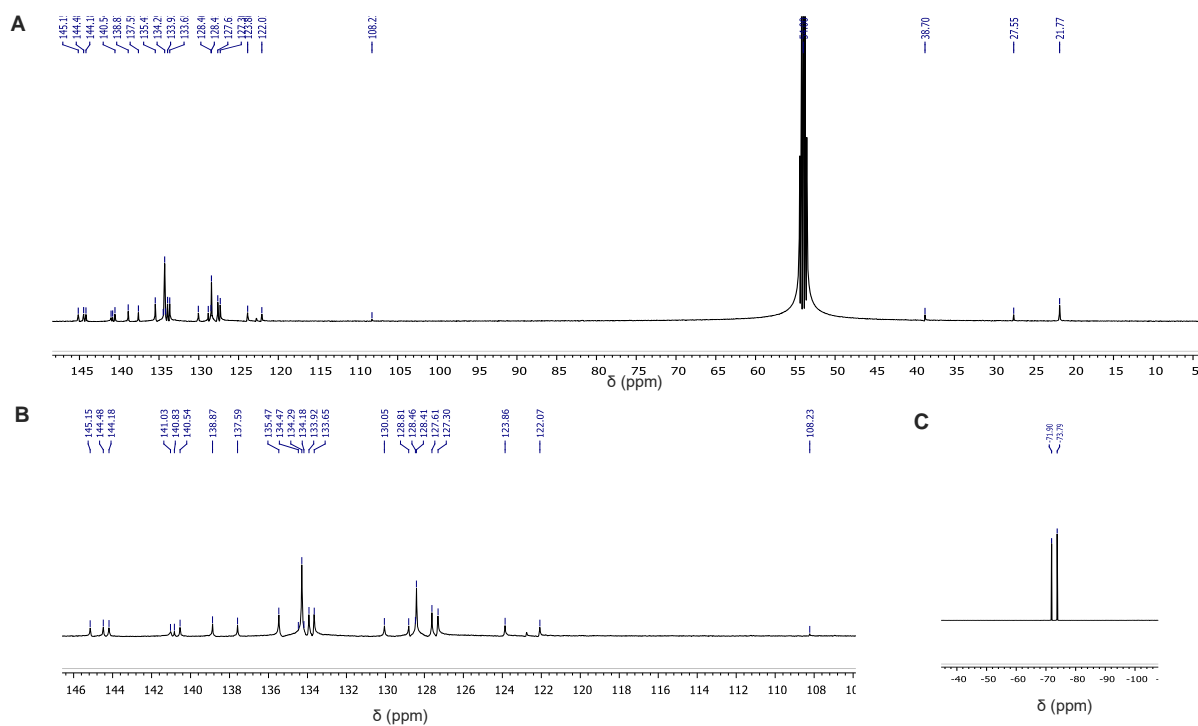


Figure S32. A) Full range B) Partial ¹³C{¹H} NMR spectrum (125.7 MHz, CD₂Cl₂) of Ni-C-PF₆. C) ¹⁹F{¹H} (376.5 MHz, CD₂Cl₂) of Ni-C-PF₆

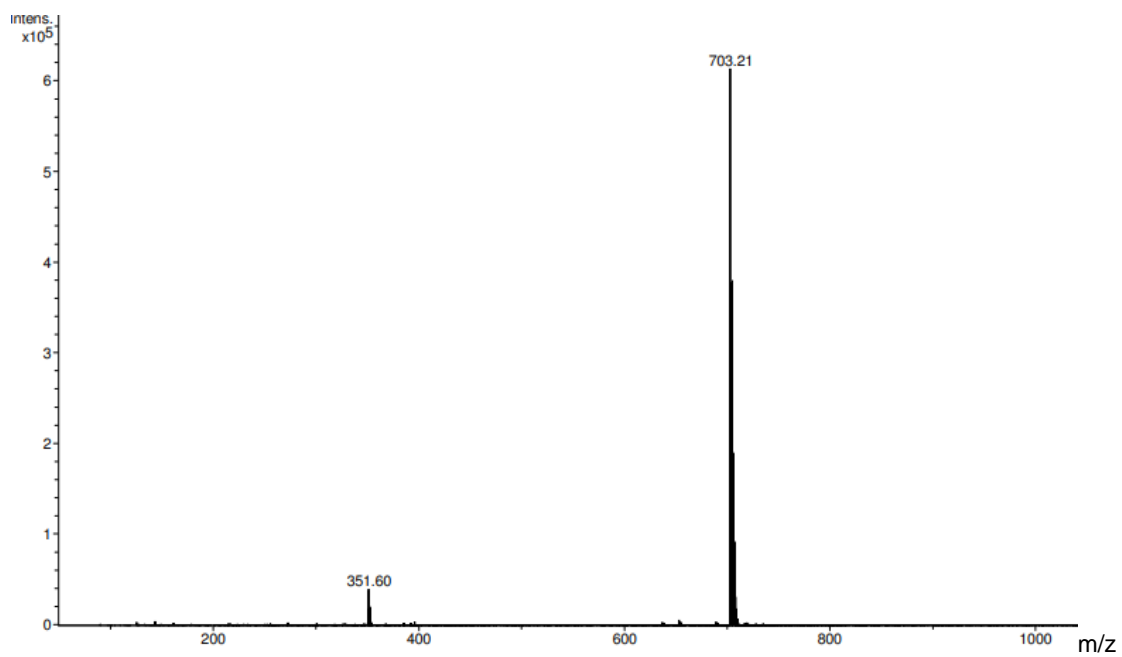


Figure S33. ESI-TOF (positive mode) mass spectra of **Ni-C-PF₆**

Porphyrin 2H-C-Rh(cod)Cl

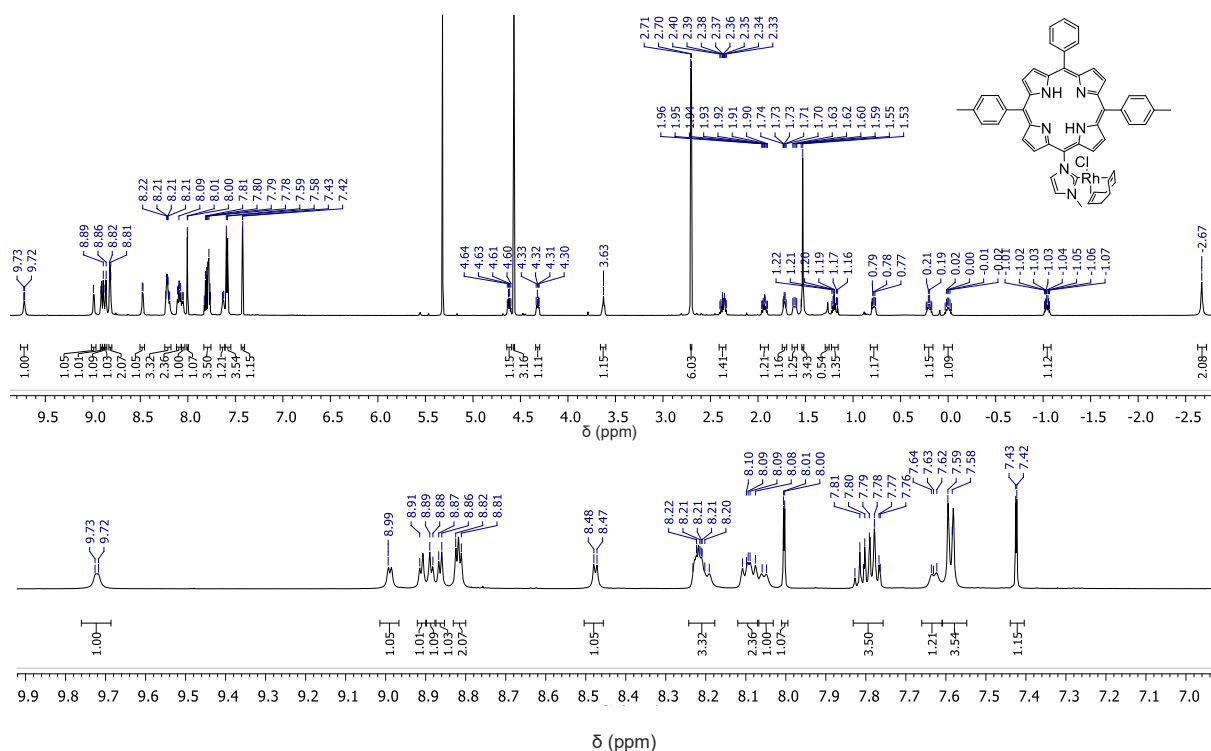


Figure S34: Full range (top) and partial (bottom) ^1H NMR spectrum (600 MHz, CD_2Cl_2) of **2H-C-Rh(cod)Cl**

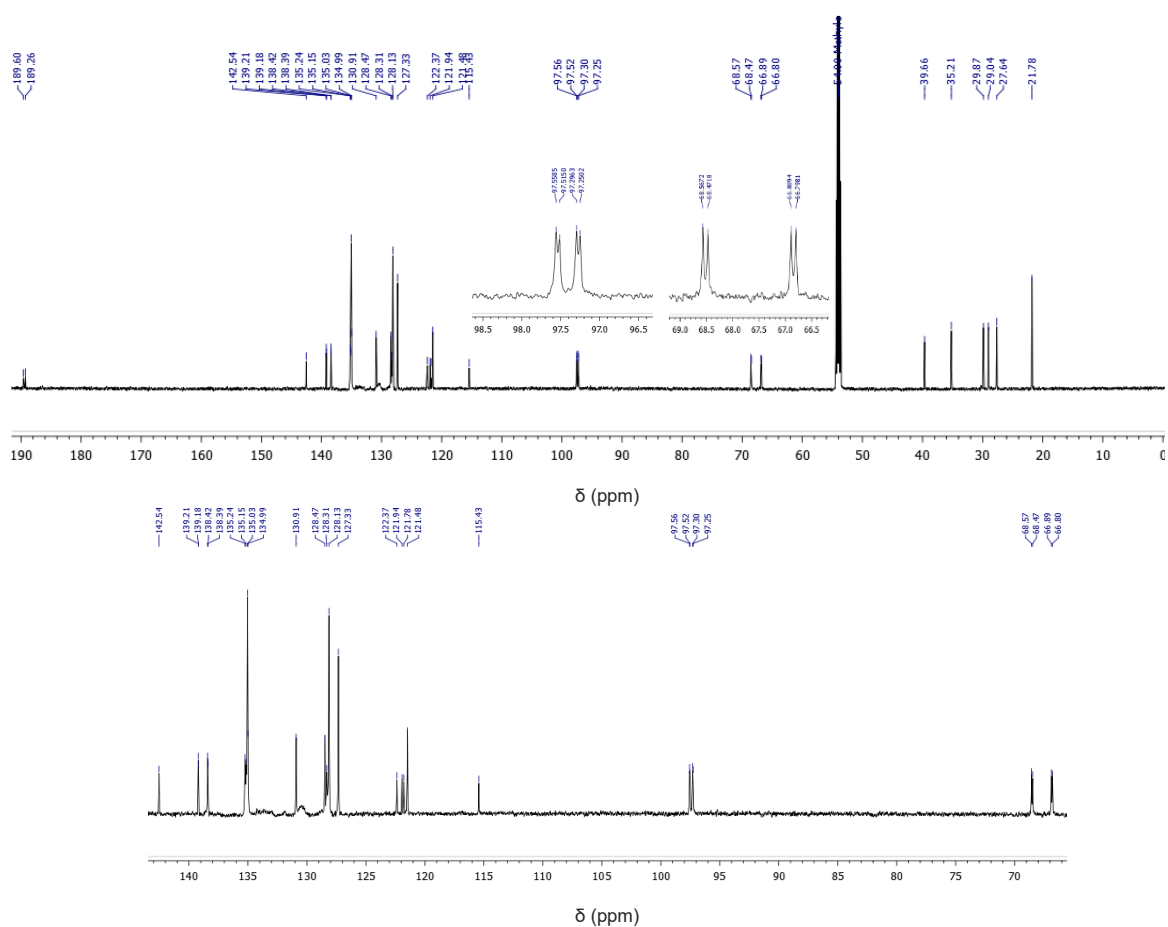


Figure S35: Full range (top) and partial (bottom) $^{13}\text{C}\{^1\text{H}\}$ NMR spectrum (150.9 MHz, CD_2Cl_2) of **2H-C-Rh(cod)Cl**

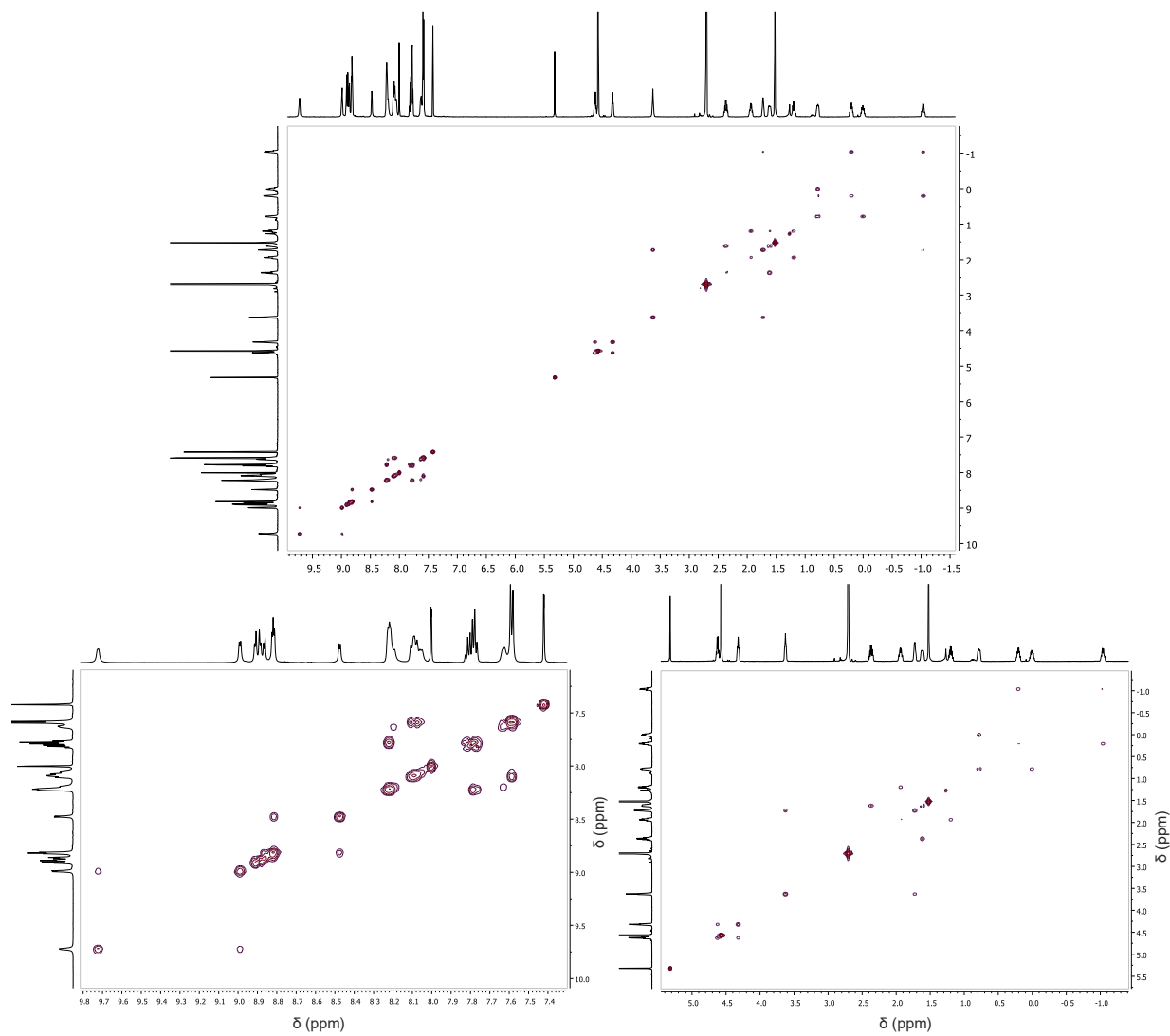


Figure S36. Full range (top) and partial (bottom) ^1H - ^1H COSY NMR spectrum (600 MHz, CD_2Cl_2) of **2H-C-Rh(cod)Cl**

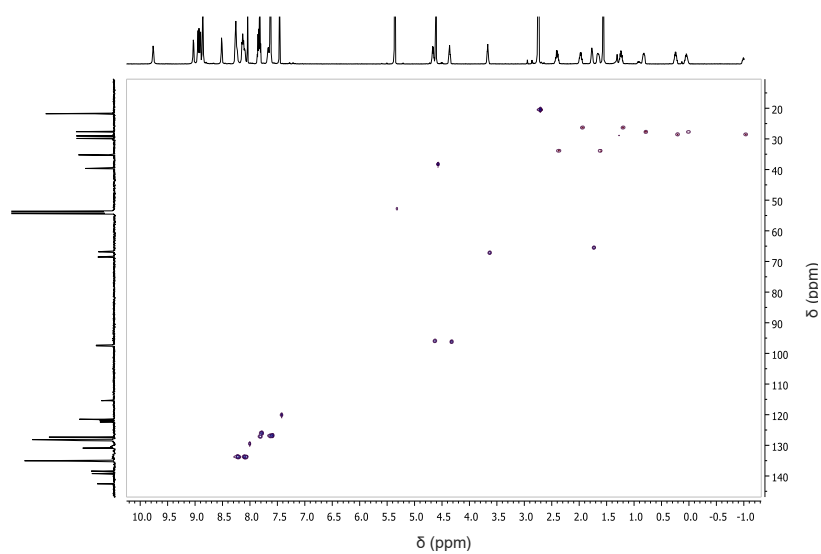


Figure S37. ^1H - $^{13}\text{C}\{^1\text{H}\}$ HSQC NMR spectrum (600 MHz, CD_2Cl_2) of **2H-C-Rh(cod)Cl**

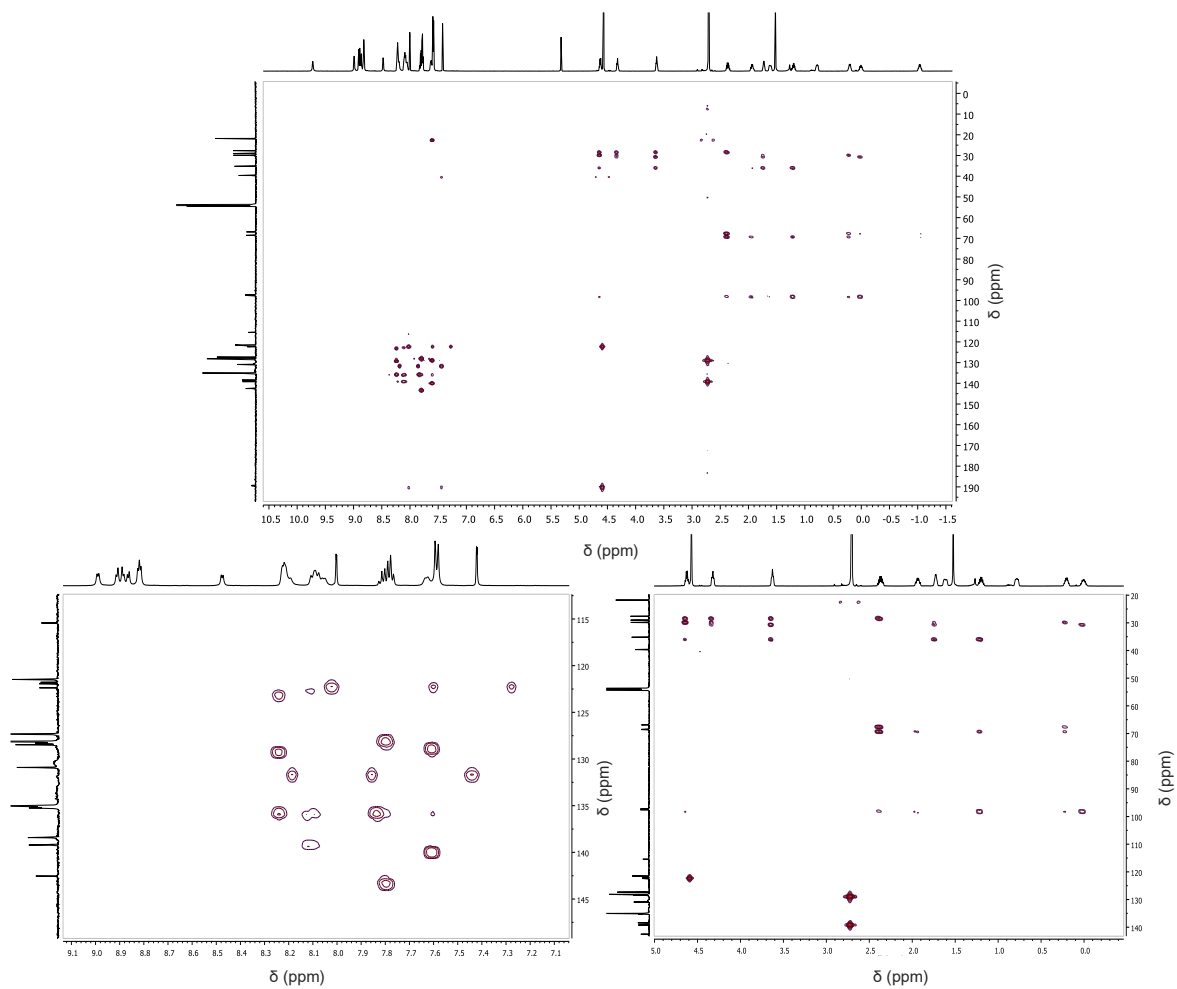


Figure S38. Full range (top) and partial (bottom) ^1H - $^{13}\text{C}\{^1\text{H}\}$ HMBC NMR spectrum (600 MHz, CD_2Cl_2) of **2H-C-Rh(cod)Cl**

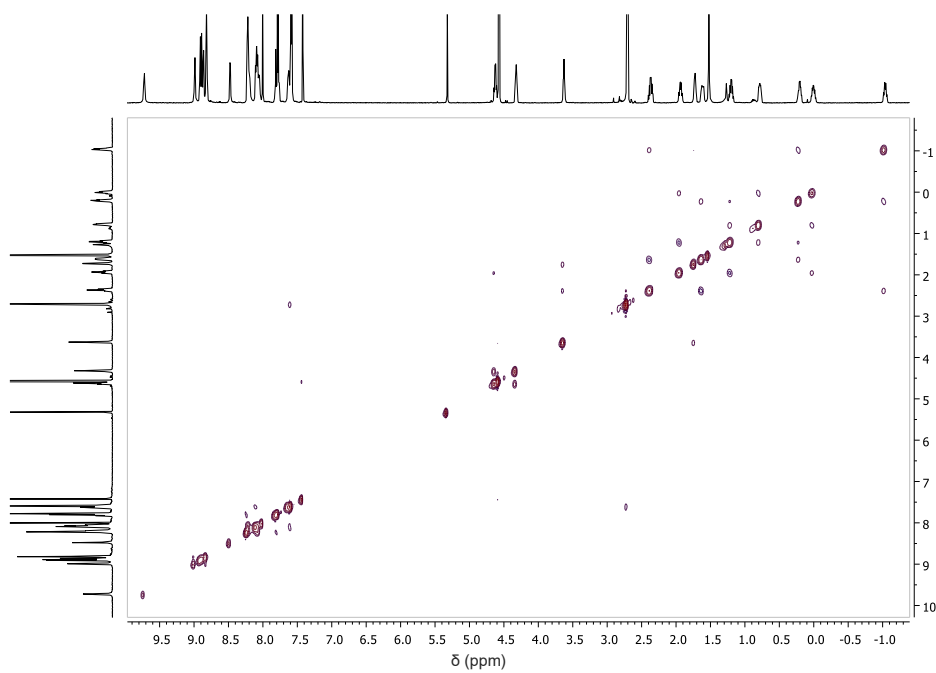


Figure S39. ^1H - ^1H ROESY NMR spectra (600 MHz, CD_2Cl_2)

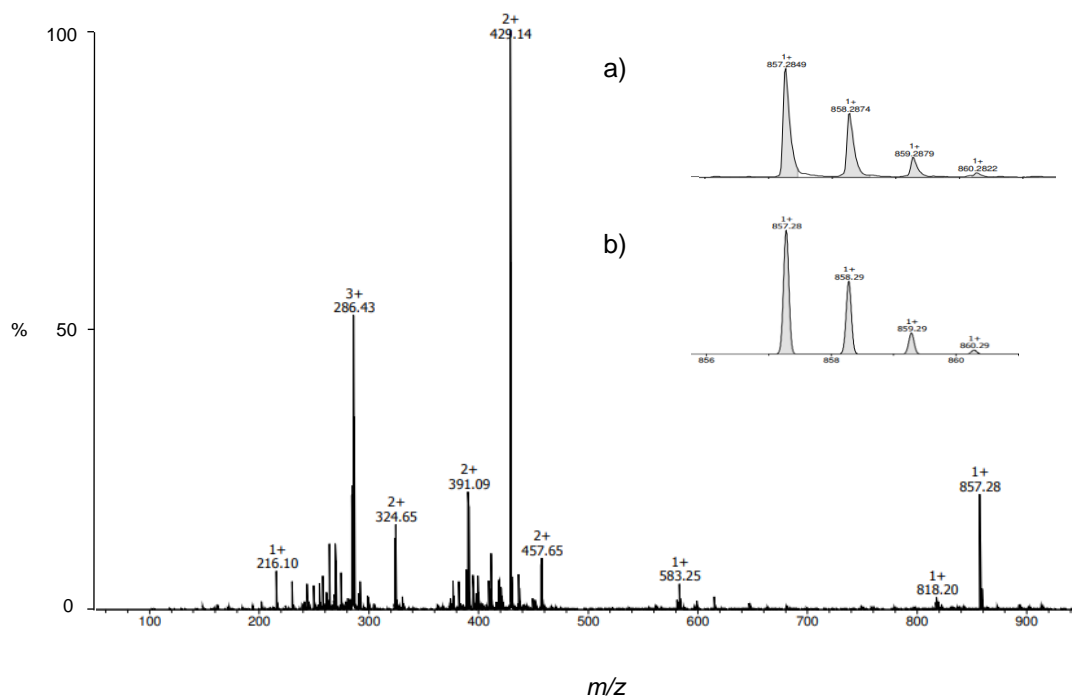


Figure S40. ESI-TOF (positive mode) mass spectrum of **2H-C-Rh(cod)Cl** (left). Experimental (a) and theoretical (b) isotopic patterns (right)

Porphyrin Zn-C-Rh(cod)Cl

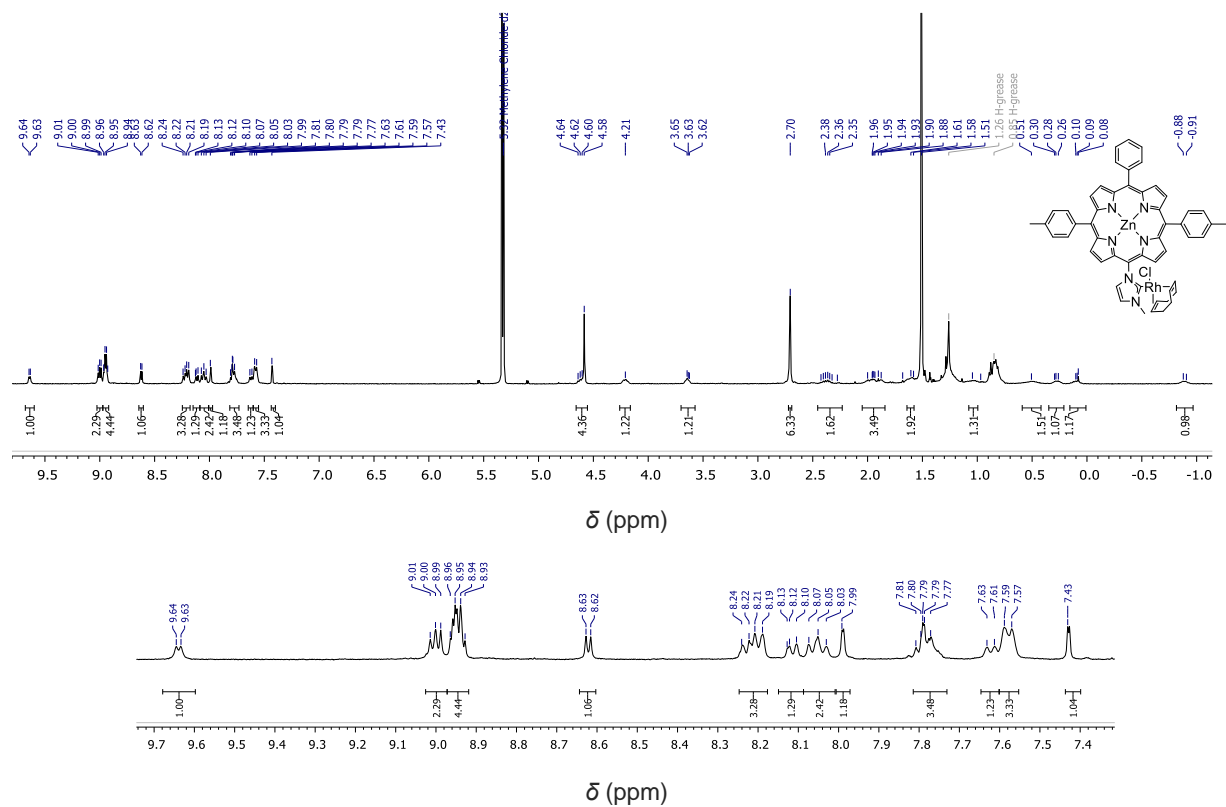


Figure S41. Full range (top) and partial (bottom) ¹H NMR spectrum (600 MHz, CD₂Cl₂) of Zn-C-Rh(cod)Cl

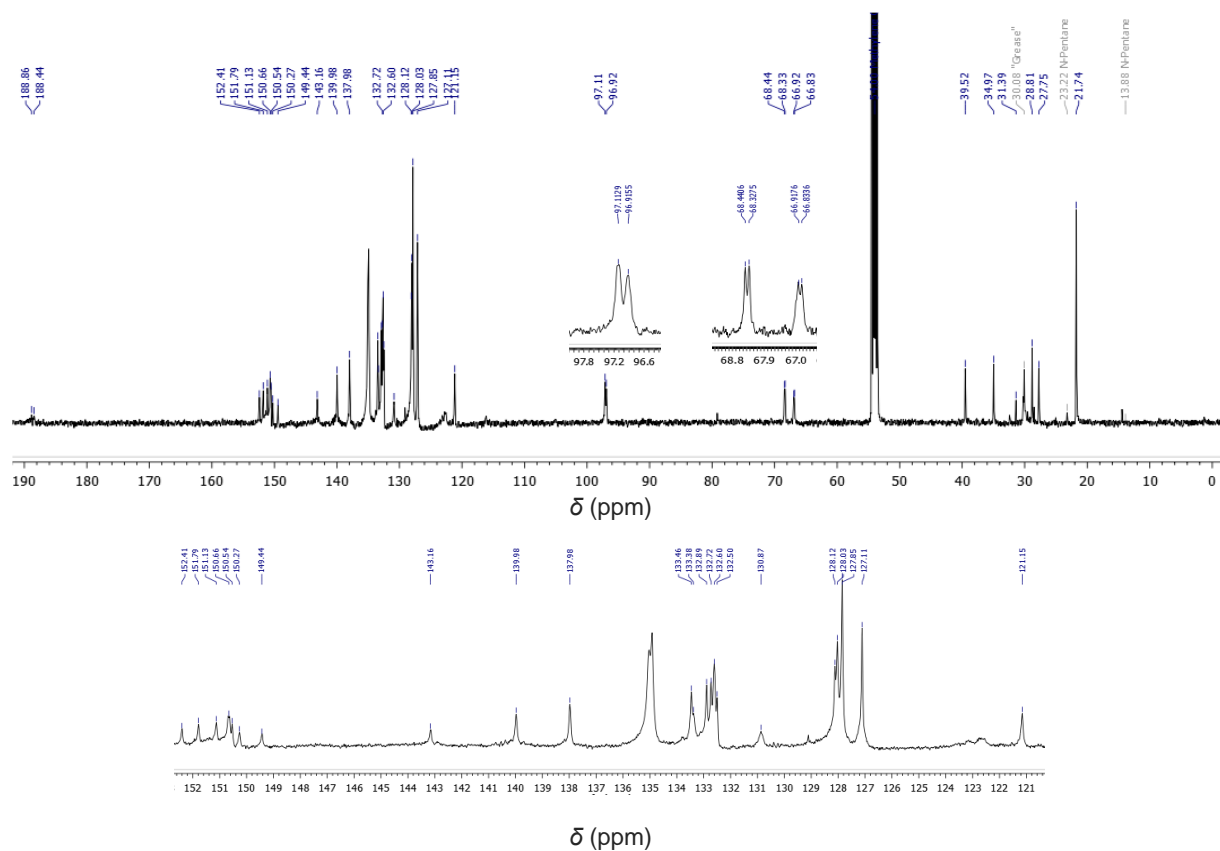


Figure S42. Full range (top) and partial ¹³C{¹H} NMR spectrum (150.9 MHz, CD₂Cl₂) of Zn-C-Rh(cod)Cl

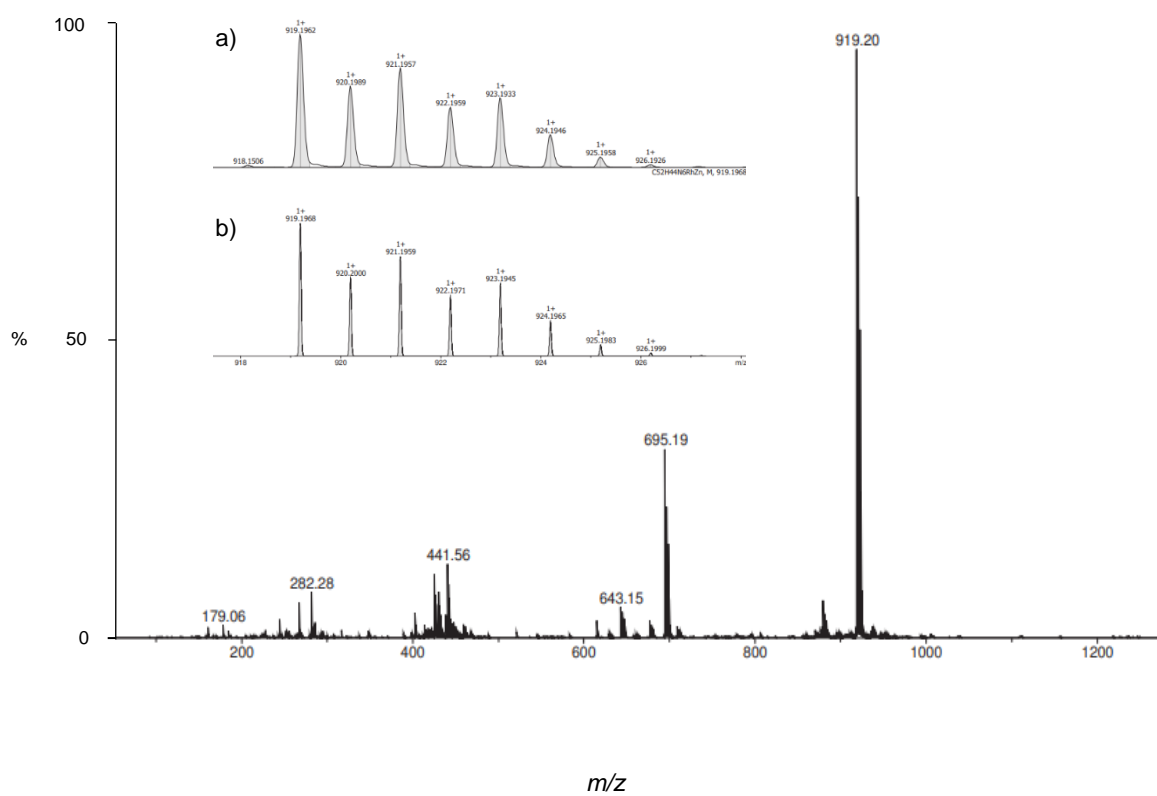


Figure S43. ESI-TOF (positive mode) mass spectrum of porphyrin **Zn-C-Rh(cod)Cl** (right). Experimental (a) and theoretical (b) isotopic patterns (left)

Porphyrin Ni-C-Rh(cod)Cl

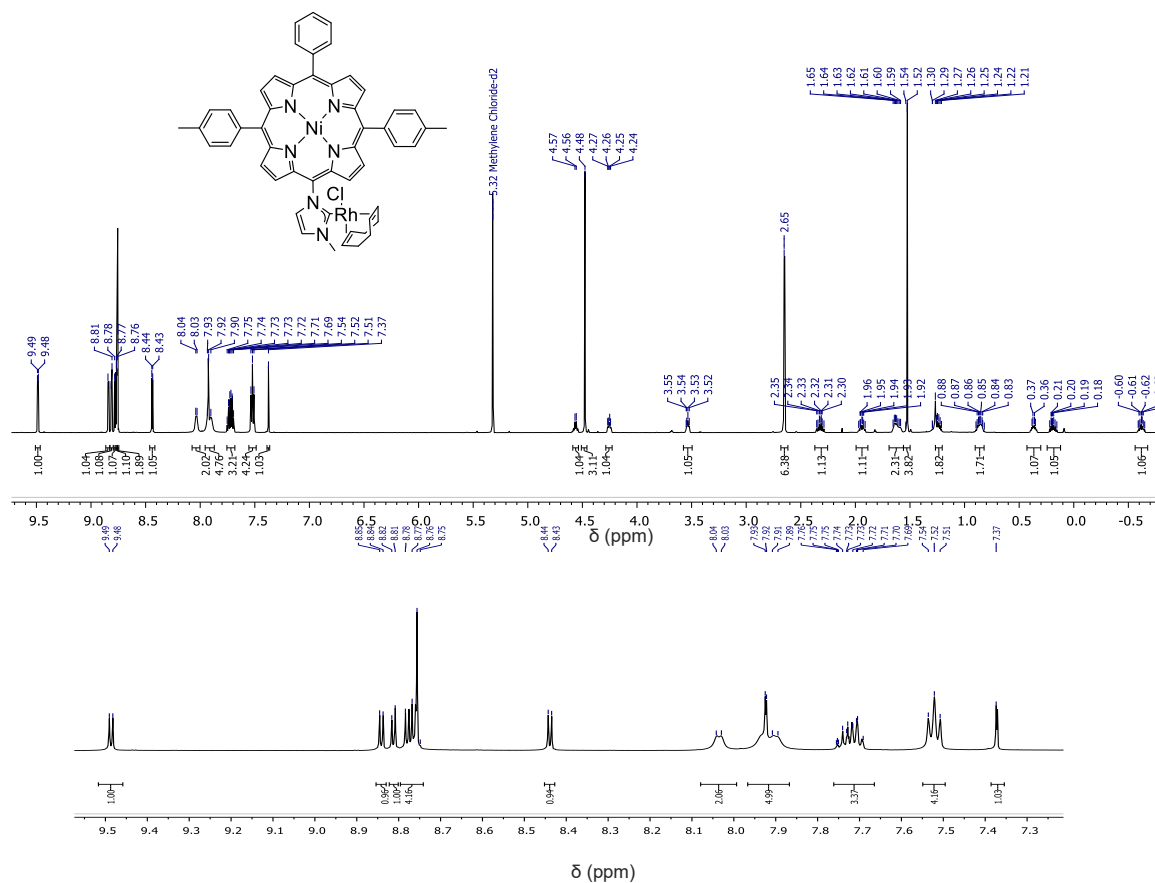


Figure S44. Full range (top) and partial (bottom) ^1H NMR spectrum (600 MHz, CD_2Cl_2) of Ni-C-Rh(cod)Cl

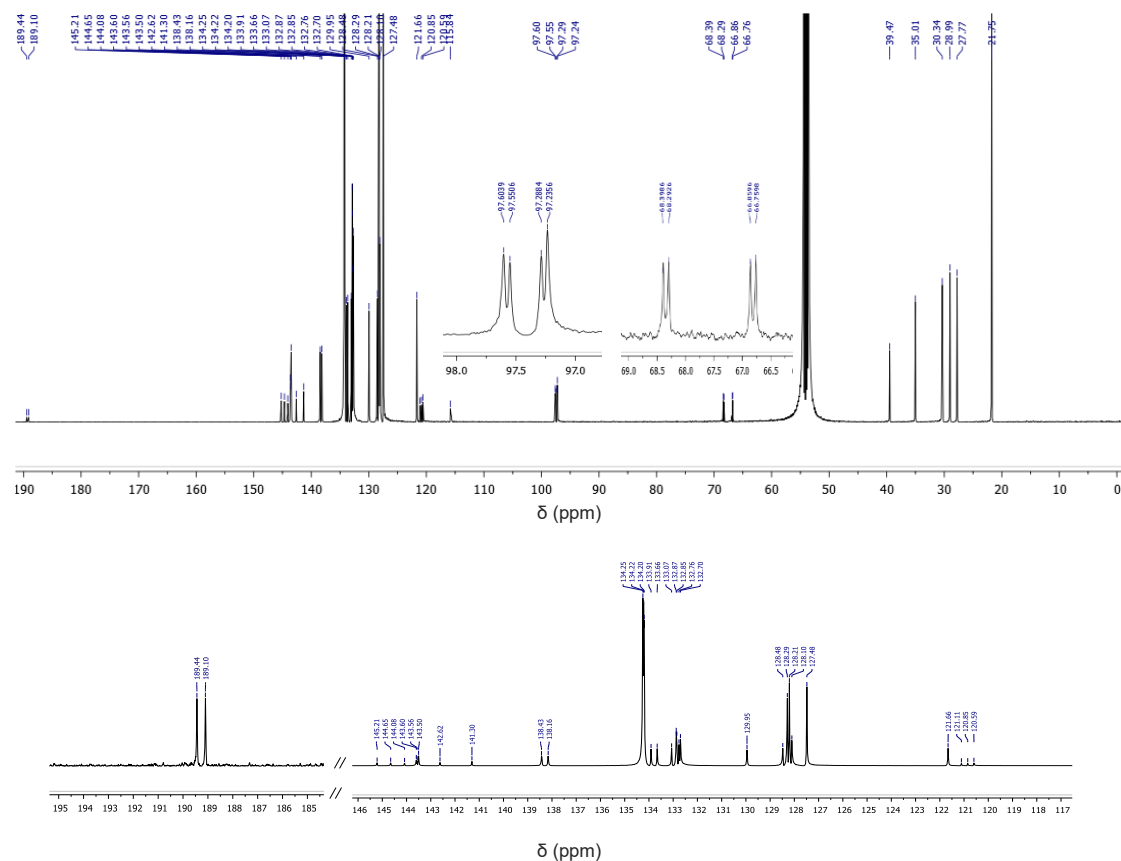


Figure S45. Full range (top) and partial (bottom) $^{13}\text{C}\{^1\text{H}\}$ NMR spectrum (150.9 MHz, CD_2Cl_2) of Ni-C-Rh(cod)Cl

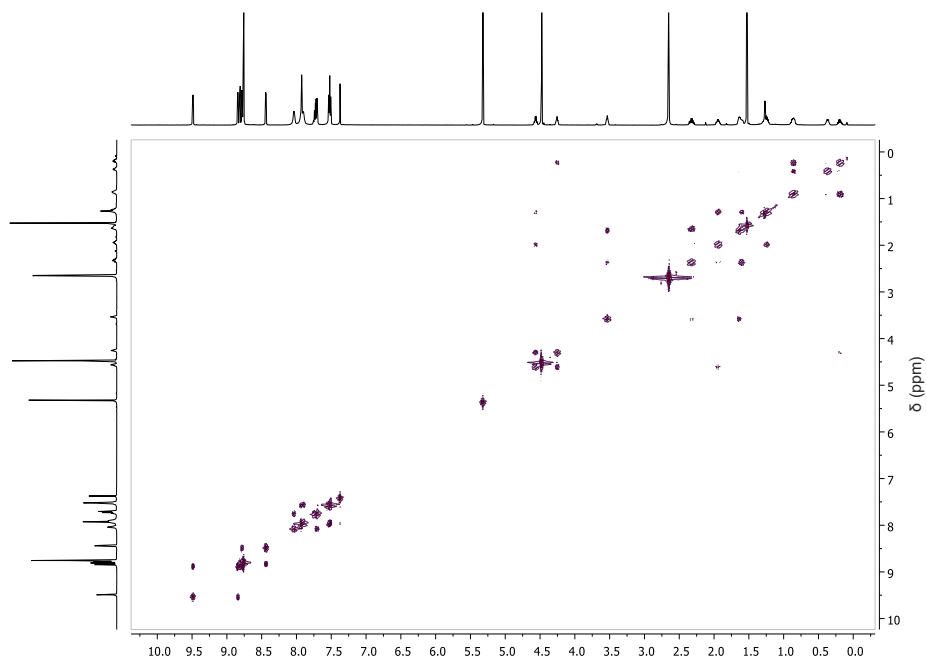


Figure S46. Full range ^1H - ^1H COSY NMR spectra (600 MHz, CD_2Cl_2) of porphyrin Ni-C-Rh(cod)Cl

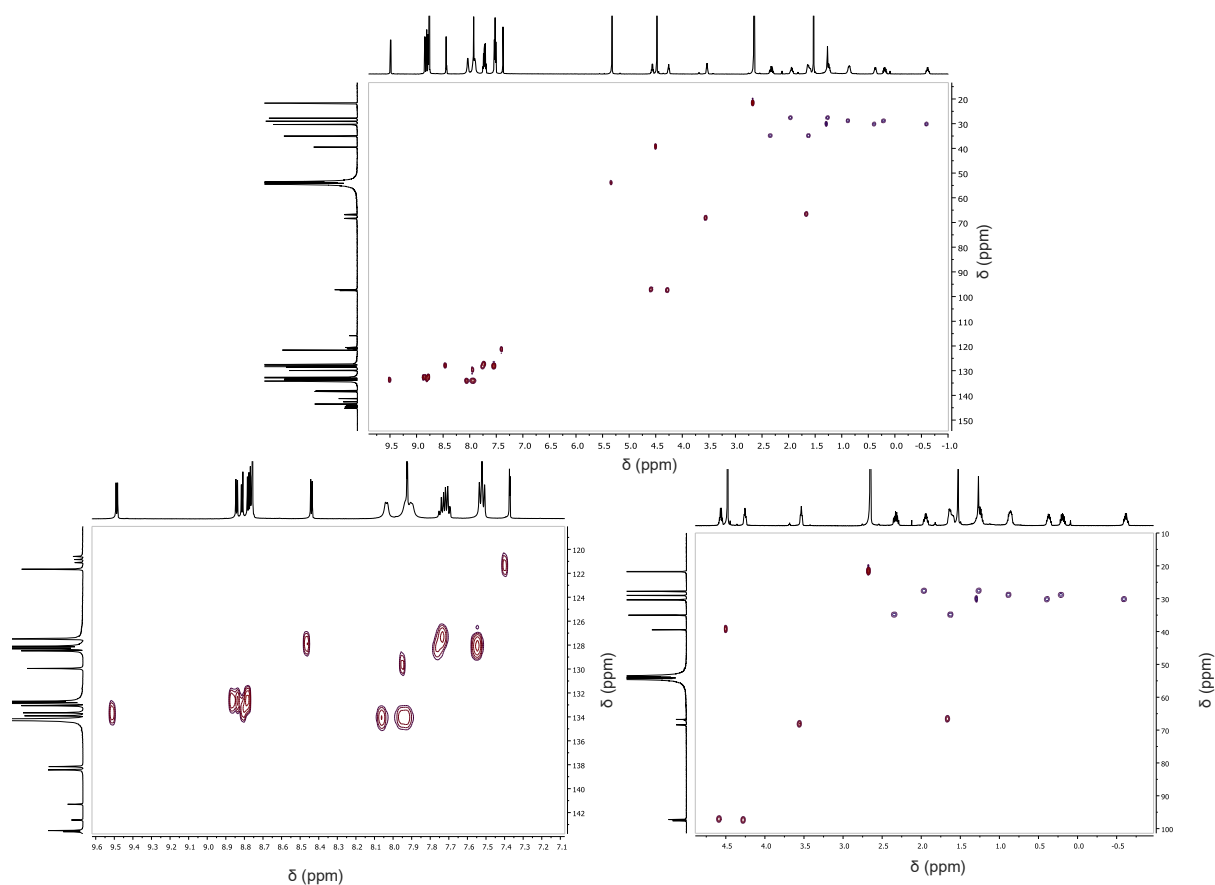


Figure S47. Full range (top) and partial (bottom) ^1H - $^{13}\text{C}\{^1\text{H}\}$ HSQC NMR spectrum (600 MHz, CD_2Cl_2) of Ni-C-Rh(cod)Cl

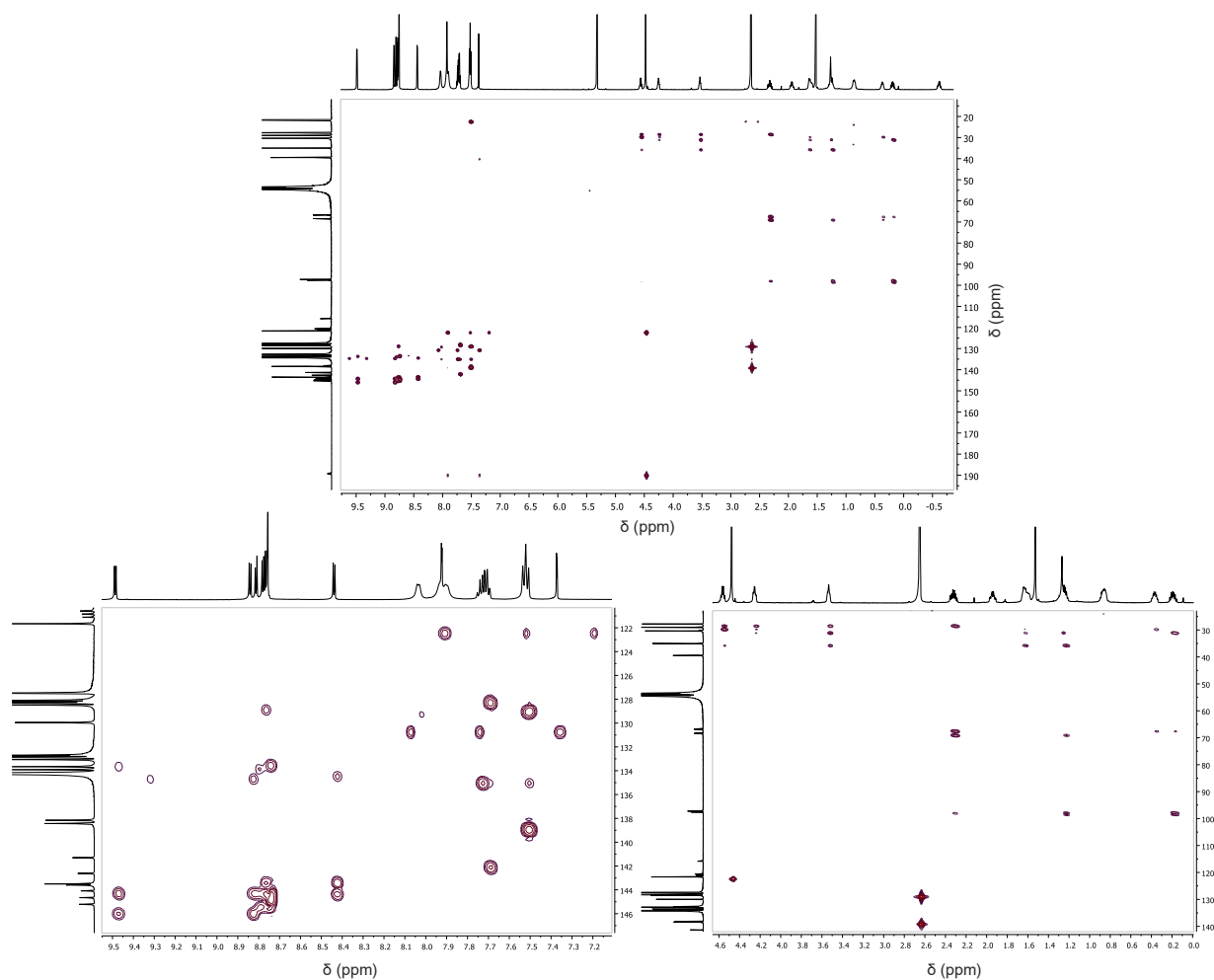


Figure S48. Full range (top) and partial (bottom) ^1H - $^{13}\text{C}\{^1\text{H}\}$ HMBC NMR spectrum (600 MHz, CD_2Cl_2) of **Ni-C-Rh(cod)Cl**

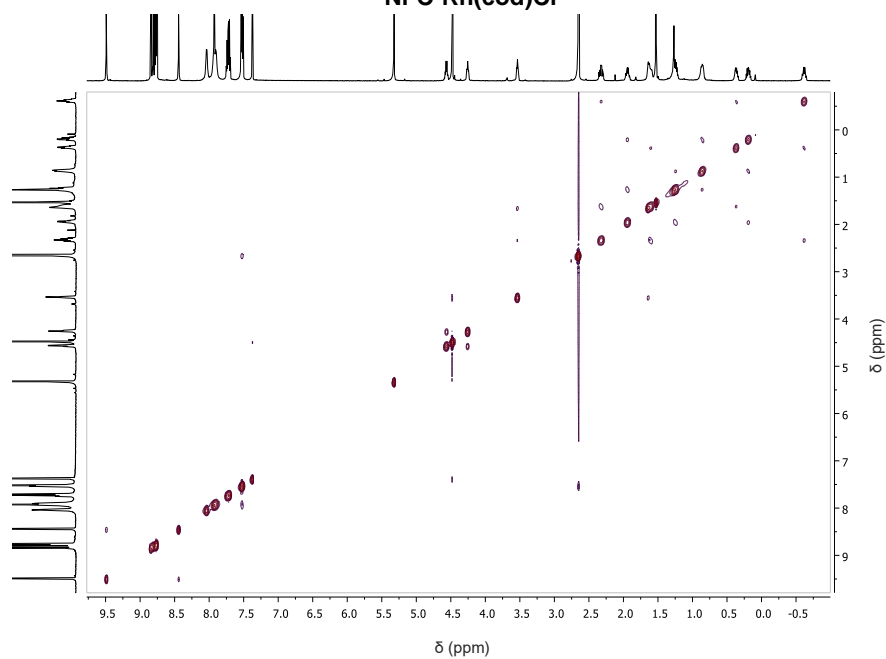


Figure S49. Full range ^1H - ^1H ROESY NMR spectrum (600 MHz, CD_2Cl_2) of **Ni-C-Rh(cod)Cl**

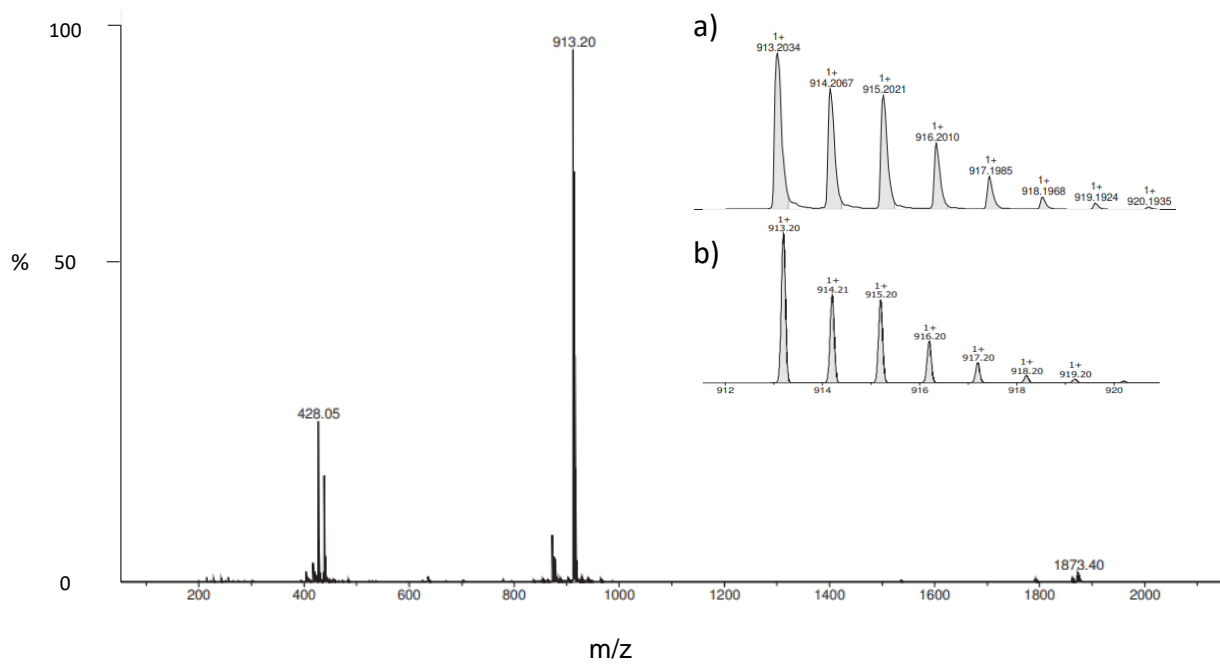


Figure S50. ESI-TOF (positive mode) mass spectrum of **Ni-C-Rh(cod)Cl** (left). Experimental (a) and calculated (b) isotopic patterns (right)

DFT optimized geometries

Gaussian16 has been used to perform quantum mechanical calculations.⁹ B3LYP^{10,11}, including Grimme's dispersion correction for nonbonding interactions was employed using atom pair-wise additive scheme¹², the DFT-D3 method. The Stuttgart/Dresden (SDD) valence basis set and effective core potential have been used for Rh atom¹³ in conjunction with the 6-31G** basis set for rest of the atoms. Full geometry optimizations, without any constrains, have been carried out in implicit toluene ($\epsilon = 2.4$), the solvent used for the catalytic experiments, using the PCM continuum solvation model as implemented in Gaussian 16¹⁴.

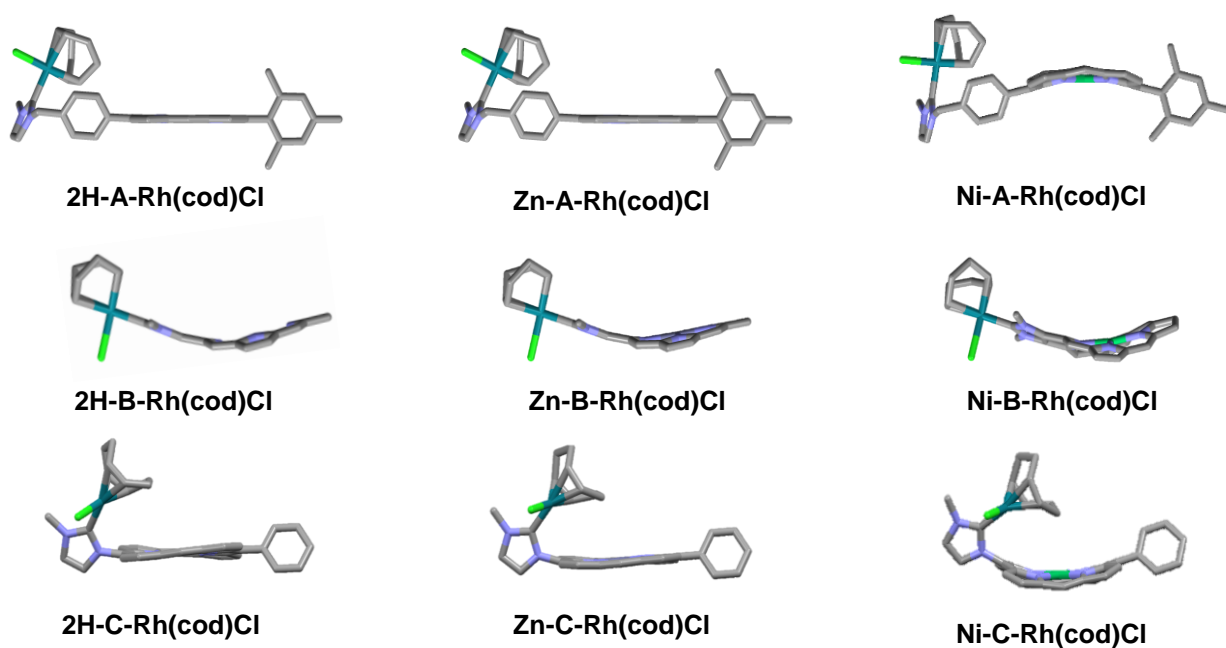


Figure S51. DFT optimized structures of complexes **M¹-A-Rh(cod)Cl**, **M¹-B-Rh(cod)Cl** and **M¹-C-Rh(cod)Cl** with $M^1 = 2H, Zn$ and Ni (meso p-tolyl groups and H omitted for clarity).

Topographic steric maps

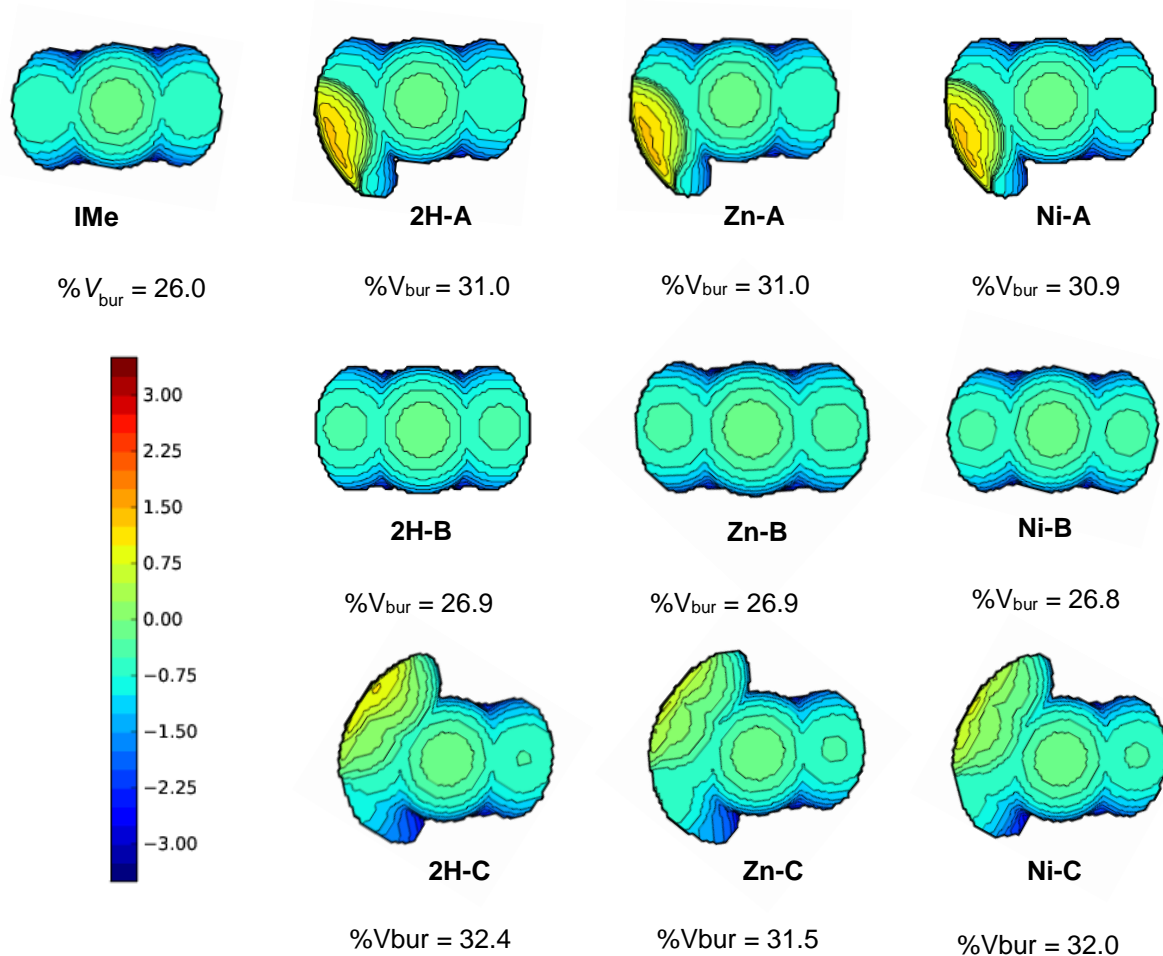
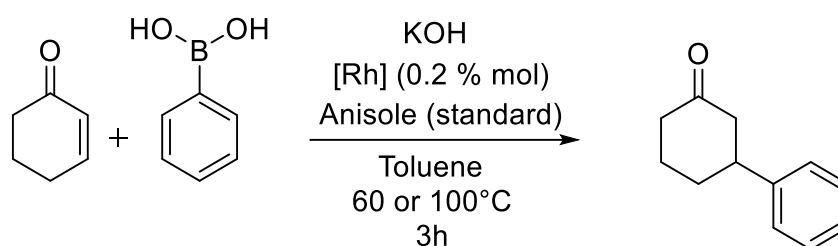


Figure S52. Steric maps of the complexes **M¹-A-Rh(cod)Cl**, **M¹-B-Rh(cod)Cl** and **M¹-C-Rh(cod)Cl** with M¹ = 2H, Zn and Ni in optimized geometries of the corresponding complexes calculated with the SambVca 2.1 tool with the following standard inputs: Bondi radii 1.17 Å, Rh–C_{NHC} 2.00 Å, r_{sphere} = 3.50 Å, mesh spacing 0.10 Å, H atoms excluded.¹⁵

Catalytic studies

General procedure for catalytic studies



Cyclohex-2-en-1-one (48.0 mg, 0.499 mmol, 1eq) and anisole (54.0 mg, 0.499 mmol, 1eq) used as internal standard were dissolved in anhydrous toluene (2 mL) in a degassed 10 mL vial. Phenylboronic acid (121.7 mg, 0.999 mmol, 2 eq) was added under argon and the mixture was stirred until complete dissolution. KOH (5.2 mg, 0.093 mmol, 0.2 eq) and the catalyst (0.2% mol, 0.998 μmol) were added under argon and the mixture was protected from light and stirred at 60 or 100°C for 3 hours. Conversion of cyclohex-2-en-1-one was monitored by gas chromatography (GC) analyses. Conversions of the cyclohex-2-en-1-one and yields of 3-phenylcyclohexan-1-one after 3 hours were determined by gas GC analyses and by ^1H NMR spectroscopy. All reactions were performed minimum in triplicate with reproducible results.

Monitoring of the reactions by gas chromatography (GC)

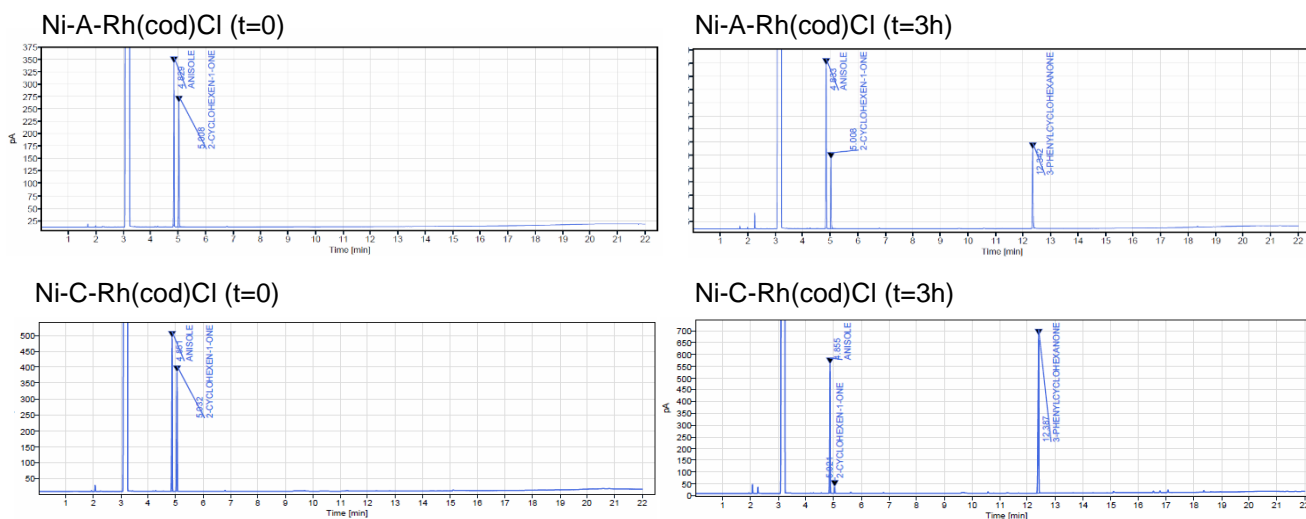


Figure S53. GC chromatograms obtained from reaction mixtures with **Ni-A-Rh(cod)Cl** (top) and **Ni-C-Rh(cod)Cl** (bottom) at 100°C with t=0 (left) and t=3h (right).

Time profile of the reactions

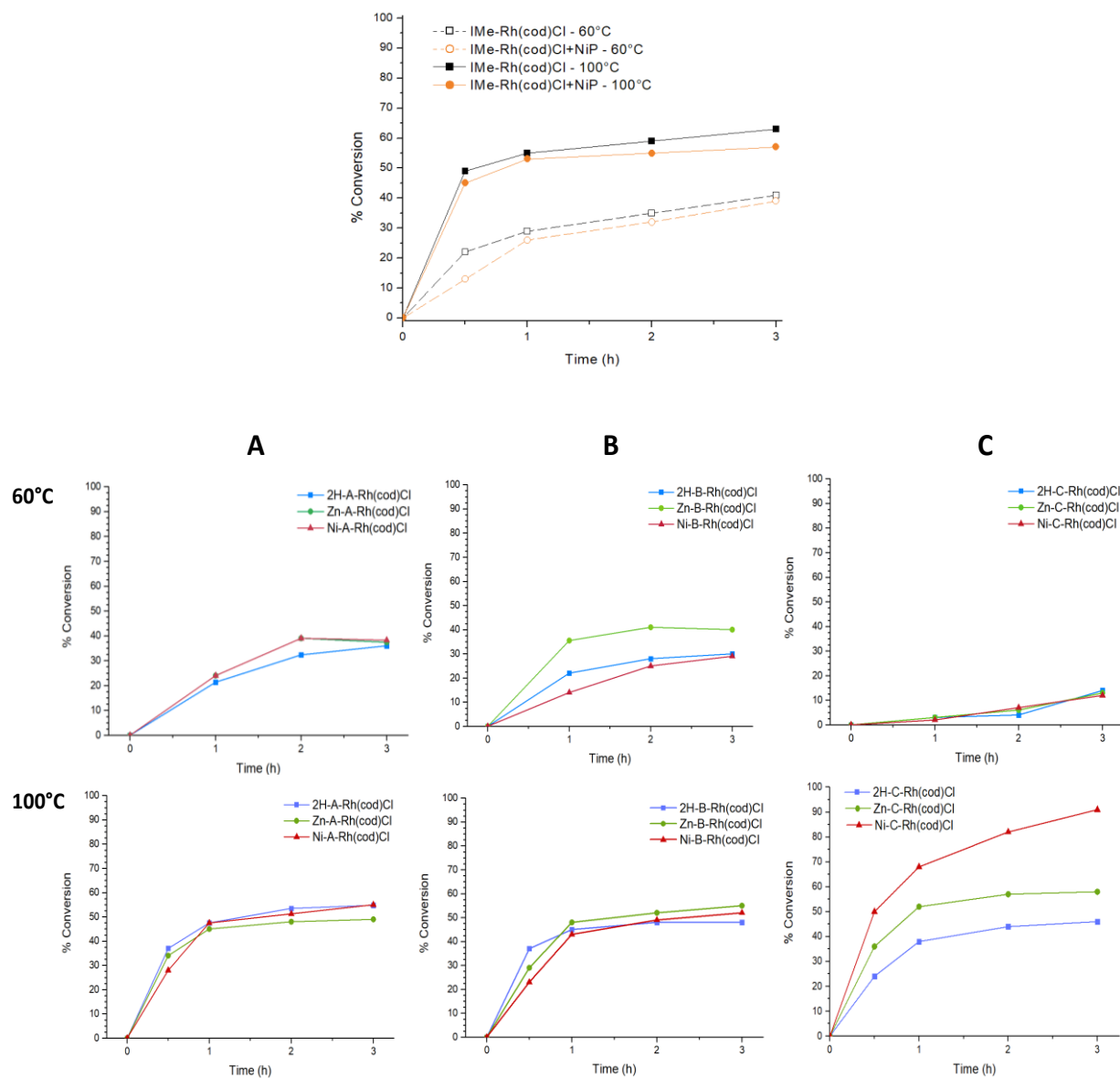
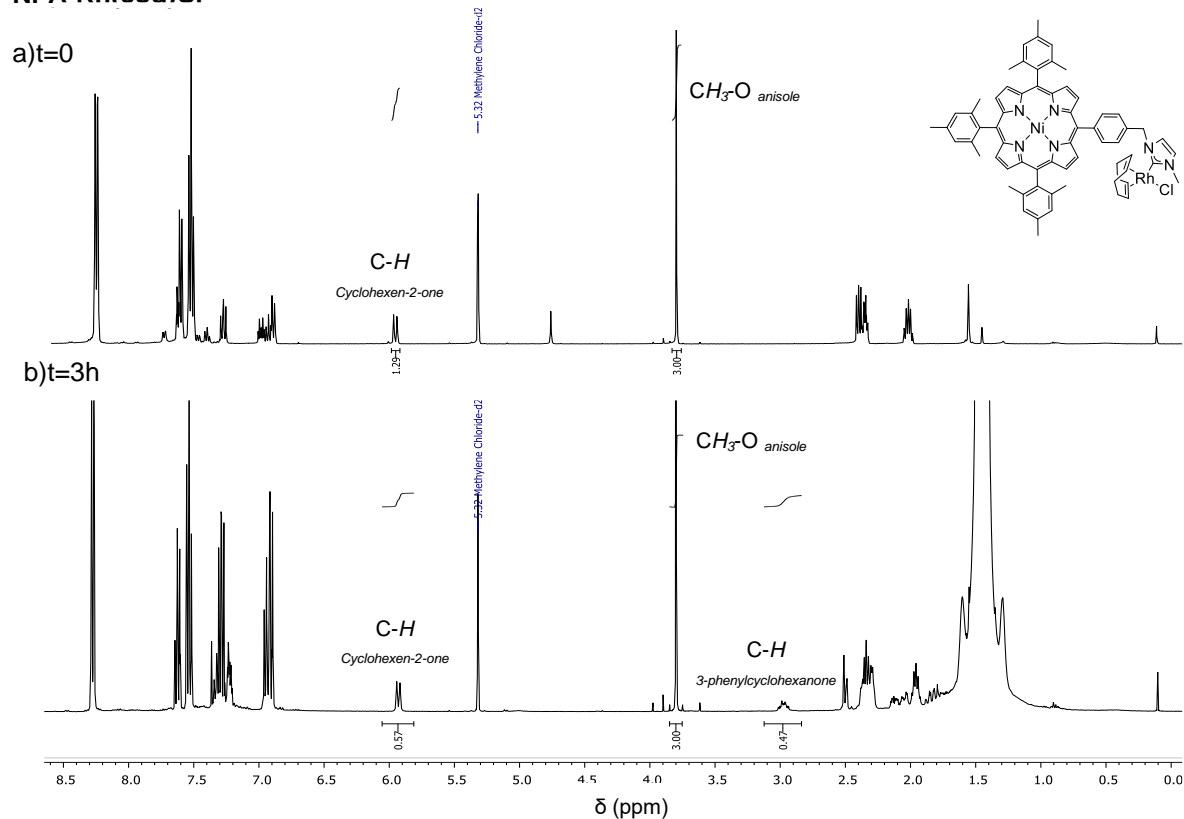


Figure S54: Time profiles of the conjugated addition of phenylboronic acid to cyclohexen-2-one catalysed by **IMe-Rh(cod)Cl** (black), **IMe-Rh(cod)Cl + NiP** (orange) at 60°C and 100°C (top); Time profiles of the same reaction catalysed by **M¹-A-Rh(cod)Cl**, **M¹-B-Rh(cod)Cl** and **M¹-C-Rh(cod)Cl** (M¹ = 2H in blue, Zn in green and Ni in red) at 60°C and 100°C.

Monitoring of the reactions by ^1H NMR spectroscopy

Ni-A-Rh(cod)Cl



Ni-C-Rh(cod)Cl

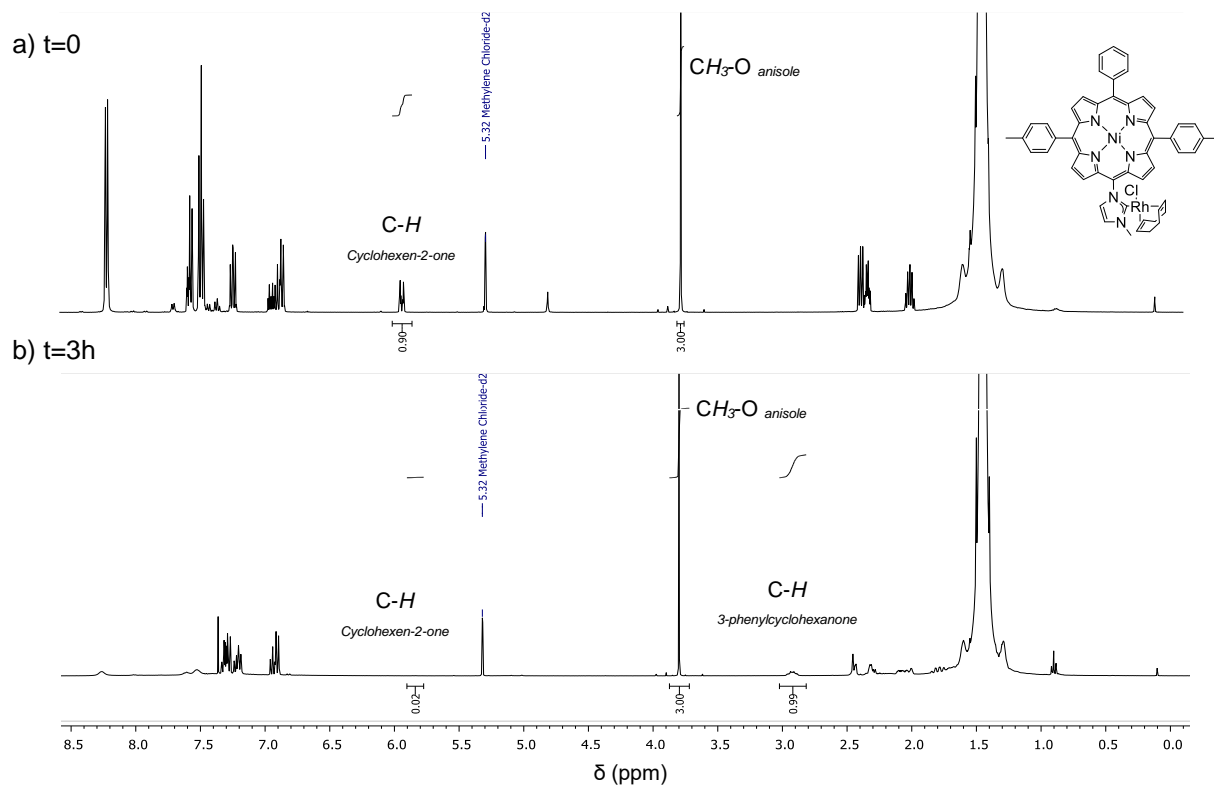


Figure S55. ^1H NMR spectra of the reaction mixtures with **Ni-A-Rh(cod)Cl** (top) and **Ni-C-Rh(cod)Cl** (bottom) complexes at $t = 0$ (up) and $t = 3$ hours (down). A drop of the reaction mixtures was taken at $t = 0$ and $t = 3$ h and diluted with CD_2Cl_2 for ^1H NMR spectroscopy analysis.

Monitoring of the catalysis reactions by UV-visible absorption spectroscopy

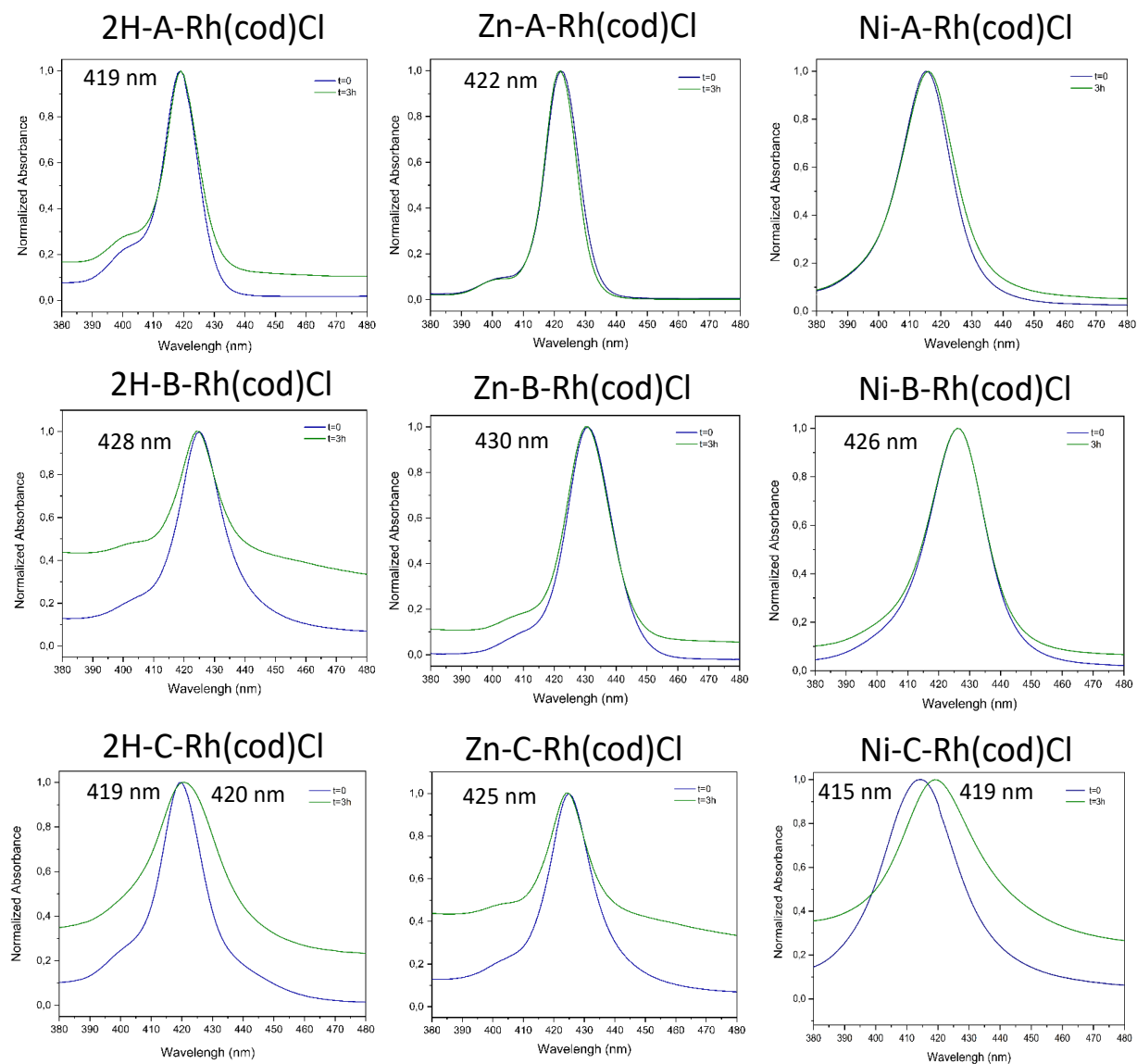


Figure S56. UV-visible absorption spectra in CH₂Cl₂ of the reaction mixtures of the conjugated addition of phenylboronic acid to cyclohexen-2-one at 100°C catalysed by **M¹-A-Rh(cod)Cl**, **M¹-B-Rh(cod)Cl** and **M¹-C-Rh(cod)Cl** (M¹ = Ni, Zn, 2H) at t = 0, blue and t = 3h, green.

Stability of 2H-C-Rh(cod)Cl and Ni-C-Rh(cod)Cl

Catalysts $M^1\text{-C-Rh(cod)Cl}$ ($M^1=\text{Ni}$ or 2H) (10 mg) were dissolved in toluene (15 mL) and mixed with KOH (100 eq), heated to 100°C for 3h. At $t = 0.5\text{h}$ and $t = 3\text{h}$, 7mL of the reaction mixture were take-off and concentrated for $^{13}\text{C}\{^1\text{H}\}$ NMR spectroscopy, UV-visible absorption spectroscopy and Electrospray Ionization Time-of-Flight mass spectrometry.

Monitoring of the stability of complexes 2H-C-Rh(cod)Cl and Ni-C-Rh(cod)Cl by $^{13}\text{C}\{^1\text{H}\}$ NMR spectroscopy

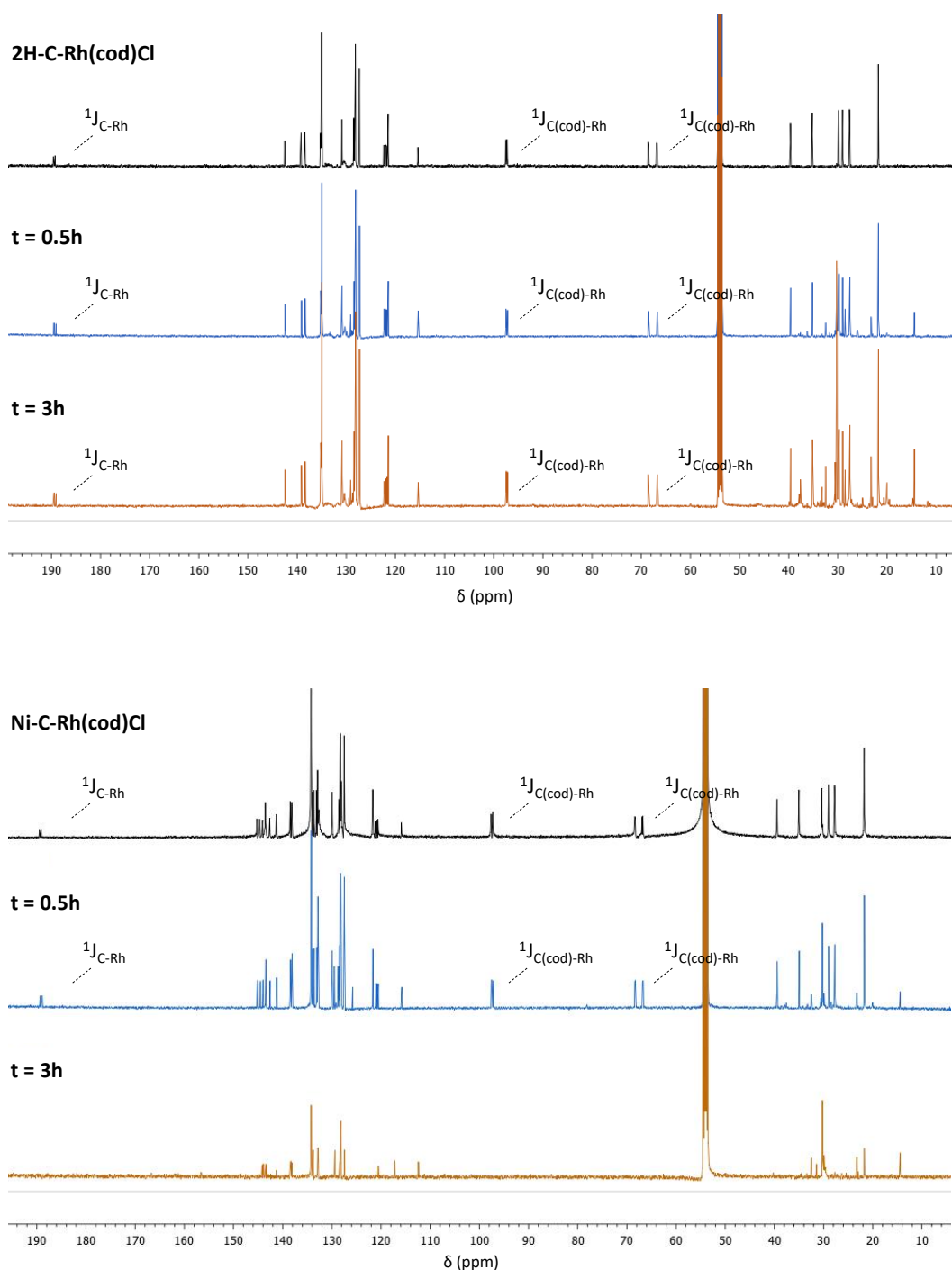


Figure S57. Monitoring of the stability of complexes **2H-C-Rh(cod)Cl** (top) and **Ni-C-Rh(cod)Cl** (bottom) in the presence of KOH (100 eq) in toluene at 100°C ($t = 0$, black; $t = 0.5\text{h}$, blue; $t = 3\text{h}$, orange) by $^{13}\text{C}\{^1\text{H}\}$ NMR spectroscopy (500 MHz, CD_2Cl_2).

Monitoring of the stability of Ni-C-Rh(cod)Cl by UV-visible absorption spectroscopy

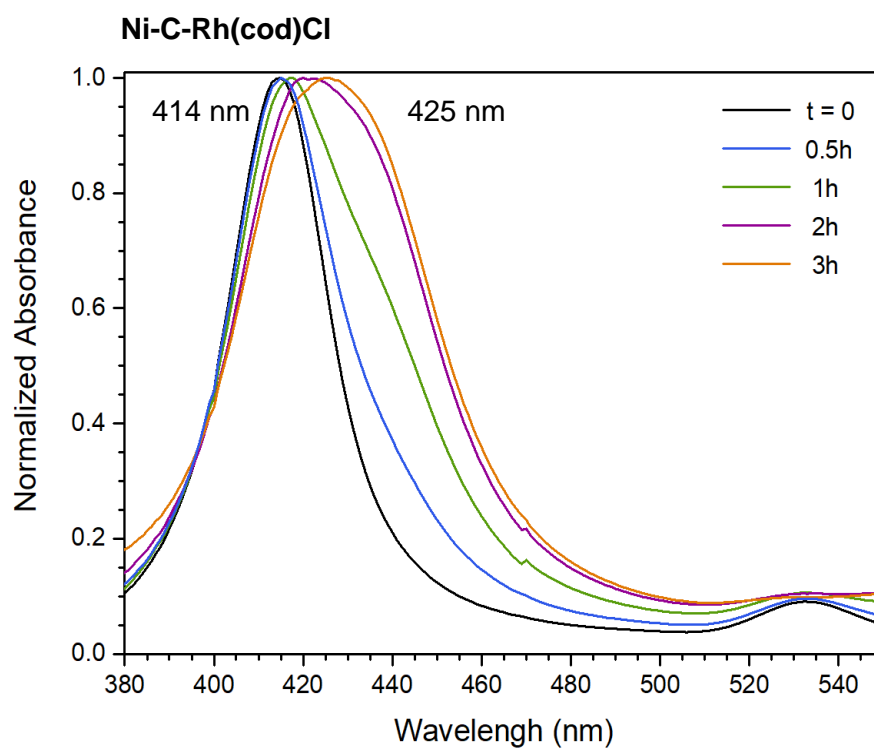


Figure S58: Monitoring of the stability of complex **Ni-C-Rh(cod)Cl** in the presence of KOH (100 eq) in toluene at 100 °C (t = 0, black; t = 0.5 h, blue; t = 1h, green, t = 2h, purple, t = 3h, orange) by UV-visible absorption spectroscopy in CH₂Cl₂.

Monitoring of the stability of complex Ni-C-Rh(cod)Cl by Electrospray Ionization Time-of-Flight mass spectrometry.

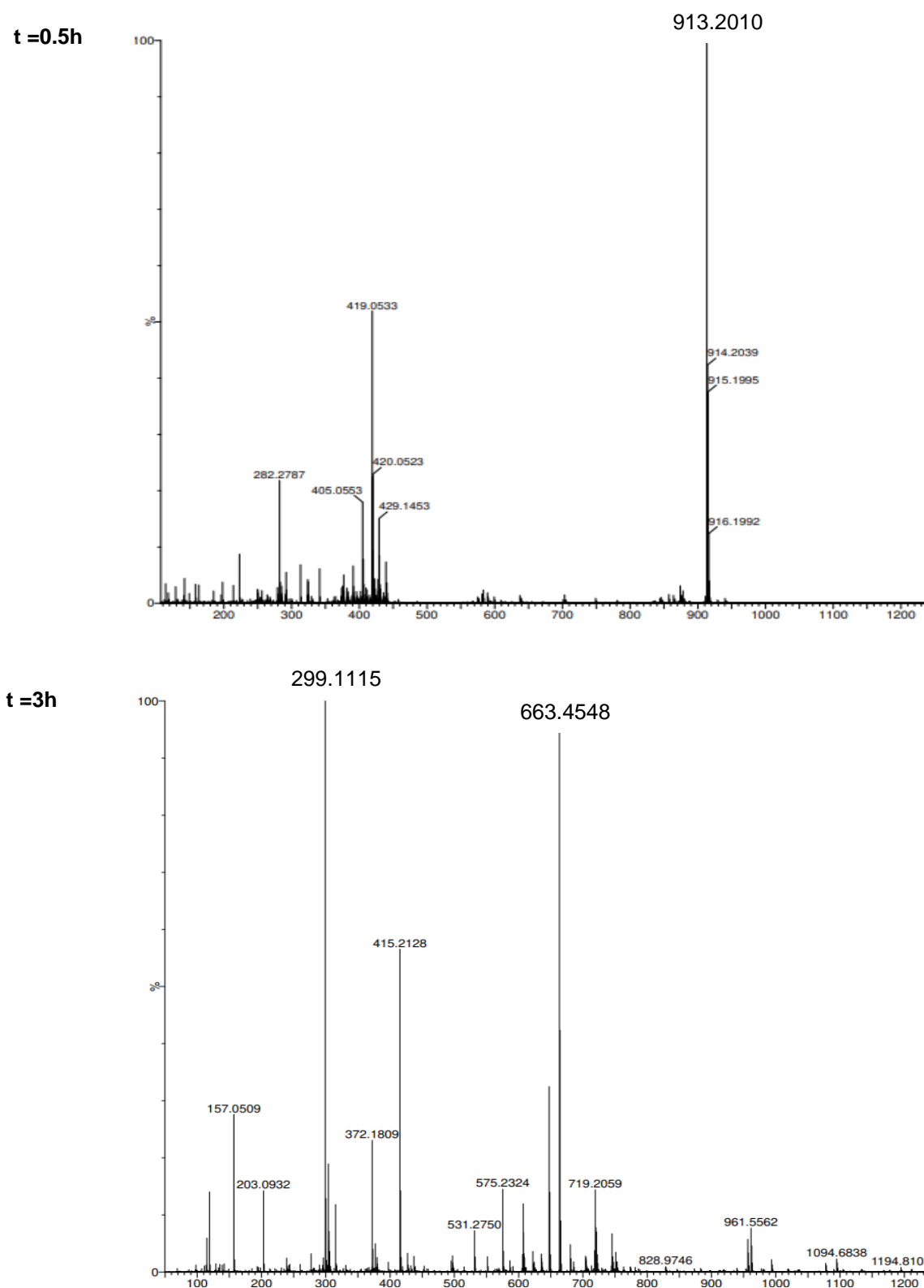


Figure S59: Monitoring of the stability of complex Ni-C-Rh(cod)Cl (m/z calc for $C_{52}H_{44}N_6NiRh [M-Cl]^+$: 913.2030) in the presence of KOH (100 eq) in toluene at 100 °C ($t = 0.5h$ (top) and $t = 3h$ (bottom)), by ESI-TOF mass spectrometry.

References

- (1) J. Li, J. Peng, Y. Bai, G. Lai, X. Li, *J. Org. Chem.*, 2011, **696**, 2116-2121.
- (2) J. S. Lindsey, S. Prathapan, T. E. Johnson, R. W. Wagner, *Tetrahedron*, 1994, **50**, 8941-8968.
- (3) J.-F. Lefebvre, D. Leclercq, J.-P. Gisselbrecht and S. Richeter, *Eur. J. org. Chem.*, 2010, 1912-1920.
- (4) (a) J.-F. Lefebvre, M. Lo, J.-P. Gisselbrecht, O. Coulembier, S. Clément and S. Richeter, *Chem. Eur. J.*, 2013, **19**, 15652-15660 ; (b) J.-F. Lefebvre, M. Lo, D. Leclercq, *Chem. Commun.*, 2011, **47**, 2976-2978.
- (5) J.-F. Lefebvre, J.-F. Longevial, K. Molvinger, S. Clément, S. Richeter, *C. R. Chimie*, 2016, **19**, 94-102.
- (6) C. H. Devillers, S. Hebié, D. Lucas, H. Cattey, S. Clément, S. Richeter, *J. Org. Chem.*, 2014, **79**, 6424-6434.
- (7) C. Rose, L. Lichon, M. Daurat, S. Clément, S. Richeter, *C. R. Chimie*, 2021, **24**, 83-99.
- (8) T. Dröge, F. Glorius, *Angew. Chem., Int. Ed.*, 2010, **49**, 6940–6952.
- (9) M. J. Frisch, G. W. Trucks, H. B. Schlegel, G. E. Scuseria, M. A. Robb, J. R. Cheeseman, G. Scalmani, V. Barone, G. A. Petersson, H. Nakatsuji, et al. G16_C01 2016, Gaussian 16, Revision C.01; Gaussian, Inc.: Wallingford, CT, USA, 2016.
- (10) A. D. Becke, *J. Chem. Phys.*, 1993, **98**, 5648–5652.
- (11) C. Lee, W. Yang, R. G. Parr, *Phys. Rev. B: Condens. Matter Mater. Phys.*, 1988, **37**, 785–789.
- (12) S. Grimme, J. Antony, S. Ehrlich, H. A. Krieg, *J. Chem. Phys.*, 2010, **132**, 154104.
- (13) D. Andrae, U. Häußermann, M. Dolg, H. Stoll, H. Preuß, *Theor. Chim. Acta.*, 1990, **77**, 123.
- (14) J. Tomasi, B. Mennucci, R. Cammi, *Chem. Rev.* 2005, **105**, 2999–3093.
- (15) L. Falivene, Z. Cao, A. Petta, L. Serra, A. Poater, R. Oliva, V. Scarano and L. Cavallo, *Nat. Chem.*, 2019, **11**, 872-879.